Università degli Studi di Parma

Dottorato di ricerca in Progettazione e Sintesi di Composti Biologicamente Attivi

XXVI ciclo

TITOLO DEL PROGETTO:

Design and Synthesis of Human Serine Racemase inhibitors, a challenge to modulate NMDAR dysregulation and neurodegeneration induced.

Coordinatore:

Chiar.mo Prof. Marco Mor

Tutor:

Chiar.mo Prof. Gabriele Costantino

Studente: Chiara Pecchini

Abstract

Mammalian Serine Racemase (SR) is a pyridoxal-5′-phosphate (PLP) dependent enzyme, responsible for the biosynthesis of the neurotransmitter D-Serine, which activates *N*-methyl-d-aspartate receptors (NMDAR) in the CNS.

Inhibition of SR could be a means to control D-Serine levels, which on turn may limit the NMDAR- mediated neurotoxicity in neurodegenerative diseases such as Alzheimer's disease, amyotrophic lateral sclerosis, Parkinson's disease, and protect against cerebral ischemia.

The aim of this work is to identify new compounds that can interact with SR with satisfactory potency and selectivity, either with a competitive or with a non-competitive mechanism of action. In particular, a number of cyclopropane-1,2-dicarboxylic acid derivatives were synthetized, leading to the identification of *cis*-(±)-cyclopropane-1,2-dicarboxylic acid, that interacts with the enzyme in a non-covalent manner and shows an affinity of~ 240 μM. However, as described herein, the modification of the hit compound was found to be particularly problematic.

The search for covalent inhibitors, led to the synthesis of a second class of compounds that interact with the PLP moiety of the enzyme, and inhibit the enzyme in a time–dependent manner.

This finding opens the possibility of exploring a new class of SR covalent inhibitors.

Tables of Contents

1. Introduction

Glutamate is the major excitatory neurotransmitter in mammalian central nervous system, and many of its effects are mediated through the interaction with NMDA receptors (NMDAR). NMDAR signaling pathways are considered suitable pharmaceutical targets for a variety of neuropathological conditions, and a variety of NMDAR blocking agents have been identified, although they are affected by a variety of undesirable effects.

D-serine, endogenously synthetized from L-serine by Serine Racemase, a PLP dependent enzyme, is a natural co-agonist of NMDAR, binding it at the glycine site. It is hypothesized that inhibition of Serine Racemase could represent a valuable pharmaceutical intervention in order to regulate NMDAR excitotoxicity.

1.1 Glutamate receptors.

The effects of glutamate, in the central nervous system, are regulated by metabotropic and ionotropic receptors. Metabotropic glutamate receptors (mGluRs) are a family of G protein-coupled receptors, which modulate slow synaptic transmission through intracellular second messengers. Ionotropic glutamate receptors (iGluRs) are multimeric ion channels responsible for fast synaptic transmission[1].
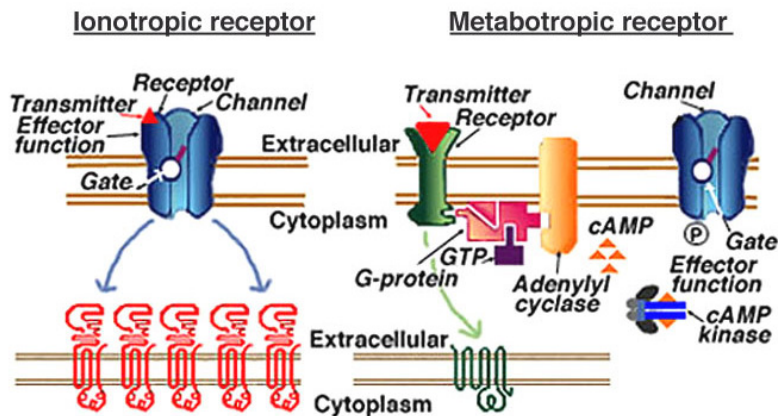
Scheme 1. GLUTAMATE RECEPTORS. Ionotropic receptors and their associated ion channels. Each iGluR is formed from the co-assembling of multiple subunits. Metabotropic receptors are coupled to their associated ion channels by a second messenger cascade. Each mGlu is composed of one polypeptide wich is coupled to a g-protein. *From Kandel et al.1991*

1.2 Metabotropic glutamate receptors (mGluRs)

mGlu receptors play important modulatory roles, and they are involved in many functionalities of the mammalian CNS, amongst others the regulation of neuronal excitability, synaptic transmission and neuronal plasticity through the activation of a multitude of signaling pathways.

To date, molecular cloning has identified eight members of this G-protein-coupled glutamate receptor family (mGlu1-mGlu8)[2], based on their sequence similarity, signal transduction mechanisms and relative pharmacology, these receptors have been further classified into three subgroups: group I (mGluR 1 and 5), group II (mGluR 2 and 3) and group III (mGluR 4, 6, 7 and 8)[2].

Group I mGluRs are coupled to Gq/Gn proteins and allow for signal transduction through increasing the phospholipase C activity and the breakdown of inositol phospholipids; group II and group III receptors are coupled to Gj/G0 proteins and inhibit the adenylyl cyclase activity[3].

mGluRs are spread throughout the CNS with individual family members exhibiting distinct spatial and temporal expression profiles[4]. In the adult rat, mGluRs are mainly expressed in neuronal cells. Group I mGluRs are typically localized in the post synaptic membrane, while group II and III receptors are mostly localized presynaptically to regulate the neurotransmitter release [4].

1.3 Ionotropic glutamate receptors

Ionotropic glutamate receptors are divided into three families named after their most specific agonists: α-amino-3-hydroxy-5-methyl-4-isoazolepropionic acid (AMPA), 2-carboxy-3-carboxymethyl-4-isopropenylpyrrolidine (kainate) and N-methyl-D-aspartate receptors[1].

AMPA receptor (AMPAR)

AMPAR are heteromeric tetramers, composed of four subunits (GluR1, GluR2, GluR3, and GluR4) that are produced by separate genes.

However, RNA editing and alternative splicing allows some exons to be interchangeably translated, leading to several functionally different subunits from each genes.

An important example is the so-called Flip/Flop region: this sequence is formed by 38 amino acids, and it is a part of the extracellular ligand-binding domain.[5]

Alternative splicing lead a difference of only 9-11 amino acids which contributes to the functional etherogeneity of AMPAR- mediated synaptic transmission.

The Flip/Flop isoforms are differentially expressed in the brain according to the cell type and age.[6] At the receptor level, these

isoforms influence the sensitivity to allosteric modulators and determine the speed of desensitization and resensitization; generally the Flop variants desensitize faster than the Flip counterpart.[7]

The permeability of receptors to calcium and others ions is critically regulated by the GluR2 subunit; AMPARs assembled from GluR1, GluR3, or GluR4 subunits are permeable to Ca^{2+} while GluR2 subunit containing receptors are Ca^{2+} impermeable.

The molecular determinant of calcium permeability has been identified as an Arginine residue in the pore loop, M2 domain, of GluR2; however, in the others subunits, Glutamine is the corresponding amino acid. In addition, in this case, the difference is due to RNA splicing.[8]

The prevention of calcium entry into the cell on activation of GluR2-containing AMPARs is thought to guard against excitotoxicity. [9]

The AMPAR subunits differs most at their C-terminal domain which interacts with the glutamate-receptor interacting protein (GRIP), that plays a prominent role in regulating the number of AMPARs on the synaptic surface.[10]

Kainate receptor (KAR)

Similarly to AMPAR, KARs in the CNS are made of heteromeric tetramers assembled from two subunit families, GluK1-3 and GluK4-5. The latter do not form functional homomeric receptors, as for the Glu1-3 subunits, but rather they form high-affinity kainate binding sites; there are evidences suggesting that in the absence of GluK1-3 subunits, GluK4-5 does not achieve cell surface expression, but it is held in the endoplasmic reticulum[11].

The lack of specific antibodies against KAR subunits has been a limit for the study of receptors distribution and purposes. However, through the development of selective inhibitors and hybridization studies, it has been demonstrated that KARs mainly have a modulatory role in synaptic transmission rather than being the major post synaptic target for synaptically released glutamate, as in the case of NMDAR and AMPAR.

At a presynaptic level, KAR can modulate the neurotransmitter release both in an excitatory and in an inhibitory manner, by modulating the GABAergic transmission[12].

Another peculiarity of the KARs is that they appear to transmit the signal also by a metabotropic mechanism involving G-proteins and second messengers. This non-canonical metabotropic signaling of KARs was confirmed by demonstrating that it is independent from ion flux[13].

2. NMDA Receptor (NMDAR)

Broadly distributed throughout the brain, NMDARs have the highest affinity for glutamate and permeability to calcium among all of the glutamate receptors.

2.1 NMDARs structure and distribution

Cloning studies revealed that NMDARs are assembled as heteromers that differ in the composition of the subunits. To date, seven different subunits, falling into three subfamilies according to sequence homology, have been identified: the GluN1 subunit, four distinct GluN2 subunits (GluN2A, GluN2B, GluN2C and GluN2D), which are encoded by four different genes, and two GluN3 subunits (GluN3A and GluN3B), arising from two separate genes.

Combination of different subunits generates functionally specific oligomeric NMDARs, which are expressed in a specific spatiotemporal manner and have distinct biophysical and pharmacological characteristics[1]. NR1 subunit is mandatory expressed throughout development and adulthood, whereas NR2B and NR2D subunits reach higher levels early in development, and decrease thereafter. NR2A and NR2C subunits show the opposite pattern.[14]

The various NMDAR subtypes display distinct gating and permeation properties. Transfection studies in heterologous systems have shown that NR1A/NR2B heterodimers have greater

permeability and Ca2+ influx, and are activated at lower Glu concentrations than NR1A/NR2A heterodimers. Insertion of the NR1A subunit with the NR2A and NR2B subunits generates receptors that are highly sensitive to magnesium block, and that are activated only under depolarized conditions.[14]

Although the NMDAR quaternary structure has yet to be resolved, functional studies suggested that the activation of the NMDAR requires the simultaneous binding of two different agonists.

Functional NMDAR is commonly formed by a heterotetrameric structure composed by two dimers embodying the NR1-NR2 subunits; each of these NR1 subunits has a glycine/serine binding site, and each of the NR2 subunits has a glutamate binding site[15].

GluN3-containing NMDARs are either glutamate/glycine-activated triheteromeric receptors composed of GluN1, GluN2, and GluN3 subunits or glycine-activated diheteromeric receptors composed of GluN1 and GluN3 subunits[16].

Although each subfamily is encoded by different genes, each ionotropic receptor subunit has a very similar molecular structure, and is divided into 4 functional domains: *1)* an amino-terminal extracellular domain (NTD); *2)* a ligand-binding domain (LBD); *3)* a transmembrane region formed by 4 hydrophobic segments (M1 to M4), with M2 partially entering the membrane to form the ion channel; and *4)* a carboxyl final domain (CTD) in the intracellular region.

In addition to natural glycine and glutamate binding sites, the extracellular region of NR2 contains binding sites for endogenous ligands such as polyamines, protons and zinc. They may wield a regulatory effect on NMDAR activity by increasing or decreasing calcium flux under physiological and pathological conditions. At the same time, the intracellular domain undergoes to multiple modifications such as phosphorylation, nitrosylation, glycosylation, and ubiquitination, which affect the cellular localization and the functions of the receptor[17].

2.2 NMDAR and CNS development

NMDARs are distributed throughout the CNS and play a key role in its development, which occurs through many stages of neurogenesis, migration, proliferation, axonal outgrowth, and synapses formation and elimination.

During development of the CNS, a large number of neurons are produced, but only a few are integrated into the neuronal circuits. This selective process is achieved through neuron apoptosis. Neurons that are stimulated by glutamate or other excitatory neurotransmitters survive, while those that do not receive stimulation undergo programmed death[18]. There is evidence that local activation of NMDARs induces production of neurotrophic factors such as brain-derived neurotrophic factor in the post-synaptic neuron[19], which diffuses and activates receptors on the presynaptic neuron, resulting in an up regulation of genes that encode proteins critical for cell survival, like Bcl-2 and antioxidant enzymes [20].

Beyond shaping the mature neuronal circuits, NMDARs also have a role in neurogenesis. Neurons and glial cells are produced by asymmetric divisions of self-renewing neural progenitor cells. Studies report that neurogenesis is promoted by neurotrophic factors released upon NMDAR activation[21]. Moreover, the functional heteromeric NMDARs may be expressed constitutively in neural progenitor cells before differentiation to play a crucial role in differentiation to neurons. In particular, neurospheres obtained from neuronal progenitor cells isolated from adult mouse hippocampus,

express the NR1, NR2A, and NR2B subunits, and the exposure to NMDA leads to a noticeable expression of c-Fos, Fos-B, Fra-2, and c-Jun proteins[22].

2.3 NMDAR and pathological conditions

Since the importance of glutamate in CNS development and functionality, abnormalities in glutamate transmission have the potential to mediate a cellular damage that plays a crucial role in many neurological disorders.

Hyper-activation of glutamate receptors, especially NMDARs, results in neuronal death through necrosis or apoptosis, a condition that is more generally known as excitotoxicity.

NMDARs over activation causes a Ca^{2+} overload in cells, which increases the activity of proteases and lipases, destroying the plasma membrane. In addition, it generates an excess of nitric oxide (NO), reactive oxygen species (ROS) and peroxynitrite, which damage membrane lipids, DNA and proteins.

This dual behavior of NMDARs is stimulated by neuronal damage and insult, but seem to be also due to the location of the receptors.

NMDARs localized in extra synaptic site[23] (cell body, dendritic shaft, the neck of the dendritic spine and adjacent to the post-synaptic density) are involved in regulating the neurotoxicity. In particular, extra synaptic NMDARs are involved in the suppression of CREB

activity and stimulation of FOXO nuclear import, whit the result to promote the transcription of pro-death genes.[24]

A recent work has specifically implicated the extra synaptic NMDAR activation in the etiopathophysiology associated with an acute and a chronic form of neuronal dysfunction such as ischemia and Huntington's disease.

In the case of Huntington's disease, the mutant Huntingtin seems to stimulate the expression of containing GluN2B NMDARs in extra synaptic site.[25]

Similarly, the reverse glutamate uptake that happens during an ischemic episode, activates the extrasinaptic NMDARs with consequent activation of neuronal death. [26]

On the opposite side, a hypofunction of NMDAR is involved in schizophrenia and in the early stage of Alzheimer's disease.

IN Alzheimer's disease the β amyloid- suppresses the long term potentiation of NMDAR and enhance endocytosis of the receptor complex in the cortical neurons [27-28].

2.4 NMDAR agonists and modulators

NMDARs are unique among ligand-gated ion channels. The activation of the receptors requires binding of both two molecules of glutamate and two co-activator molecules (either glycine or D-Serine), and a depolarization of the membrane to remove the magnesium block of the ion channel in a voltage-dependent manner[29].

Opening of the channel permits a massive entry of calcium and sodium, and the increase of the intracellular calcium activates a variety of metabolic cascades, which, under physiological conditions, govern a multitude of cellular processes including cell growth, differentiation, and synaptic activity[9].

Among the diverse subunits of NMDAR, the NR1 is an obligatory subunit, which binds to glycine or D-Serine, while the NR2 subunits binds to glutamate. NR2 subunits determine the biophysical and pharmacological activity of the NMDAR.

In addition to the activation of NMDAR, the endogenous NR1 agonists have a role in neuromodulation, by influencing allosterically the NMDAR to enhance the affinity and efficacy of glutamate[30], and promoting NMDAR turnover through priming of the receptor for internalization[31].

Glycine is an abundant neurotransmitter, which binds to both inhibitory and excitatory receptors in the mammalian CNS. Upon release from the pre-synaptic terminals, glycine activates a post-synaptic strychnine-sensitive glycine receptor, which is an inhibitory

chloride channel; it also binds strychnine-insensitive sites on excitatory NMDAR as a co-agonist[32].

At the level of the NMDAR-expressing synapses, the synaptic concentration of glycine is finely regulated by glycine transporters 1 (GlyT-1), which are closely associated with NMDARs [33].

Hashimoto and colleagues first identified D-Serine at concentrations that are one-third of those of L-serine in the brain[34]. Later, evidence showed that D-Serine can activate the so-called 'glycine' site of NMDARs, and degradation of endogenous D-Serine with D-amino acid oxidase (DAAO) specifically diminishes NMDA neurotransmission[35].

These findings provide the direct evidence that D-Serine is an endogenous ligand for the NMDAR.

3. D-SERINE

D-amino acids were not thought to be present in significant amounts in eukaryotes; the discovery of large amounts of endogenous D-Serine in the brain by Hashimoto *et al.* changed the dogma that only L-amino acids are present in mammalian tissues. Like glycine, D-Serine in a co-agonist of NMDAR, displaying up to three times higher affinity than glycine toward the receptors, because it makes three additional hydrogen bonds in the binding pocket of the receptor[36] .
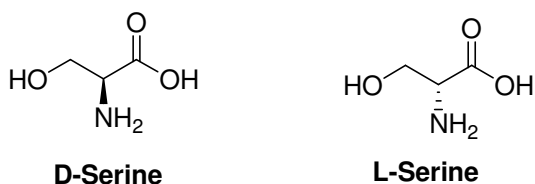
Figure 3: Structure of D-Serine and L-Serine

The actual role of D-Serine as modulator of NMDAR, was boosted by the discovery of Serine Racemase (SR), which produces D-Serine from the corresponding L isomer, and matches the regional localization of D-Serine.[37-38]

3.1 D-Serine localization

In the brain, D-Serine concentration is one-third of that of L-serine, and its levels are higher than the majority of the essential amino acids.

Early HPLC analyses have revealed a heterogeneous distribution of D-Serine throughout the brain with highest concentrations in the forebrain areas, including cerebral cortex, hippocampus, striatum, and limbic forebrain; moderate to low concentrations in the diencephalon and midbrain, and traces in the cerebellum[34].

Brain microdialysis experiments, conducted by Hashimoto *et al.*, show that the extracellular concentration of D-Serine is twice than that of glycine in the striatum, and similar to the concentration of glycine in the cerebral cortex [34].

Subsequently the Snyder's group demonstrated, through immunohistochemical studies, that D-Serine in the brain is almost co-localized with NMDAR; conversely, glycine immunoreactivity doesn't correspond to NMDAR distribution with the exception of some regions such as the hindbrain, the adult cerebellum, and the olfactory bulb, where D-Serine is also present.[39]

The selective association of D-serine with NMDARs in various districts of the brain supports the notion that D-Serine is an endogenous ligand for the receptor in these areas. So far, the specific mechanisms involved in regulating the NMDAR by D-Serine and glycine in different regions of the brain are still unclear. Although most part of D-Serine is found in the CNS, recent investigations

reveal that D-Serine and its synthesizing enzyme SR are also present in the peripheral nervous system such as Schwann cells[40], and in the supporting cells of the vestibular sensory epithelium.

On a cellular scale, D-Serine has been predominantly localized in the astrocytes[41], Mothet *et al.* have demonstrated that it can be released by a vesicular transport.[42] This evidence, along with the existence of a biosynthetic pathway and a target receptor, suggests that D-Serine behaves as an unconventional glio-transmitter.

Afterward, a large amount of D-Serine was found also in forebrain neurons, where SR is expressed at higher rates than in the astrocytes [43- 44] . This finding implicates that D-Serine could be produced in neurons and stored in astrocyte cells for an activity-dependent release.

3.2 D-Serine metabolism

Humans supply D-serine from food, gastrointestinal bacteria, degradation of proteins (which contain D-amino acids after racemization with aging), and through biosynthesis from L-serine. The key enzyme responsible for D-serine synthesis is the PLP (pyridoxal-5'- phosphate)-dependent enzyme SR, which converts L-serine into its D-isomer[37-38].

In humans and animals, L-serine is a nonessential amino acid, which can be obtained from glycolysis. 3-Phosphoglycerate, a glycolytic intermediate, can be converted to L-serine by oxidation, transamination and dephosphorylation reactions. Although L-serine can be also derived from dietary intake or from degradation of proteins and phospholipids, the blood-brain barrier has low permeability to L-serine. Hence, local synthesis is particularly important for L-serine metabolism in the brain[45].

Mammalian D-amino acids can be metabolized by the peroxisomal flavoprotein DAAO,[46] with the concomitant reduction of the co-factor flavin- adenine dinucleotide (FAD).

The activity of DAAO is selectively limited to the metabolism of neutral D-amino acids, with highest affinity for D-Serine, D-Alanine, D-Proline, D-Leucine and D-Methionine [47-48]. Glycine is not a substrate at physiological pH values, nor are the L-amino acids or the dicarboxylic amino acids[49]. The expression of DAAO is highest in the kidneys, followed by the liver and the CNS, where DAAO is particularly concentrated in astrocytes of the hindbrain and cerebellum [50].

Physiological degradation of D-Serine by DAAO was suggested by the marked regional and developmental variation in DAAO levels in a pattern reciprocal to D-Serine levels[51]. Furthermore, DAAO-KO mice manifest an increase in D-Serine levels, especially in areas with physiologically low levels of DAAO in wild type animals such as the cerebellum and periphery [42]. The relatively unchanged D-Serine levels in the forebrains of DAAO-KO mice imply that in these areas, other mechanisms might regulate D-Serine concentrations [42-50].

Accordingly, it was found out that SR displays an unusual dual activity; it can catalyze also a α,β-elimination of water from D or L-serine to generate pyruvate and ammonia.

This is not surprising, since PLP-dependent enzymes often catalyze collateral reactions (called "paracatalytic") as a result of evolution from a common ancestor enzyme. However, in the case of SR, this paracatalytic activity is highly expressed, suggesting a precise role in physiological homeostasis.

It's possible to imagine that pyruvate, formed by the dehydratase activity of SR, has a distinct metabolic role, since the SR is expressed in tissue with high metabolic demand. However, the forming rate of pyruvate by SR, and its metabolic contribution, is very low compared to the other metabolic enzymes[52].

In vitro studies conducted by Wolosker *et al.* demonstrated that at physiological concentration of L and D Serine (1mM and 0.3 mM respectively) the enzyme degrades both enantiomers. The physiological concentration of D-Ser doesn't affect the *ratio* of D-Serine dehydration, because is much below the Km of the SR

(~ 10 mM). According to this, part of D-Serine, produced by the enzyme, undergoes theα-β elimination branch, in order to limit the D-amino acid concentration at neuronal site.

On the other hand, D-Serine is stable when physically separated from SR and its elimination activity. In cells expressing SR, the release of D-Serine to the extracellular medium prevents its destruction by SR. As a result, more than 98% of the synthesized D-Serine is found in the culture medium, rather than inside the cells [53]. By restricting the accumulation of D-Serine, the α,β-elimination provides an explanation for the lower levels of D-Serine in neurons when compared to astrocytes. Thus, it is conceivable that the accumulation of D-Serine in astrocytes is mostly due to the uptake from the extracellular medium, associated to a relative low metabolism in these cells (which possess little amount of SR). Compartmentalization of D-Serine in intracellular vesicles will further contribute to its relative stability in astrocytes[54] .

However these studies about the α-β elimination activity have yet to be determined *in vivo*, and the real function of dehydratase activity of SR still remain controversial.

3.3 D-Serine storage, release and clearance

Originally, D-Serine was conceived to be produced by astrocyte and released in the extra synaptic cytosol by exocytosis.

Mothet at al. demonstrated that cultured astrocytes can release D-Serine from vesicles after AMPAR stimulation [43]. They also demonstrated that the release of D-Serine is dependent upon both intracellular and extracellular calcium levels. Also, Mothet and colleagues have found out that the release of D-serine is dependent on activity of vacuolar-type H+-ATPase (essential for maintaining the electrochemical gradient of protons across synaptic vesicle membranes), and SNARE proteins, which mediate the fusion of vesicles with plasma membrane.

Nevertheless, Ca^{2+}-dependent vesicular release of D-Serine from glia doesn't rule out the possibility that the amino acid is released by other mechanisms, especially considering that the majority of D-Serine is free in the cytoplasm [55].

These "non vesicular" pathway could involve processes that have been already associated to other glio-transmitters such as hemichannels, volume anion channels and reversal transporters [43].

In addition, release of cytosolic D-Serine can operate through neutral amino acid transporters present on the membrane of astrocytes[56].

The secondary source of D-Serine are neurons, in which the amino acid is released mostly through a cytosolic route[57].

In cortical neuronal cultures, D-Serine release is dependent upon stimulation of NMDAR, AMPAR, and KAR, and is blocked by removal of either external Ca^{2+} or Na^+; however, toxins, which usually inhibit vesicular release, do not affect it, confirming the hypothesis of a cytosolic pathway.

Because neurons expressing SR also contain NMDARs, it is conceivable that neuronal D-Serine exerts an autocrine or paracrine activation of NMDARs and its release is coordinated with glutamate release to stimulate NMDARs [60].

Both the resident microglia in CNS, amyloid and secreted amyloid precursor protein (sAPP) were found to release D-Serine upon stimulation [40-58], which indicates that D-Serine may be involved in neuroinflammation associated with Alzheimer's disease.

Neuronal or glial uptake via specific transporters is an important mechanism to terminate the synaptic activities of most neurotransmitters. Several transporter candidates for D-Serine have been identified on the membrane of glial cells and neurons. Astrocytes express a Na^+-dependent transporter with low affinity and low specificity for D-Serine, similar to the ASCT transporter that is responsible for accumulation of small neutral amino acids[59]. Fluxes of D-Serine through this transporter are coupled to L-Serine and other small neutral amino acids counter-movements, indicating an antiporter mechanism for glial D-Serine transport. It has been identified also another neutral amino acid transporter, named Asc-1, which is Na+-independent and has a high affinity for D-Serine[59]. This transporter is located at presynaptic terminals, dendrites and soma of neurons, and it's thought to be involved in the synaptic

clearance of D-Serine by neurons. A third D-Serine transporter, which is Na^+ Cl^- sensitive and has limited affinity for other neutral amino acids, including cysteine and alanine, has been described in rat brain synaptosomes[60]. These multiple transport systems may contribute simultaneously to the regulation of D-Serine concentrations at the level of the synapses.

3.4 D-Serine physiological role

Today, it is fairly clear that in several brain areas the endogenous co-ligand on NMDAR is D-Serine and not glycine [42-61]. Thus, D-Serine plays a key role in regulating NMDAR-dependent processes including synaptic transmission, synaptic plasticity, gene expression and pathophysiological phenomena like excitoxicity and neurodegenaration.

The first indication of the prominent role of D-Serine in opposition to Glycine derives from immunohistochemical studies, which co-localized NMDAR expression and D-Serine high concentration in the brain of the rat. Subsequently, *in vitro* studies demonstrated that the selective degradation of D-Serine, by DAAO, abolishes NMDAR neurotransmission in different regions of the brain[62].

Hippocampus represents the best model to study synaptic effects of NMDAR and D-Serine for the high concentration of both factors. In the hippocampus, long-term potentiation (LTP) depends on NMDAR activation[63]. Therefore, because D-Serine is an endogenous ligand for NMDAR, it was not surprising to discover that D-Serine released from astrocytes is involved in the induction of LTP in pyramidal cell synapses[64]. The pre-treatment of cells, using exogenous DAAO, inhibited this LTP, further supporting the idea that D-Serine, rather than glycine, is the endogenous ligand of NMDAR in this area of the brain and it has a crucial role in the maintenance of LTP.

A further evidence supporting this theory derives from the observation that, in aged hippocampus, D-Serine level significantly decreases, leading to impaired LTP and NMDAR-mediated synaptic

potentials which can be reversed by exogenous D-Serine [65-66]. In hypothalamic supraoptic nucleus (SON), astrocyte-derived D-Serine controls activation of NMDAR and thus the activity-dependent long-term synaptic changes[67].

In line with the crucial role of D-Serine in synaptic plasticity, defective LTP recorded in a senescence-accelerated mouse strain was brought to control levels when D-Serine was given as a supplement[68]. Furthermore, in agreement with the emerging role of D-Serine as the major ligand for the modulatory glycine-binding site of NMDAR, such a deficit in LTP is not associated with reduced levels of glycine[67]. The ability of D-Serine to control NMDAR-dependent neurotransmission has been confirmed using DAAO-deficient mice. The highest increases in D-Serine levels displayed by these mice are in the brainstem and spinal cord[69]. NMDAR-mediated excitatory postsynaptic currents recorded from spinal cord dorsal horn neurons were significantly potentiated in mutant mice [72]. Finally, knockout mice for the neuronal transporter Asc-1 display a NMDAR-dependent hyperexcitability, likely due to the elevated extracellular D-Serine levels[70].

D-Serine might also be involved in the coding and processing of sensory information. For example, in the retina, SR localized in the Müller glia controls NMDAR mediated responses resulting from application of NMDA or light stimulation, through the production of D-Serine[71]. Another potential model is the peripheral vestibular system, where there are high levels of SR, DAAO and D-Serine in the sensory epithelia[72] . Finally, astrocytes are not the only glial cells that synthesize and release D-Serine, as microglia do so as well[73].

The function of D-Serine secreted by quiescent microglia as yet unknown. But there is growing evidence that neurons in non-pathological states are frequently contacted by satellite microglia, which might promote synaptogenesis and synaptic plasticity using a large repertoire of secreted factors, such as brain-derived neurotrophic factor (BDNF) or neurotrophin 3 (NT-3).

D-Serine also promotes motility signal during brain development. In fact, it is well known that NMDARs participate to the radial migration of immature granule cells in the developing cerebellum[74]. As they migrate through the molecular layer, immature neurons are guided by Bergmann glia. Observation of cell migration in cerebellar slices revealed that glutamate, acting on NMDAR, has a crucial, modulatory effect on promoting the motility of granule cells through the molecular layer[75]. The granule cells start their radial migration after the expression of the NMDARs on the plasmalemmal surface, and the antagonists of these receptors significantly decrease the rate of glia-guided radial neuronal migration. By contrast, the rate of granule cell movement is increased by removal of Mg^{2+} or by application of NMDA or the co-agonist glycine.

In developmental cerebellum, granule neurons migrate from the external granular layer to the internal granular layer along the processes of the Bergmann glia. SR is present in the Bergmann glia of the developing cerebellum and D-Serine levels reach the higher concentration in postnatal days, and subsequently decrease because of the emergence of DAAO [76]. D-Serine released by Bergmann glia seems to be essential in promoting the migration of granule cells through activation of NMDAR[57]. Indeed inhibition of

SR, using a new series of specific inhibitors or by applying DAAO on cerebellar slices to degrade extracellular released D-Serine, blocked the migration of granule cells via inhibition of NMDAR-mediated Ca^{2+} influx[57]. In addition, GRIP adenoviral infection of the developing cerebellum increases D-Serine levels through activation of SR and concomitantly increases the rate at which granule cells migrate to their final location. D-Serine might also participate in the synaptogenesis of neural network because its ontogeny in Bergmann glia is concurrent with expression of the NR2A and NR2B NMDAR subunits in Purkinje cells[42].

The motility-promoting role of D-Serine is not restricted to the postnatal development of the cerebellum. In fact, SR is present in the perireticular nucleus, a transient area of the human fetal brain that is thought to be involved in the orientation of thalamocortical fibres[77]. Additionally, D-Serine synthesized in the placenta is exported into the fetal circulation through amino acid transporters[78]. NMDAR are present in the early phases of the gestation[79], so D-Serine is spatially and temporally expressed to control NMDAR-mediated neuronal migration and synaptogenesis. The blocking of NMDARs during neocorticogenesis[80] results in abnormal cortical development, at the same time the disruption of D-Serine metabolism during embryonic and early postnatal life might lead to the same developmental defects. Notably, impairment in cerebellar development and maturation correlate with a specific shut-down of DAAO gene expression[81], supporting the hypothesis that alterations in the signaling of D-Serine and/or NMDARs promote neuronal degeneration and inhibition of synaptogenesis.

3.5 NMDAR overactivation and D-Serine mediated neurotoxicity.

Besides NMDAR normal role in promoting neuronal development and plasticity, it is well known that they can cause cell death in many neuropathological conditions and in case of intense or chronic activation[82].

Since D-Serine regulates NMDAR activity, its dominant role within this disorders, and neurotoxicity was observed in parallel with its correlation in neuroplasticity[83-84]

Research over the past years has strongly corroborated this notion, particularly in relation to Alzheimer's disease and stroke; but recent studies show that high D-Serine levels are involved also in Amyotrophic Lateral Sclerosis (ASL), Parkinson's disease and chronic pain. On the other hand, NMDAR hypofunction, which occurs in schizophrenia, is notably ameliorated by administration of D-Serine.

In Alzheimer's disease (AD), various evidences support a central role of amyloid β-peptide (Aβ), the major component of neuritic plaques, in causing an inflammatory circumstance in microglia, which triggers neuronal death by excitotoxicity[85]. Furthermore, the activity of NMDAR is increased in the AD brain and memantine, an antagonist with moderate affinity for these receptors, has neuroprotective[86] effects. A number of observations support the idea that D-Serine might participate in the pathogenic progression of AD. Indeed, it has been discovered that the hippocampus of AD patients

displays higher SR activity and that Aβ can stimulate, *in vitro*, the synthesis and the release of neurotoxic levels of D-Serine from microglia[60]. Conversely, DAAO can protect neurons against Aβ-induced Ca^{2+} overload and neurotoxicity, thus providing evidence that D-Serine is a toxic factor induced by Aβ [60]. Deletion and site-specific mutagenesis on SR gene show that the activator protein-1 (AP-1) binding sites are responsible for responsiveness to Aβ and to lipopolysaccharide (LPS)[87]. Moreover, Aβ provokes Ca^{2+} transients in microglia and this might regulate the activity of SR at a post-translation level, because the enzyme activity is influenced by Ca^{2+}. All these *in vitro* observations fit with the increase in D-Serine levels measured in the cerebrospinal fluid of Alzheimer's disease patients[88].

The demonstration that Aβ activates the JNK-mediated modulation of AP-1-binding activity of SR gene is in agreement with the observations that, in Amyotrophic Lateral Sclerosis, microglia inflammation promotes up-regulation of SR expression in a JNK-dependent manner. Sasabe *et al.*[89] demonstrated that endogenous D-Serine mediates motoneuron cell death by excessive stimulation of NMDAR in the spinal cord of Amyotrophic Lateral Sclerosis induced mice. In Amyotrophic Lateral Sclerosis transgenic mice, activated microglia seem to be the main source of spinal D-Serine, constituting a potential therapeutic target for the patology. In addition, experimental data remark that elevated level of Glycine remained unchanged during the progression of the disease, by opposite with D-Serine whose level increases progressively along with the course of the pathology. Removal of endogenous D-Serine from spinal cord cultures of Amyotrophic Lateral Sclerosis

transgenic mice protects the motoneurons against NMDAR-mediated cell death, linking D-Serine to motoneuron degeneration. Moreover the authors also observed that the level of D-Serine and SR are greatly increased in the spinal cord of patients with familiar forms of ALS. In this context, inhibitors of SR may provide a new neuroprotective strategy against ALS.

Ischemia provides another pathological situation for studying the role of D-Serine in neuroinflammation and excitotoxicity. Exposing neurons to oxygen-free and glucose-free conditions (simulated ischemia) causes NMDAR-dependent cell death that is prevented by NMDAR antagonists[84]. Katsuki *et al.* have provided evidence that endogenous D-Serine has a significant role in neuronal damage resulting from simulated ischemia[85]: application of DAAO to ischemic brain slices protected neurons from death. This is consistent with the report by Wolosker and colleagues[90] that D-Serine deaminase offers protection against NMDA-induced neuronal insults by shutting-down the activity of NMDAR to physiological levels. However, these studies did not address the source (astrocytes, microglia and/or neurons) of D-Serine and the mechanisms leading to deleterious extracellular levels of the amino acid. It is plausible that in these cell types, ischemia and NMDAR might upregulate SR expression, and induce release of excessive amounts of D-Serine.

Other neurodegenerative diseases, such as Parkinson's disease and Huntington's disease, have been associated with hyperactivation of NMDAR and with high concentrations of D-

Serine, resulting from high levels of SR activity and low levels of DAAO activity.

On the other hand it's well documented that NMDAR hypofunction is implicated in the pathology of schizophrenia, as reduced NMDAR activity due to NMDAR antagonists or reduced numbers of NMDARs induces positive, negative, and cognitive schizophrenia-like symptoms, which can be reversed by intraventricular D-Serine administration. Compared to healthy controls, schizophrenic patients have lower D-Serine and higher L-Serine and total serine levels in the prefrontal cortex and serum[91-92].

Genetic association studies identified a plausible risk genes related to D-Serine metabolism for schizophrenia: for example G72 gene encodes for a protein that activates D-amino acid oxidase[93].

Currently, clinical trials are evaluating the effect of D-Serine administration in schizophrenia in a large group of patients, which include studies of both phase II and phase III.

4. SERINE RACEMASE

Racemases are a class of enzymes that reversibly convert L-amino acids to the corresponding D isomers. They are mainly expressed by prokaryotic cells, which use D-amino acids to build cell walls and for defense strategies. Bacterial Serine Racemase is related to vancomycin resistance; the *enterococcus gallinarum* modifies D-Ala-D-Ala peptidoglycan precursor to D-Ala-D-Ser, which is resistant to vancomycin action.

Interest in the Human Serine racemase (hSR) arises from the discovery that D-Serine, as well as other D-amino acids, such as D-Aspartate, can bind to NMDAR acting as a potent co-agonist of glutamate in the modulation of the receptor function. When Hashimoto *et al.* discovered considerable levels of endogenous D-Serine in the mammalian brain, the source of this unusual amino acid became a critical question. This intrigue was settled when Wolosker *et al.* in 1999 cloned the full-length mouse SR gene and purified the enzyme from rat brain. These discoveries helped to legitimize D-Serine as an endogenous signaling molecule. Co-localization of D-Serine with NMDAR expression in most part of the brain along with the fact that degradation of D-Serine abolishes NMDAR neurotransmission in different brain regions, supported the notion that D-Serine is an important endogenous ligand for the NMDAR, participating broadly in synaptic events associated with development, plasticity, learning, memory and excitotoxicity.

4.1 Serine Racemase localization

SR distribution reflect the local abundance of D-Serine: in mammals, SR is most abundant in the forebrain regions. SR is highly expressed in hippocampus, amygdala, retina and various cortical regions.

As regarding the cellular distribution it is controversial, indeed first studies indicates SR was present predominantly in glial cells, with only marginal presence in neurons[38-42].

However, the exploitation of more specific and sensitive antibodies for *in vivo* recognition of SR [54] and of SR-KO mice [45] has significantly changed this view. Present findings indicate that SR is predominantly localized in the cytosol of neurons and only marginally in astrocytes. Thus, D-Serine might act with either autocrine or paracrine signals to NMDARs localized on neurons. A "shuttle" hypothesis has been recently proposed that involves the transfer of D-Serine produced within neurons to astrocytes and then, upon NMDAR stimulation, back in the synaptic space for full receptor activation. Consequently, neurons are suggested to be the primary source of D-Serine but astrocytes may act as the primary storage site[46]. As a result, the amount of available D-Serine for receptor binding is controlled at different stages, including partition of SR neuronal and astrocytes activity between L-Serine racemization and L- and D-Serine β-elimination, and neuronal and glial export and import systems.

4.2 Serine Racemase structure.

hSR belongs to serine /threonine dehydratase of the fold type II family of PLP-dependent enzymes.

SR structures shares from 35% to 91% homology, with highest values among mammalian and the lowest between yeast and mammalian. The residues involving the binding of PLP and other modulators such as ATP and cations are generally conserved[94].

At present there are 8 X-ray structures registered in PDB, all including a Mn^{2+} or Mg^{2+} cation in the metal binding site and PLP cofactor.

1. Human SR (hSR): 3L6B and 3L6R, both with malonate as ligand. 3L6R is selenomethionine hSR [95].

2. Rat SR (rSR): 3HMK and 3L6C, in the holo form and complexed with malonate, respectively[97].

3. *Schizosaccharomyces pombe* SR (SpSR): in the holo form (1V71) with 5'-adenylyl methylenediphosphate (AMP-PCP) (1WTC), modified with PDD (lysino-D-alanyl residue) in the holo form (2ZPU) and modified with PDD and complexed with serine (2ZR8)[96-97].

All the structures are dimers because, in solution, SR forms a dimeric structure with traces of tetramers. A homology model of hSR revealed that the dimers are stabilized mainly by hydrophobic interactions, without the participation of any disulfide bridge. Neither
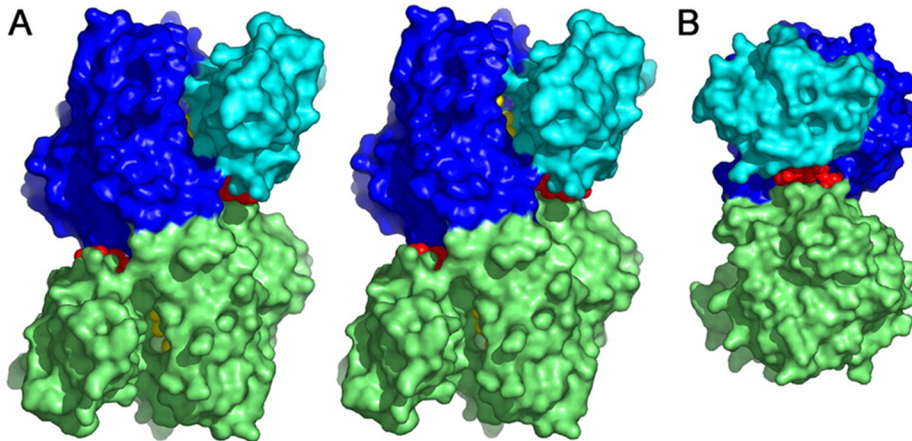
Figure4. Dimeric and monomeric structures of spSR.A, stereo view of the spSRw complex with AMP-PCP. Fig. **4A** The small and large domains of one subunit are shown in light and deep blue, respectively, and the other subunit is shown in green. A large deep groove is formed at the domain interface. The cofactor PLP shown by a space-filling model (yellow) is bound to the bottom of the groove. The groove extends to the subunit interface. AMP-PCP (red) is bound to the groove located at the boundary between the domain interface and the subunit interface on the right or left side of the molecule. N-ter, N terminus; C-ter, C terminus. **Fig. 4B**, side view of the molecule perpendicular to the two-fold axis. The image structure is turned 90° counterclockwise around the vertical axis relative to the image in Fig. 4A. The groove embracing AMP-PCP is further extended to the subunit interface formed at the back of the molecule. Binding of AMP-PCP induces the rotation of both subunits to widen the back groove. From Goto et al, JBC (2009), 248; 25944-25952.

ATP or cations influence the oligomer state, instead covalently cross-linked dimers were observed in the presence of active nitrogen and oxygen species[96-98-99].

The global SR structure shows a globular protein with two domains, typical of the fold type II enzymes. The large and the small domain exhibit an open α-β architecture and both contribute to the active site formation, which is localized at the interface between the two domains.

The large domain is made up of residues 1-68 and 157-340, organized in a twisted six stranded β-sheets, surrounded by ten α-

helices, and contains the PLP factor. Residues 78-155 form the small domain that is organized in four-stranded parallel β-sheets enclosed by three α-helices, two located on the domain interface and one on the solvent side. The linker between the two domain is formed by a flexible loop not fully resolved in human structure, made up by residues 69-77.

Baumgart *et al.* studied the flexible c- terminus on the yeast SR structure[96]. This four carboxy- terminal residues (SVSV in hSR) is believed to interact with glutamate receptor interacting protein (GRIP1), through its PDZ domain. The same motif is used by SR to interact with protein kinase C1 (PICK1). Some SR structures from plants, yeast and mammalian does not present this interaction sequence.

PLP cofactor, in the active site, is bound to a lysine or a lysinoalanil residue, that in human numbering is at position 56[99]. The other residues interacting with PLP are typical of the fold type II enzymes and are conserved among all the SR orthologs and in many other PLP-dependent enzymes. Specifically the PLP phosphate group interacts with the tetraglycine loop (Gly185-188), Met189 and three water molecules. Asn86, belonging to the asparagine loop, interacts with three hydroxyl groups forming a hydrogen bond, while Ser313 bonds to the pyridine nitrogen group[99]. Both Asn86 and Ser313 seems to play an essential role in regulating the electronic state of the PLP-base conjugate.
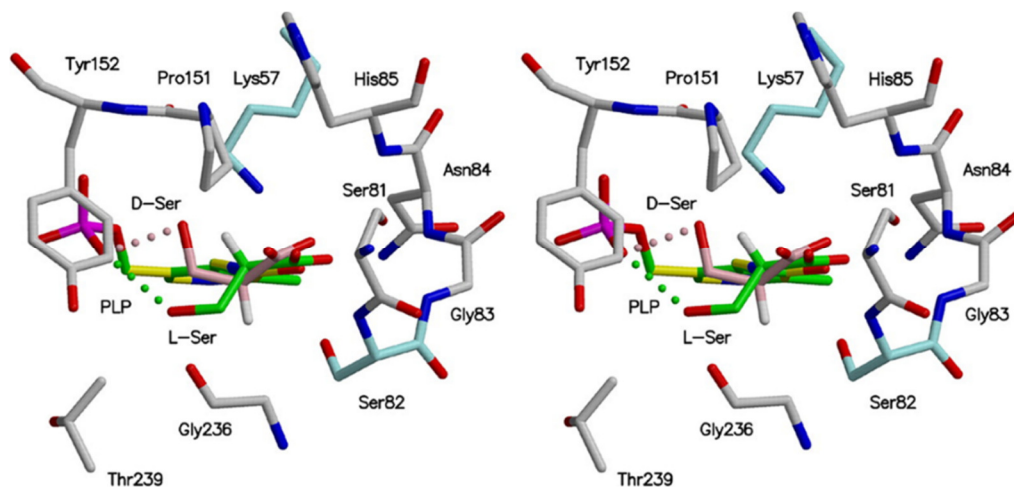
Figure 5. Superposition of external aldimine models between spSRw D-Serine and L-serine. The substrates, L-serine and D-Serine are shown in green and pink respectively. The catalytic bases Lys56 and Ser82 resides on the *si* and *re* face of PLP. From Goto et al, JBC (2009), 248; 25944-25952

Another important residue for SR catalytic action is Ser84, located in proximity of the *re*-face of PLP. This residue functions as one of the two proton shuttles, removing hydrogen from the substrate and adding hydrogen to the carbanion intermediate to produce D-Serine[98-100].The catalytic base that remove and adds hydrogens on the *si*-face of PLP is Lys56, which, also, is essential for PLP binding. Goto *et al.* have performed two studies to elucidate residues involved in racemization by generating a Ser82A and Lys56A mutants from yeast.

The mutation of Ser82 with an alanine residue, in *dictyostelium discoideum,* showed no racemase activity on L-Serine, a reduced dehydrase on D-Serine but maintains the elimination activity on L-Serine. This mutation essentially convert SR in L-Serine dehydrase, suggesting the catalytic mechanism may be stereoselective.

On the contrary the mutation of Lys56 to alanine results in an accumulation of PLP external aldimine, whit a lower formation of pyruvate, aminoacrilate and D-Serine.

Mammalian SR is activated by the presence of divalent cations[96]; experiments carried out with spSR have shown that, in presence of EDTA, the enzyme loses its catalytic activity, that it is restored upon the addition of Mg^{2+} or Ca^{2+}. All the PDB structures show that the metal molecule is octahedrally coordinated by two oxygen atoms of the terminal PLP, three structural water molecules and three conserved residues Glu210, Ala214 and Asp216. Random mutagenesis studies demonstrate that also Cys217 and Lys 221 are fundamental for metal binding as well as the enzymatic activity[101] . However, the divalent cation is located in the larger domain, close to PLP binding site, but outside to the active center, therefore it is not considered directly involved in the catalytic action, but in the stabilization of the protein folding.

ATP binding site

Mammalian SR is strongly activated by the presence of ATP, in spite of this, few studies around the ATP binding site were conducted and only one x-ray structure, from *Schizosaccharomyces pombe,* with an ATP analog has been detected[98].

Goto *et al.* showed that AMP-PCP (an ATP analog) bound to the groove formed at the intersection between the subunit and the domain interface, modifying the relative orientation between the two

subunits. Only the dimer is able to provide the necessary number of interaction to stabilize the complex.

The ATP binding site is surrounded by Ala115 and Tyr119, belonging to the small domain, and by Phe50, Asn51, Lys52, Met53, and Asn311, belonging to the large domain. Moreover several residues belonging to the large domain of the second subunit interacting with AMP-PCP structure.

The adenine ring of the nucleotide is sandwiched by Ala115 and the guanidine moiety of Arg275 of the second subunit. The O3' of the riboso moiety interacts with the side chain of Asn311, and the phosphate group interacts with Asn25, Phe50, Tyr119 and many water molecules.

Many of the residues are conserved in human and rat SRs, whereas only two residues are conserved in threonine dehydrase from *E.Coli*.

Recently, Jiraskova-Vanickova *et al.* reported a docking model of ATP with a coordinate molecule of Mg^{2+} into the hSR dimer, using the yeast complex as the template[102]. Two molecules of ATP are placed with the phosphate groups hidden inside the dimerization interface, while the adenosine moieties are pointed toward the solution. The key interactions are represented by an aromatic staking of Tyr121 with the adenosine portion, a charged-assisted hydrogen bond between Thr52, Gly53 and the phosphate group, and a magnesium ion coordinated with the side chain of Gln50. Other interactions include several charged-assisted hydrogen bonds. Overall, the Mg/ATP complex is stabilized by ten interactions, among which four are bifurcated with the phosphates.

Gln89, which participates in the formation of the active site of SR, might also be important in the stabilization of the ATP binding site by keeping in place Tyr121 and Thr52 residues.

In general, this study leads to the conclusion that ATP binding pocket in SR resembles that of other ATP sites, underlying that one monomer alone is not able to form the necessary interaction to maintain the ATP in place. When compared with the yeast protein crystallized in absence of AMP-PCP, the structure in the presence of the nucleotide does not reveal any significant change in the cofactor or side chains organization, but only a different relative orientation between the two subunits.

Moreover the O3' of PLP is linked to the ribose hydroxyl group of AMP-PCP by a network of hydrogen bond formed by Met53, Asn84, Gln87,Glu281, Asn311 and water molecules. This bond warren might play an essential role by tuning the active site of SR and activating the catalysis; in particular, the binding of ATP might affect the passage of the enzyme from an open to a close conformation after substrate binding.

Ligand induce open to close conformation

The co-crystallization of hSR with the inhibitor malonate has shown that the binding of a substrate induces a shift of the small domain carrying the overall structure of the enzyme in the so-called "close conformation". This shift is supported by a large flexibility of the

intradomain interface, which allows the small domain to assume different conformations.

The small domain undergoes to a rotation of 20 degrees towards the large domain with the effect of a reduced exposure of the surface to the solvent and a reorganization of the active site by placing the active residue Ser84 in the close proximity to the substrate, allowing the hydroxyl group to donate the proton required for isomerization[97].

The alignment of rat *holo* structure shows the H6 helix of the small domain is tilt of 4.5 Å compared to the human and rat structures in complex with malonate, and the active residue Ser84 is too distant (more than 5 Å) to be involved in the catalysis.

Is also evident from the close structure of the malonate bound to hSR that the access of L-serine to the active site is hampered by the tight cleft between the two domains, suggesting that SR undergoes to a closure of the small domain after substrate binding.

4.3 Reaction Mechanism.

PLP-dependent enzymes are broadly distributed among the organisms and are deputed to perform the majority of the reactions involved in amino acids metabolism.

SR, exploiting the electron withdrawal capacity of PLP, allows the conversion of L-Serine in D-Serine and *viceversa*.

Usually PLP enzymes catalyze more than one reaction on the substrate and the same enzyme can process more than one substrate. Accordingly, SR can catalyze the racemization of L-serine to D-Serine as well its β-eliminationto give pyruvate. If the racemization is highly specific towards Serine (L-Serine in particular) the dehydration reaction can be accomplished on a variety of amino acids and their derivatives.

On bacterial enzymes, the mechanism of racemization has been extensively studied; this is true in particular for Alanine Racemase, because of its importance as antibiotic target. However, the low expression rate of mammalian SR does not permit an comprehensive study about its mechanism, that was mainly deduced from data on bacterial enzymes and from structural information.

According to Yoshimura and Goto[98-103] SR mediated racemization proceeds through a two-bases mechanism.

The amino acid, either L or D-Serine, attacks the C4 of the Schiff base of the internal aldimine, formed by PLP co-factor and the

residue Lys56, with an unprotonated α-amino group, to form the external aldimine with the release of Lys56.

With regard to L-Serine, the free amino group of the residue Lys56 is in proximity of the hydrogen of the Cα atom of the external aldimine, allowing the side chain of Lys56 to extract the proton and form a quinoid or carbanionic planar intermediate. In this point the Ser82 (or 84, following human numeration) is on the *re*-face of this intermediate: such orientation enables the hydroxyl group of Ser82 to donate its hydrogen to the Cα atom of the intermediate, and therefore results in the formation of D-Serine. The subsequent attack of Lys56 on the PLP forms the Schiff base and thus releases D-Serine as the product.

Similarly, if the starting substrate is D-Serine, Ser82 is likely to be protonated, favoring the extraction of hydrogen from the Cα atom of PLP-D-Serine. The resulting planar intermediate allows Lys56 amino group to provide a proton from the *si*-face. As a result, Lys56 reacts with PLP to form the Schiff base and releases the L-Serine as the final product.

Normally, this kind of mechanism takes place in PLP-dependent enzyme should reduce the chance for competing reactions to take place, because the acid is pre-positioned to quickly reprotonate the intermediate.

Usually in fold-type I or IV enzymes, the pyridine nitrogen is protonated and the positive charge is stabilized by a conserved negatively charged residue. In fold-type II enzymes, as SR, a polar/neutral amino acid is always facing the pyridine nitrogen that

is consequently unprotonated. In SR, the involvement of the N-1 atom in a neutral hydrogen bond with Ser308 reduces the electron withdrawing effect of pyridine ring destabilizing the quinonoid intermediate forms during catalysis by SR. The reaction may proceed through the formation of a true carbanion with no delocalization of the negative charge to the pyridine ring[98]. However, for alanine racemase, it was suggested that formation of a rather unstable quinonoid intermediate helps in controlling reaction specificity by kinetically preventing the conformational changes needed for transamination. Further investigations are needed to establish if this applies also to SR, in view of the relative efficiency of the competing β-elimination reaction.

Elimination reaction proceeds with the protonation of the quinonoid intermediate on the β-hydroxy group that is subsequently eliminated as water to form the α-aminoacrylate[97-98], which, after the formation of the Schiff base between PLP and Lys56, is released and quickly degrades to yield pyruvate and ammonia. Protonation of the β-hydroxy group requires a strong acid. In the case of mammalian serine dehydratase the phosphate group of PLP acts as an acid. It was proposed that also for SpSR the phosphate group is in the most suitable orientation to donate a proton to the leaving β-hydroxy group[98].
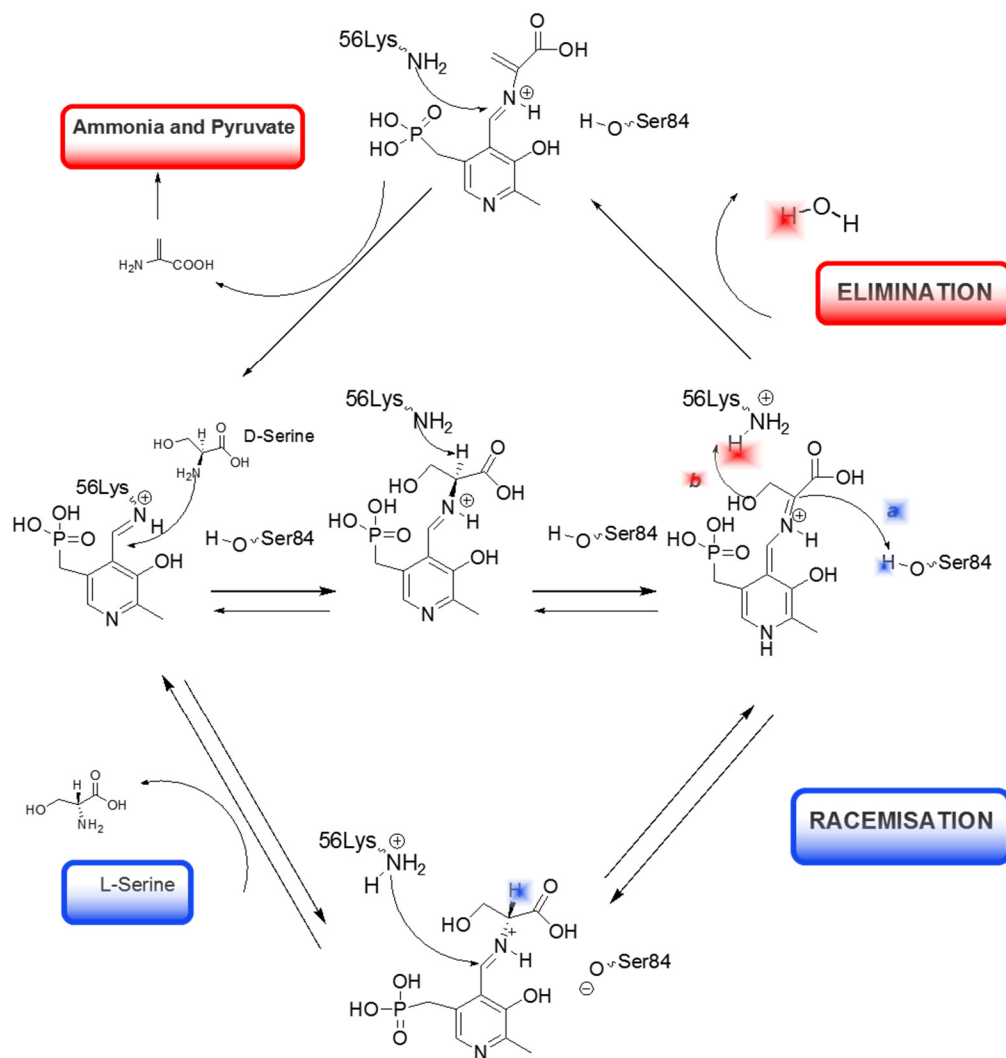
Fig 6. The racemase and dehydratese reaction mechanism of SR. The racemase can attack the L-serine with either Lys56 or Ser84. The Ser-84 hydrogen from the hydroxyl side-chain attacks the Cα from the opposite side to where the L-serine Cα-hydrogen was removed and racemization occurs resulting in D-Serine. Or the lysyl-NH3-group and the hydroxyl-group from Cβ of L-serine lose H and OH, respectively, to form water and follow the dehydratase reaction path. In the transition state a planar sp2-configuration of the L-serine Cα is created by removal of the Cα-hydrogen at which point the racemase can proceed with either reaction.

However, hSR seems to work with a slightly different mechanism: indeed mutation of Lys56 resulted in a complete loss of activity both for racemization, as well as for β-elimination. Ito and Goto[102] observed that DdSR Lys56A accumulates only the external aldimine without the formation of aminoacrilate, stressing the essentiality of Lys56 for its formation. To explain their evidence they supposed that β-elimination can occur through an E_2-type concerted mechanism without forming a distinct carbanionic or quinoid intermediate. One of the possible mechanism for the concerted reaction of α-hydrogen abstraction and hydroxyl group elimination is that the abstracted hydrogen is transferred to the hydroxyl group that is eliminated as water, a better leaving group.

The reaction of elimination is conserved through evolution, suggesting that it is involved in important biological roles. Specifically, under physiological conditions, β-elimination effectively degrades D-Serine, thus modulating the concentration of the neurotransmitter, especially in those areas of the brain where DAAO is missing. It is also plausible that pyruvate produced by dehydrase reaction could play a role in neuronal energy metabolism, similarly to the product of serine dehydratase. Nevertheless, it has been calculated that the rate of production of pyruvate by SR is less than 0.1 % of that displayed by glycolysis.

4.4 Serine Racemase regulation.

A major unanswered question in the field of D-Serine concerns the regulation of SR dynamics. Several regulatory mechanisms and protein interactions have been proposed to play a role in modulating SR activity and D-Serine release, but the *in vivo* relevance of the large majority of proposed mechanisms is not known. Enzymology studies of SR reveal that SR activity is modulated in many ways by various factors. SR activity is enhanced by PLP, magnesium, ATP, calcium, and D-Serine; inhibition of SR activity has been reported for NO, glycine, and membrane lipids like PIP2. Furthermore, SR activity is augmented by physical interactions with other proteins, such as glutamate-receptor-interacting protein (GRIP) and protein interacting with C kinase (PICK1).

ATP and divalent cations.

The first modulators of hSR to be discovered were ATP and divalent cations[104 -105]. ATP and Mg^{2+} act in synergy inducing an increase in the racemization reaction of fivefold. Moreover when Wolosher *et.al* identified for the first time SR, couldn't be able to detect the β-eliminase activity[106].Indeed, only in the presence of ATP and Mg^{2+} the dehydrase activity of the enzyme is detected with a ratio between pyruvate and D-Serine produced from L-serine of four. Subsequently, it was demonstrated that SR is activated also by other nucleotides than ATP, like ADP, GTP and, to a minor extent,

CTP and UTP, with nucleosides monophosphates being almost ineffective[106].

Ca^{2+} also activate SR [106-107], with an affinity similar to that of Mg^{2+}. Cook *et al*[107] have shown that calcium binds directly to recombinant SR and increases its activity. Fluorescence and circular dichroism techniques reveal that upon chelating of calcium by EDTA, SR undergoes to a conformational change. However, the physiological significance of a Ca^{2+}-dependent regulation of SR is debatable: indeed, the half-maximum stimulation of SR activity by calcium is 26 µM, which is at least two orders of magnitude higher than the residual concentration in the cell[107]. In addition, SR in resting cells is already fully saturated by Mg^{2+} and an increase in Ca^{2+} concentration induced by a stimulus would probably not result in a further activation of SR. *In vivo* experiments indicate that production of D-Serine is positively influenced by intracellular calcium concentration in astrocytes[64]. These data imply that SR could be regulated by calcium not through direct binding but through some calcium-dependent signal pathways.

For this reason, ATP and Mg^{2+} are believed to be the *in vivo* natural effectors of mammalian SR and bind to the enzyme as Mg-ATP complex.

In the presence of magnesium, ATP maximally activates SR at 10 µM, a concentration that is considerably lower than the endogenous ATP level (3-6mM) in most cells[107-108]. It is conceivable that SR might be saturated with ATP under physiological conditions. During stress, ATP depletion might change the activity of SR towards elimination by which SR catalyzes L-serine to pyruvate for providing

ATP. Perhaps SR switches between forming D-Serine and forming pyruvate depending on the energy status of the cell [54-106].

In the case of mammalian SR, ATP binding does not cause any effect on the aggregation state of the protein[110]. In addition, ATP is not hydrolysed during catalysis and, therefore, non-hydrolysable analogs are effective[106-107]. ATP and Mg^{2+} should thus exert their function as allosteric effectors of SR. In SpSR, the binding site of ATP was found to be connected to the active site by the conserved residue Gln89[98]. Mg-ATP binding might act causing a conformational change that is transmitted to the active site[104-109].

Nitrosylation

Nitrosylation is a very common mechanism to regulate protein activity. Some evidence shows that SR activity can be directly regulated by D-Serine and nitric oxide (NO) inversely[109]. SR activity is inhibited by nitric oxide (NO), probably through nitrosylation, and enhanced by D-Serine by denitrosylation. Further studies show that there might be an indirect way for NO and D-Serine to regulate SR activity[110]. D-Serine causes dose- and time-dependent inhibition of neuronal nitric oxide synthase (nNOS) which catalyzes the production of NO by using arginine as a substrate. So D-Serine actually decreases NO production to effect de-inhibition of SR activity.

In particular, the activation of SR by ATP binding seems to be modulated by cysteine nitrosylation. Indeed, Cys113, one of the

seven cysteine residues of hSR (Cys2, Cys6, Cys46, Cys113, Cys128, Cys217 and Cys309), was found to be nitrosylated by S-nitroso glutathione (GSNO)[111]. This post-translation modification leads to a decrease of SR activity with respect to controls and the SR mutant Cys113A that showed no change in activity upon exposure to GSNO.

Because of Cys113 is localized within the ATP binding site, its nitrosylation interferes with ATP binding and enhancement of SR activity, explaining the effect of Cys113 nitrosylation on SR activity.

It has been speculated that the reaction of NO with Cys113 represents a feedback regulation of NMDAR activity. Indeed, it is known that NMDAR activation stimulates neuronal NO-synthase. NO can react with both SR, causing a decrease in activity, and DAAO, with a subsequent activation. Both chemical modifications result in the decrease of D-Serine level, which, in turn, leads to a decrease of NMDAR-dependent neurotransmission[113]. It might also be hypothesized that glutathione, and not NO, reacts with Cys113[104], accounting for the observed effects on activity. Indeed, when a different NO donor is used, there was no formation of the thionitrosyl derivatives[109]. An attempt to explain this evidence might come from experiments using free NO and from a full characterization of the cysteine reactivity of hSR. Furthermore, it has been reported that reducing agents, such as dithiothreitol or reduced glutathione, [103-113] are essential for SR activity, [109] suggesting the detrimental effect of disulfide bond formation.

Phosphorylation.

In addition to small simple molecules, lipids can also regulate SR. Data from Snyder and colleagues shows that SR binds to phosphatidylinositol (4,5)-bisphosphate (PIP2), a kind of phospholipids present in cell membranes; this binding leads to a decrease of enzyme activity[112]. Selective mutation of amino acids identifies Lys96, Lys137, and Leu168 as the essential residues for binding to PIP2 and membrane association. Structural modeling of SR indicates that those amino acids are located in proximity of the ATP binding site. Occupation of the ATP binding site by PIP2 was demonstrated *in vitro* by competition experiments, where the effect of Mg-ATP on SR activity decreases in the presence of PIP2[114]. Therefore, the binding to PIP2 interferes with the ATP binding to the enzyme, causing inhibition of SR activity.

Stimulation of astrocytes by glutamate released in the synaptic space through the metabotropic glutamate receptors mGluR5, causes the activation of phopholipase C with a subsequent degradation of PIP2 and an increased SR activity, which is abolished by inhibiting phospholipase C[114]. Activation of SR increases the intracellular D-Serine concentration that is subsequently released into the synaptic space where it will bind to NMDAR activating the glutamatergic transmission.

Another report about SR interaction with cell membranes comes from Wolosker and colleagues[113]. Their data shows that, upon NMDAR activation, cytosolic SR is trans-located to the cell membrane, resulting in reduced D-Serine synthesis. Biochemical

analysis of this association indicates membrane binding is mediated by fatty acid acylation of SR, which occurs through the formation of an oxyester bond with serine or threonine residues. In addition, phosphorylation of Thr-227 is also required for steady-state binding of SR to the membrane under basal conditions. These findings are thought to be responsible for a fail-safe mechanism to prevent NMDAR overactivation through a negative feedback regulation of SR.

Interacting proteins

In addition to allosteric effectors and post-translational modifications, SR function is regulated *in vivo* by changes in subcellular localization and interactions with specific proteins. The C-terminus motif, located near ATP binding site, is important in terms of SR regulation, because mediates the interaction with protein partners such as GRIP and PICK1.

Since the published crystal structures do not contain the last 11 C-terminal residues, several interactions have been discovered using yeast two-hybrid screening. Kim *et al* [114] showed that rat or mouse SR interacts with the protein Glutamate Receptor Interacting Protein 1 (GRIP1). GRIP1 is a large synaptic protein that interacts with AMPAR and contains several PDZ domains. One of these, PDZ6, was found to bind to the C-terminal region of SR[110].

Released glutamate stimulates AMPARs on closely adjacent astrocytes, causing GRIP to dissociate from AMPARs and to bind to

SR, enhancing the formation and release of D-Serine. This process is involved in granule cell migration during cerebellum development. The activation of SR by GRIP is also confirmed by Baumgart *et al.* that demonstrated that full-length GRIP activates SR by modulating the enzyme's conformation[110].

SR was also found to bind to Protein Interacting with C-Kinase (PICK1), again by the C-terminus domain[115]. PICK1 is another PDZ domain-containing scaffold that binds a large number of protein structures, including AMPARs. PICK1 knockout mice showed decreased concentrations of D-Serine in the brain, suggesting that PICK1 may be involved in the regulation of SR function in a spatially and temporally specific manner[116]. However, the mechanism by which this effect takes place is unclear, since PICK1 does not directly activate SR and the level of SR protein is unchanged in the PICK1-deficient animals[118]. Fujii and colleagues have proposed that PICK1 might act driving protein kinase C (PKC) to its target, leading to phosphorylation of SR.

Dumin *et al.* identified the third SR binding partner with a yeast two-hybrid assay in astrocytes. They found out that Golgin subfamily A member 3 (Golga3) protein interacts with SR and significantly increases SR half-life by decreasing ubiquitylation of SR, which prevents its degradation by the ubiquitin-proteasome system[117]. Golga3 is present on the cytosolic surface of the Golgi apparatus, which plays an important role in transduction of some apoptotic signals and membrane trafficking. It is possible that Golga3 mediates SR binding to the Golgi membrane, and the membrane-

bound SR could play a role in the vesicular storage or release of D-Serine.

A further interaction of SR has been found with Disrupted-In-Schizophrenia-1 (DISC1), one of the few proteins whose mutations have been linked to the genetic of schizophrenia. A recent work by Ma *et al.* [118] has shown that the scaffold protein DISC1 binds to and stabilizes SR. Mutant DISC1 truncated at its C-terminus failed to bind to SR, facilitating ubiquitination and degradation of SR, with a consequent decrease in D-Serine production. These results suggest a very direct pathway by which DISC1 can modulate the production of D-Serine and NMDAR neurotransmission, relevant to the pathophysiology of schizophrenia and other neuropsychiatric disorders.

Effector/post translational modification	Reaction	Effect
Mg/ATP	α-elimination	k_{cat}/K_M (↑4x)
	α-elimination (D-Ser)	k_{cat}/K_M (↑13x)
	Racemization (L-Ser)	k_{cat}/K_M (↑2x)
	Racemization (D-Ser)	k_{cat}/K_M (↑7x)
S-nitrosylation of Cys113	Racemization (L-Ser)	Specific activity (↓2x), V_{max} (↓)
Ca⁺⁺	Racemization (L-Ser)	Specific activity (↑< 2x)
PIP2	Racemization (L-Ser)	V_{max} (↓)
Phosphorylation	Racemization (L-Ser)	Specific activity (↑2x)
GRIP1		D-Serine release from cells (↑)
	Racemization	↑ (+ 65%)
PICK1		D-Serine release from cells (↑)

Table 1. Effect of effectors and post-translational modifications on SR activity.

4.5 Serine Racemase inhibitors.

SR is a potential target for the treatment of several neurological diseases such as stroke, AD, amyotrophic lateral sclerosis and PD, where NMDAR deregulation and D-Serine overproduction play a crucial role.

However, in spite of the relevance of SR, the development of potent inhibitors or effectors is surprising limited. This might depend on the low stability and yield of the purified enzyme that make inhibition studies problematic. Furthermore, the source of the enzyme and the reaction condition, in particular the presence or absence of ATP, DTT and divalent cations, influence the outcome of the assay and the results of experiments carried out under different conditions can be conflicting.

In order to generate specific inhibitors, the structural features of SR active site and the known reactivity of PLP cofactor have been exploited.

To date, SR inhibitors have been developed to reduce the excitotoxic effects of high levels of D-Serine. In particular, these compounds aimed at reducing SR activity, thus decreasing D-Serine concentration. SR effectors discovered so far can be classified, based on their mechanism of action, in compounds that target PLP, and those that target the active site of the enzyme.

PLP- targeting inhibitors

All the proteinogenic amino acids and a number of non-proteinogenic ones, have been tested. Non proteinogenic amino acids failed to show any activity, while for proteinogenic amino acids the outcome depends on the SR reaction mixture.

Panizzuti *et al.*[119] provided the most complete screening of AA's, testing also the D-forms of AAs without significant affinity. They observed inhibition from L-Cysteine, which was confirmed also by Cook,[120] who discovered that L-Cysteine can reduce the racemase activity at 2 mM concentration.

However, Dunlop and Strisovsky did not confirm this data; they tested independently several amino acids and discovered that Glycine is a competitive inhibitor with a K$_i$ from 0.15 to 1.64 mM.

The concentration of Glycine in cells is around 0.5-0.7 mM, consistent with its K$_i$ values, suggesting that the inhibition of SR by glycine is physiologically relevant.

A comprehensive analysis of compounds derived from Serine results in loss of activity for any modification on Serine skeleton, except for L-Serine-O-sulfate (L-SOS).

L-SOS behaves as a substrate of SR, able to shift the racemase activity of the enzyme toward the eliminase activity [121] with a K$_i$ of ~2 mM.

The replacement of O-Sulfate group by structural analogs led to the identification of the most active SR competitive inhibitor, (2S,3R) L-

erythro 3-hydroxyaspartate (L-EHA), with a K_i of 43 µM for murine enzyme and 11 µM for human.

On the other hand, the isomer L-*threo*-3-hydroxyaspartate (2*S*,3*S*) acts as a substrate of SR, by which is degraded to oxaloacetate and ammonia. This peculiarity is probably due the fact that SR is a close relative of bacterial L-*threo* 3-hydroxyaspartate dehydratases. [121-104].

To elucidate the binding of L-EHA, Jiraskova-vanikova performed a docking studies using the hSR crystal structure, showing how all the functional groups of the inhibitor are involved in 8 hydrogen bonding within the SR active site. In particular, one carboxylic group of L-EHA interacts with the backbone nitrogen of Ser84 and His87, the other with Arg135, Asn154 and Ser242, while the hydroxyl moiety interacts with the side chain of Gly239.

L-*threo*-3-hydroxyaspartate is also bound to the active site, but with longer H-bonds than the *erythro* isomer, and with a different orientation. Indeed, it lacks the interaction with Asn154 and shares an additional H-bond with the phosphate group of PLP.

With the aim of identifying new inhibitors acting with a different mechanism of action, the same group tested a small family of hydroxamic acid derivatives.

The most effective products were found to be succinodihydroxamic acid and L-aspartic acid β-hydroxamate. The K_i value calculated for succinodihydroxamic acid was ~3 µM, resulting the most potent SR inhibitor identified so far, whereas L-aspartic acid β-hydroxamate exhibited a K_i of ~100 µM. A clear disadvantage of hydroxamic acid

derivatives as SR inhibitors and potential drugs more in general, is their lack of specificity, as they react with a broad range of PLP-dependent enzymes[121].

Active-site targeting compounds.

This approach aims at identifying compounds that do not react specifically with PLP, but rather exploit their tight functional group and structural complementarity with the active site.

Strisovky mapped the influence of several dicarboxylic acids differing for the chain length and the conformation. Malonate was found to be the strongest binder with a K$_i$ of 33 µM for hSR and 71µM for mSR[101].
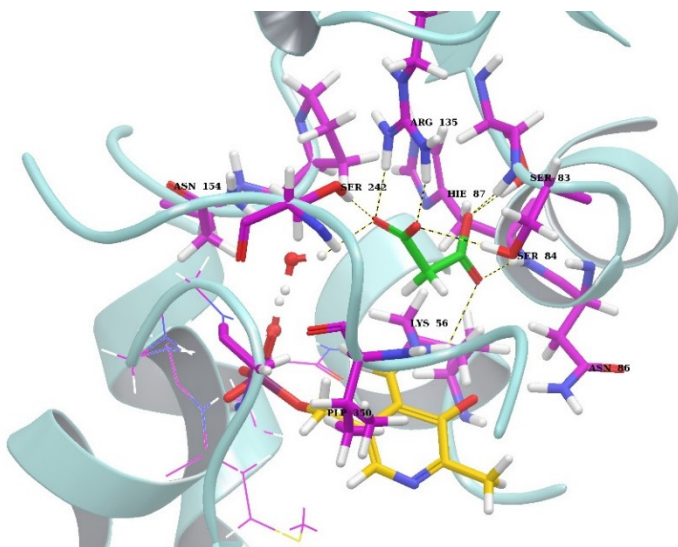
Figure 8. Malonate interaction in hSR (PDB 3B6L). Keys interactions of malonate (green) with Ser84, Lys56, Arg135 and Ser242.

Malonate is a dicarboxylic acid that is orthosteric with L-Serine. Its ability to interact with SR is probably due to the small dimension and the carboxylate groups that make strong ionic bonds with active site residues. One carboxylate

of malonate interacts with the nitrogen backbone of Ser84, Asn86 and His87, with the side chain of Ser83 and with one water molecule, while the other forms salt bridge type ionic interactions with Arg135, and also makes interactions with Ser84, Ser242, Lys56 and two molecules of water. Interestingly, Arg135, which seems to be fundamental for the stabilization of the enzyme-inhibitor complex, is not conserved in other PLP-dependent enzymes belonging to the fold-type II family[98]. A series of malonate derivatives were synthesized and tested [104]. No significant improvement with respect to the parent molecule was observed.

Dixon *et al.* identified several moderate peptide inhibitors, the most potent compound having a K*i* of 320 µM. All the active compound are bulky tripeptides containing either histidine or phenylpropionic moieties, lacking any sort of similarity to the substrate. Although the authors claim that these compounds are active site inhibitors, their steric hindrance suggest that they could compete on the ATP binding site[122].

To date, there has not been any attempt to develop compounds that can act as allosteric modulators on the ATP or the metal binding site.
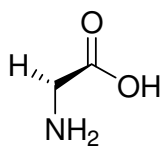
Glycine
K$_i$ 360 μM
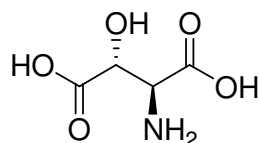
L-EHA
K$_i$ 11 μM
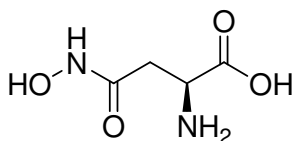
L-aspartic acid
β–hydroxammate
K$_i$ 10 μM
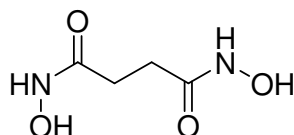
Succinodi-Hydroxammic
acid
K$_i$ 3 μM
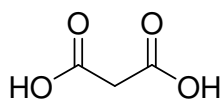
Malonate
K$_i$ 33 μM
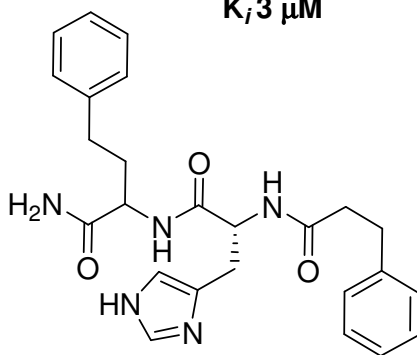
Positive hit
by Dixon et al.
K$_i$ 3 μM

Figure 9: overview of competitive SR inhibitors with Ki values referred to hSR.

5. <u>AIM OF THE WORK.</u>

SR activity in the brain serves as the only endogenous mechanism to generate D-Serine, which is a co-agonist of the NMDAR. Inhibition of SR could be a means to regulate D-Serine levels and to limit the NMDAR mediated neurotoxicity in Alzheimer's disease, amyotrophic lateral sclerosis, Parkinson's disease, and to protect against cerebral ischemia. A number of SR inhibitors have been developed, including dicarboxylic acids, small peptides, and hydroxamic acids; however the development of potent and selective inhibitors still remains a challenge due to the difficulty in enzyme expression and purification, and the poorly understood mechanism of SR catalytic activity and regulation.

The aim of this work is to identify new compounds that can interact with SR with satisfactory potency and selectivity.

The disclosure of hSR x-ray structure in presence of malonate has confirmed that the domains of SR are connected by a flexible linker and can adopt different conformations with respect to each other. Moreover, the ligand-induced rearrangement of the small domain, organizes the active site for the turnover of the substrate. Indeed, the open and the close SR structure represents the starting point for rational drug design and hold promise for the synthesis of novel molecules that could modulate the enzyme activity, possibly by blocking the movement of the small domain.

5.1 Analysis of Serine Racemase conformational flexibility[123].

Mammalian SR adopts the expected fold of β-family PLP-dependent enzymes, showing a large domain and a small, flexible domain that rearranges upon the binding of the substrate to shape the active site, thus allowing L-Serine processing.

Smith *et al.*[97] demonstrated that the orthosteric inhibitor malonate binds to the active site promoting the conformational changes towards a closed conformation and eventually hindering the entry of the substrate. Moreover, they speculated that individual ligands could recognize different enzyme conformations.

Since SR undergoes to large conformational changes during ligand recognition, the limited number of individual enzyme conformations captured by X-ray crystallography are not sufficient to delineate all the features needed for a proper interaction with the substrate or the inhibitors, nor represent the actual conformational space explored by the protein. This is particularly important for structure-based drug design, because the choice of a specific enzyme conformation may warp a subset of features or limit the ligand size, with the result of neglecting other potentially relevant information.

In order to overcome this problem, Bruno *et al.*[125] conducted a target molecular dynamic (TMD) study with the aim of simulating the transition between the open and the closed conformation of SR in the presence of either the natural substrate L-Serine or the orthosteric inhibitor malonate.

The aim of the study was to highlight the molecular mechanism of the enzyme closure by identifying key residues responsible for the conformational movements. Moreover, using the targeted trajectories between the open and the closed conformations of SR, it could be possible to sample, through clustering analysis, the most relevant enzyme conformations to be used for docking/virtual screening purposes.

To set up the study, the x-ray structure of malonate bound to hSR (PDB code 3L6B) and the holo enzyme of the rat (PDB code 3HMK) were selected as representative of a full close and a full open conformation, respectively.

The sequence identity between the two orthologs is more than 90%, and rSR was "humanized" by manual point mutation on the different residues.

The starting structure of the malonate-bound to open SR was prepared by superimposing the large domain of both open and close conformation and by pasting the coordinates of malonate from the close to the open conformation. With this method malonate maintains the H bonds with Ser242 and Ser83 (Ser81 in rat) in the open conformation, but misses the interaction with Arg135, which is located in the small domain.

Similarly, L-Serine was positioned in the active site of the open conformation by superimposing the carboxylic group of α–amino acidic moiety to one of the carboxylic groups of the malonate. Therefore, the carboxylic group of L-Serine forms a hydrogen-bound to Ser83, while the amino group faces the phosphate of PLP and the

internal aldimine moiety, ready for the subsequent covalent attack to form the Schiff base.

The structure preparation required also the assignment of the ionization state of the PLP cofactor. In agreement with the literature data[98], all the simulation experiments were performed by using PLP with the 3-hydroxy group in the ionized form, the immino nitrogen positively charged, and the pyridine nitrogen in its neutral form.

During the TMD simulation of the two complexes (SR-L-Serine and malonate), it appeared that the malonate-bound complex closed faster and required lower energy respect to L-Serine complex. Besides, SR, when in complex with L-Serine, reopens faster than with malonate. This supports the hypothesis that malonate inhibits SR by stabilizing the closed form[97]. However, even if L-Serine requires a closed conformation to be properly processed by the enzyme, its stabilization is given by the formation of the covalent Schiff's base with PLP. This simulations are unable to model the chemical steps leading to the Schiff's base formation, and it is not surprising that L-Serine is less effective than malonate to stabilize the closed conformation under the above described simulation conditions.

Through TMD simulations, it was possible to identify subsets of previously unreported residues, whose interactions may contribute to the conformational transition; namely, the ionic lock formed by Lys77 and Glu147, and the essential role played by Ser242 and His82. It can be speculated that the interaction between the inhibitor and some suitable residues in the active cleft (Ser242, in particular), triggers the conformational transition along the hinge region domain

(HR), where the formation of a salt bridge between Glu147 and Lys77 plays an active role. As a result, the small domain moves toward the large domain, thus bringing together residues such as Arg135 and His82, which in turns lead to the correct orientation of Ser84, critical for the catalysis. The salt bridge between Lys77 (located at the C-terminus of HR) and Glu147 (located at the C-terminus of the helix 6) is maintained during the entire simulation and can be considered as an unprecedented ionic lock, potentially involved in the long distance transmission of movements between individual SR domains. Moreover, a correlated motion between Ser84 and Arg135 was identified. From the analysis of the crystal structure, Arg135 is involved in malonate binding. An inspection of SR behavior during the TMD simulations revealed that Arg135 and Ser84 are distant in space, and His82 mediates their concerted motion.

The conformations generated by the dynamics were then clustered. Six representative structures, covering the whole transition from the open to the closed malonate-complexed forms, were selected and used for docking a small library of known SR inhibitors and closely related inactive analogs. Better results were achieved when docking was applied to the TMD generated conformations rather than to the individual crystallographic structures, indicating the relevance of including protein flexibility in computational simulations.

5.2 Design of Serine Racemase inhibitors.

From the TMD simulations, it seems that the passage between the open and close conformation of SR is a dynamic process not characterized by discreet states. This evidence enormously complicates any attempt of rationally projecting drugs based on docking studies.

As such, our attempts to synthesize novel inhibitors of SR has followed approaches other than the Structure-Based Drug Design. Moreover, to make a more comprehensive study, competitive and non-competitive inhibitors were projected and synthesized, as described herein:

- For the synthesis of competitive inhibitors, the design relied on the structure of malonate (Fig.8), which has demonstrated to possess a moderate activity. In particular, two approaches were followed:
    - constrain of the structure, to favour a stronger interaction at the target binding site;
    - modification of the malonate core, in order to define which substituents could be tolerated;
- For the synthesis of covalent non-competitive inhibitors, the structure of highly reactive amino acids, properly modified, was explored.

6. DESIGN AND SYNTHESIS OF POTENTIAL COMPETITIVE INHIBITORS.

Malonate was chosen as the reference compound to be suitably modified in order to identify molecules with a satisfactory inhibitory activity. We have reasoned that the structure of the molecule was amenable to a various range of modifications, leading to a refined structure-activity relationship study. Moreover, malonate showed good physicochemical parameters such as solubility and lipophilicity, along with good overall predicted drug-likeness.

It was hypothesized that a cyclopropane-1,2-dicarboxylic acid might have mimicked the conformation of malonate, in particular with respect to the two carboxylic moieties. Indeed, as reported in figure 10, the superimposition of malonate (blue) and cyclopropane-1,2-carboxylic acid (green), shows how the carboxylic moieties maintain the same pose. Moreover, maleic acid, also reported as a moderate inhibitor of SR, shows the same pattern of superimposition with both maleate and cyclopropane-1,2-dicarboxylic acid,(fig.10, yellow), further confirming the likeness of our hypothesis.
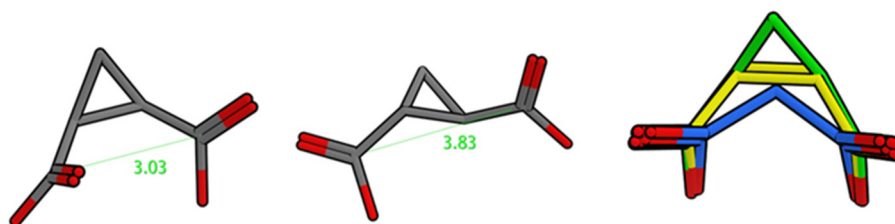
Figure 10. Representative distances between the carboxylic group of *cis* and *trans* cyclopropane-1,2-dicarboxylic acid , and superimposition between the malonate (blue), the maleate (yellow) and the cyclopropane nucleus (green).

Therefore, we prepared a small library of compounds enclosing the malonate structure in the rigid conformation of a cyclopropane, considering that the more rigid structure could have led to a stronger interaction at the target-binding site, as reported previously.

6.1 Design and Synthesis of substituted cyclopropanes.

The investigation started with the synthesis of a series of cyclopropane-1,2-dicarboxylic acids and monoesters both in *cis* and *trans* conformation, in order to identified which isomer was better

R=H, Et, *i*Pr, *i*Bu, *p*CF$_3$Ph

Figure 11. Dicarboxyl cyclopropane derivatives
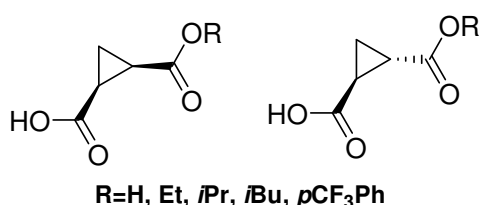
tolerated; then, we wanted to check if it was possible to introduce a steric hindrance and less polar substituents.

The synthesis of *cis*-cyclopropane derivatives started from commercially available 3-oxabicyclo[3.1.0]hexane-2,4-dione, which was hydrolyzed with various solvents, affording the desired compounds in good overall yields.

1 R = H   **2** R = Et
3 R = iPr   **4** R = iBu
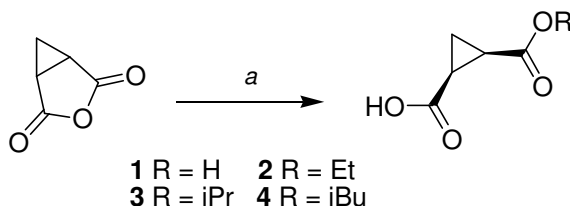
Scheme 1. reagents and conditions *a)* for **1**, H$_2$O, 2h at reflux; for **2**, EtOH, 2h at reflux; for **3**, *i*PrOH, 2h at reflux; for **4**, *i*BuOH, 2h at reflux

The synthesis of (±)*cis*-2-[(4-methylphenoxy)carbonyl]cyclopropanecarboxylic acid (scheme 2) started from compound **1,** which was condensed with 4-

(trifluoromethyl)phenol using DCC as coupling agent, and a catalytic amount of DMAP.
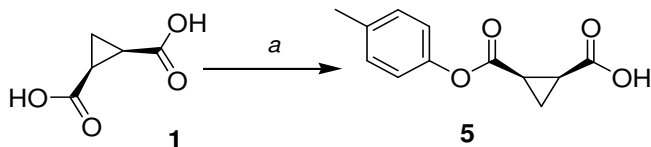
Scheme 2. reagents and conditions *a) p*CF₃Phenol, DCC, DMAP, DCM, 0 C° to RT, 12h.

To obtain the *trans* derivatives, diethyl (1*R*,2*R*)-cyclopropane-1,2-dicarboxylate was hydrolyzed in the presence of a stoichiometric amount of potassium hydroxide (Scheme 3) .

6 R = H   **7** R = Et
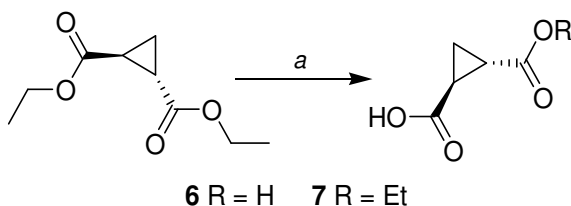
Scheme 3. reagents and conditions *a)* for **6**, H₂O, 2h at reflux; for **2**, EtOH, 2h at reflux; for **3**, *i*PrOH, 2h at reflux; for **4**, *i*BuOH, 2h at reflux.

The encouraging activity of **1** (see discussion below) prompted us to further explore this scaffold, synthetizing different 1',2'-disubstitued-1,2-dicarboxylic acid cyclopropanes in order to verify if bulkier
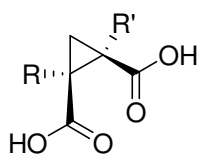
8 R = H, R' = Me
9 R = Me, R' = Me
10 R = H, R' = Et
11 R = H, R' = Ph
12 R = Me, R' = Ph
13 R = H, R' = Bn

Figure 12. (1',2')-1,2-dicarboxylic acid cyclopropanes derivatives

substituents could be tolerated and/or could enhance the activity. The compounds synthesized are reported in the figure 12.

For the synthesis of **8-13**, the key intermediate 1,2-diethyl-1,2-cyclopropanedicarboxylate was prepared by the reported McCoy procedure, [124-125] starting from the corresponding acrylates and α-halo esters, giving a ready access to the *cis*-cyclopropanedicarboxylic esters.

Of note, in the cyclopropanation reaction, solvent plays a key role in the *cis/trans* ratio, and the use of toluene was found to be essential to obtain the desired *cis* conformation of the dicarboxylic moieties.

**8a, 9a,
10a,11a,12a,13a**

**8,9,
10,11,12,13.**
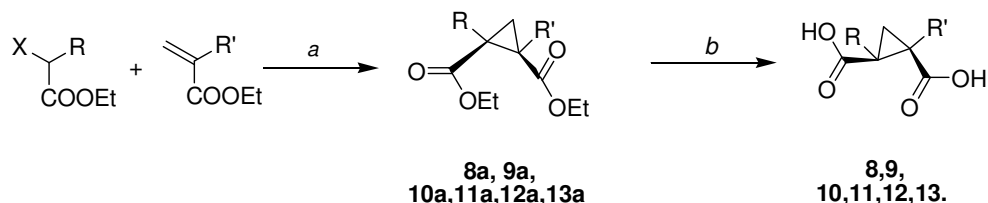
Scheme 4. reagents and conditions *a)* NaH, toluene, 0°C to RT, 48-72 h. *b)* KOH, THF/water (1:2) from 0°C to 50°C 4 days. Yield 30%-60%.

The suitable substituted acrylate and ethyl 2-halocarboxylate were reacted in toluene in the presence of stoichiometric amount of NaH. Reaction proceeds slow with yield from moderate to good. The subsequent hydrolysis in basic aqueous media afforded the title compounds.

Moreover, to determine whether the presence of the two carboxylic groups was essential, we submitted to biological tests also compounds with monoacidic functionalities such as cynnamic acid, that is known to be active[104], and its derivative (1*R*,2*R*)-2-phenylcyclopropanecarboxylic acid.

14   **15**
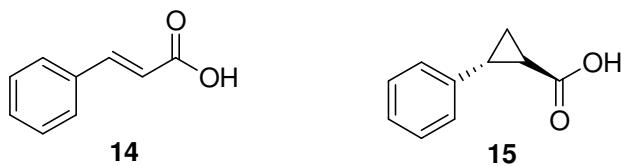
Figure 13. Cynnamic acid and (1R,2R)-2-phenylcyclopropanecarboxylic acid.

6.2 Design and Synthesis of malonate derivatives.

Along with the synthesis of constrained structure, we deemed relevant to investigate a small set of α-substituted malonates and also some bioisosteres. The aim of this investigation was to refine the structure activity relationship for malonate derivatives, as yet undetermined, and to control if such a small structure could be elaborated to yield a better inhibitor.
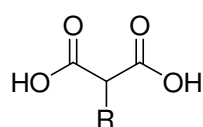
16 R = Me
17 R = OH
18 R = C=O
19 R = Bn
20 R = Phenyl-Ethyl
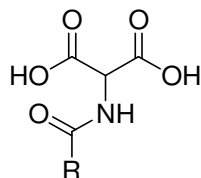
21 R = Me
22 R = Ph-pCF$_3$

Figure 14. Malonate derivatives

First, we wanted to evaluate the presence of small polar and apolar groups in the α-position, then bulkier groups and groups with different electrochemical characteristics were used as substituents.

To perform the synthesis of malonate analogues **19** and **20**, we started from the diethyl malonate that was reacted with (2-bromoethyl)benzene or (bromomethyl)benzene, in presence of

16a,17a,18a,19a, 20a   **16,17,18,19, 20**
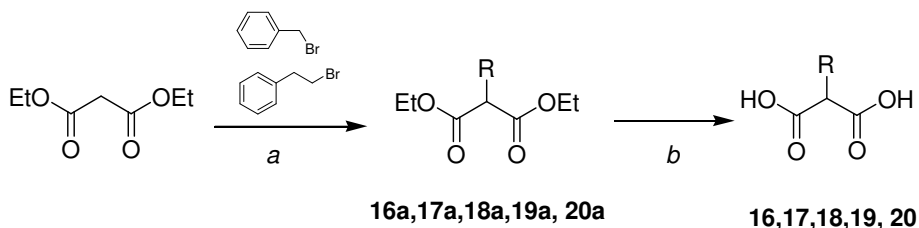
Scheme 5. Reagents and conditions *a)* NaH, THF, from 0°C to RT 12h. *b)* NaOH 1N, RT 12h.

NaH. The diethyl esters derivatives **19a**, **20a**, were then hydrolyzed by NaOH in water to afford the desired compounds.

Compound **18** was obtained from the commercially available diethyl

18
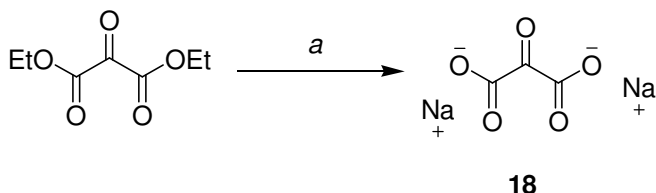
Scheme 6: Reagents and conditions *a)* NaOH stoichiometric, THF/H$_2$O (2:1), RT 12h.

oxopropanedioate through hydrolys in THF/Water in the presence of NaOH. Due to poor solubility of the dicarboxylic acid derivative the biological assay was carried out on the disodium salt.

The introduction of the amidic moiety on the malonate scaffold (**21** and **22**) was obtained through the coupling between 2-amino malonate and the suitable acyl chloride, in the presence of an organic base a room temperature. The following hydrolysis in aqueous solution of NaOH 1N gave the titled compound.

21a, 22a   **21, 22**
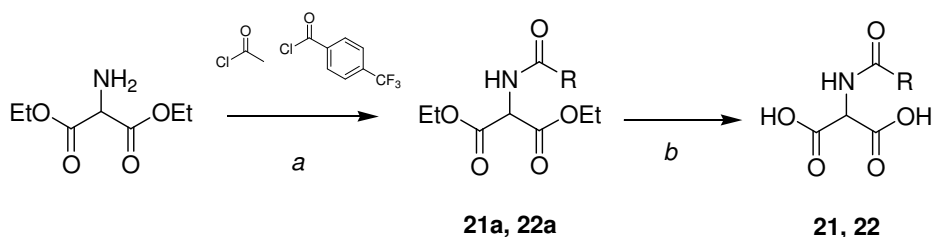
Scheme 7. Reagents and conditions. *a)* TEA, MeCN, RT 12h. *b)* NaOH1N, RT 12h.

Compounds **16**-**17**, as well as the carboxylic bioisosters **23** and **24**, were commercially available.
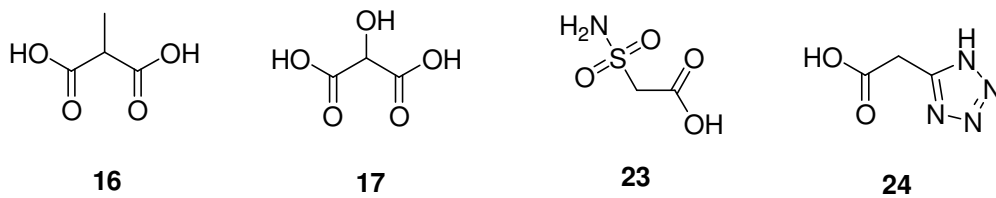
Figure 14. Structure of 2-methyl and 2-hydroxyl malonic acid (**16** and **17**), 2-sulfamoylacetic acid (**23**) and 2-(1H-tetrazol-5-yl)acetic acid (**25**).

7. DESIGN AND SYNTHESIS OF VINYL GLYCINE ANALOGUES AS POTENTIAL COVALENT-INHIBITOR.

Along with the synthesis of competitive inhibitors, aim of this work was also to prepare covalent inhibitors of hSR. Therefore, the synthesis of small amino acidic molecules, which could interact with the PLP co-factor, was planned and performed.

We reasoned that the synthesis of α-vinyl amino acids, in which the α-proton is replaced by a vinyl group, might have led to the uncompetitive inhibition of SR. The parent and simpler member of this family, α-vinylglycine, is a natural product known to act as a suicide substrate for a number of PLP-dependent enzymes (fig 15).[126]
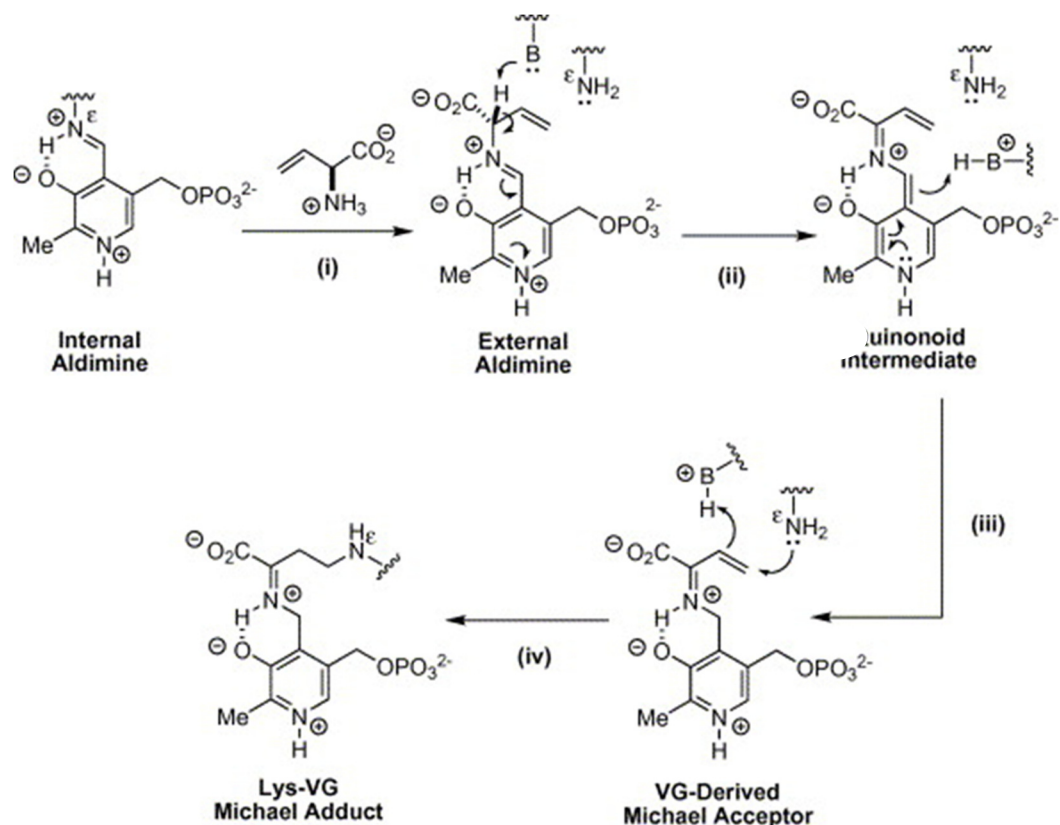
Figure 15. Proposal mechanism of vinyl glycine. The amino group of vinyl glycine forms the external aldimine with PLP, which is deprotonated at the α-carbon to form of quinoid intermediate. In the following step, the protonation of the intermediate result in a Michael acceptor that react with basic residues, present in the binding site to give the Michael adduct with the subsequent inactivation of the catalytic circle of PLP.

Moreover, the anti-epileptic drug vigabatrin (γ-vinyl-GABA) is an irreversible suicide inhibitor of gamma-aminobutyric acid transaminase (GABA-T)[127]. Introduction of a fluorine atom on the vinylic moieties of glycine may lead to a likely more electrophilic Michael acceptor, as it has already been reported for γ-(2'-fluoro)-γ-vinyl-GABA[128]. Interestingly, in that case, the (*Z*)- and (*E*)-(2'-fluoro)vinyl triggers different profiles of action, highlighting the importance of accessing single geometric isomers.

With the intent to trap the PLP cofactor of SR we decided to synthetize fluorine vinyl glycine analogs represented in figure 15.
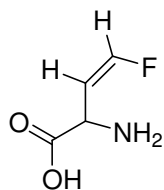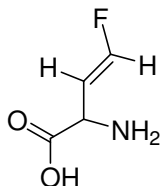
Figure 15. Structures of vinyl glycine derivatives (Z) **25** and (E) **26** 2-amino-4-fluorobut-3-enoic acid

25   **26**

The synthesis of compounds **25** and **26** was performed through the fluoro methylenation route reported by McCarthy in which the Garner aldehyde was condensed with α-fluoro-α-(phenylsulfonyl)methylphosphonate in a Wittig-type reaction, to obtain a Z/E mixture of α-(2'-fluoro)vinylglycinol isomers[129](figure

McCarthy's Reagent
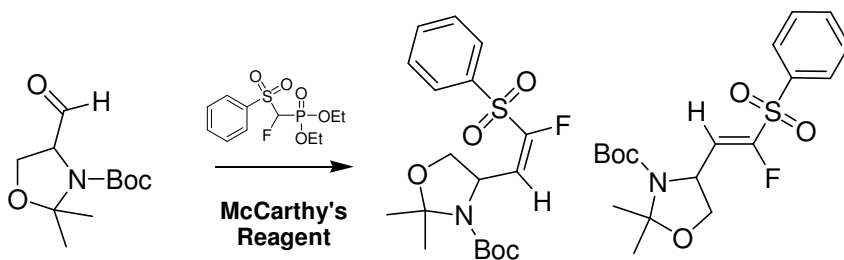
Figure 16. Floromethylenation route by McCarthy

16).

For the synthesis of compound **25** and **26**, racemic Serine was first protected on the amino and the carboxylic group, and then at the remaining OH an NH functionalities. Thus the distillation of a mixture of 2,2-dimethoxypropane in the presence of a catalytic amount of *para*-toluensulfonic acid in benzene resulted in the formation of the

oxazolydine. The following treatment with DIBALH led to the Garner aldehyde.

The Garner aldehyde was then processed with the anion of the Emmons Wittig reagent, generated *in situ* from fluoro methylphenyl sulfone, diethyl chlorophosphate and two equivalents of lithium hexamethyldisilizane, providing the fluoro-vinyl sulfones in 92% yield.

These fluoro-vinyl sulfones were then converted in fluoro-vinyl stannane in good to excellent yield, by treatment of **31** with tributyl tin hydride and AIBN in ciclohexane. At this point, it was possible to separate the Z and E isomers by flash chromatography, and the two syntheses proceeded in a parallel way.

Cleavage of the tributyl stannane was accomplished by sodium methoxide in refluxing methanol without epimerization of the isomer.

The isopropilydene group was then removed with *para*-toluensolfonic acid in methanol, to give 36 and 38 as a white solid and colourless oil, respectively. Oxidization of the alcohol to the carboxylic acid was accomplished with PCC in acetic acid at room temperature, and the Boc protection was removed with HCl in ethyl acetate.
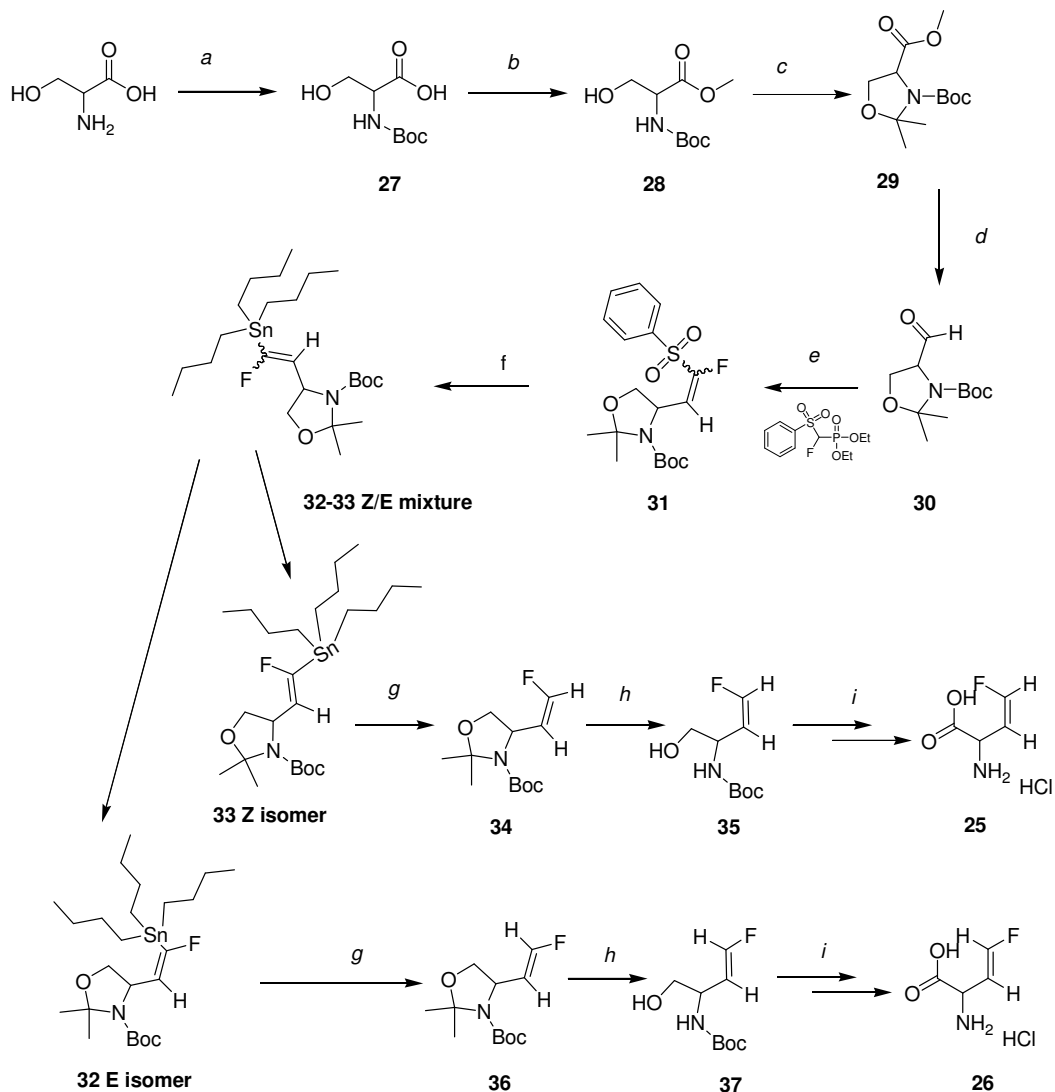
SCHEME 8. Reagents and conditions. *a)* Boc₂O, 1N NaOH, Dioxane, from 0°C to RT. 3,5 h. *b)* MeI, K₂CO₃, DMF, from 0°C to RT for 2h. *c)* DMP, *p*-TSA, Toluene, reflux for 6h. *d)* DIBALH, toluene, -78°C for 2h. *e)* fluoro methyl sulphone, dimethyl chlorophosphate, Lithium Bis, toluene, from -78°C to RT overnight. *f)* (ᵗBu)₃SnH, AIBN, toluene, reflux 5h. *g)* NaOMe, MeOH, 50°C for 2h. *h)* *p*-TSA, MeOH, 60°C for 24h. *i)* PDC, AcOH, RT for 2h. and HCl, EtAc rt for 2h.

8. BIOLOGICAL RESULTS AND DISCUSSION.

The synthetized compounds were tested on hSR enzymes. Since racemization and elimination reactions are known to share the same enzymatic active site, it is possible to study SR activity by analyzing either reaction.[104] The products that can be detected are L-or D-Serine (depending on the substrate), pyruvate and ammonia.
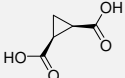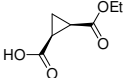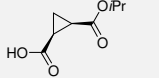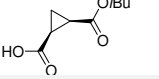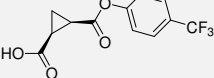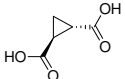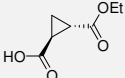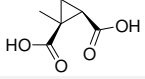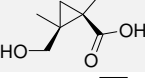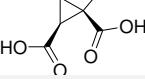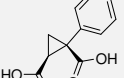
In this case, the rate of the β-elimination of L-Serine on hSR was monitored, by coupling this reaction with lactate dehydrogenase (LDH). The rate of pyruvate production was calculated by measuring the redox reaction of pyruvate to lactate by means of LDH and following NADH disappearance at 340nm. All the compounds were tested at 330 µM concentration, unless properly specified in the table.
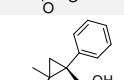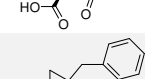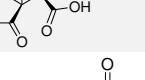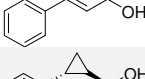
8.1 Cyclopropanes.

The residual activity of hSR after treatment with compounds **1**-**15**, along with their K_i, is reported in table 2.

With regard to the cyclopropane derivatives, the activity of compound **1**, although weak, was thought to serve as a starting point for the synthesis of more potent analogues. However, the synthetic efforts aimed at rationally expand the series, led only to compounds that were inactive at the concentration tested. Bulky groups, as well as small functional groups, or polar atoms, as well as more lipophilic substituents, led only to higher K_i. Moreover, it seems obvious that constraining of the molecule is detrimental to activity: likely, the conformation adopted by the two carboxylic groups is not compatible with the conformation imposed by the cyclopropane structure. To be noticed, compound **14,** reported as active[104], under this assay condition resulted devoid of any activity, somehow confirming how outcome of the assay is strongly influenced by experimental conditions.

Compound	Structure	hSR %residual Activity	Ki(µM)
1		60	~ 240
2		100	> 600
3		100	> 600
4		100	> 600
5		100	> 600
6		100	> 600
7		100	> 600
8		93	> 600
9		88	> 600
10		98	> 600
11		96	> 600
12		92	> 600
13		97	> 600
14		100	> 600
15		100	> 600

TABLE 2. Biological activity of compounds **1-15** on hSR evaluating β-eliminase reaction rate

8.2 Malonate derivatives

The residual activity of hSR after treatment with compounds 16-24, along with their K_i, is reported in table 3
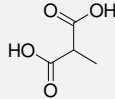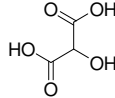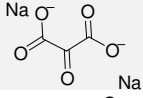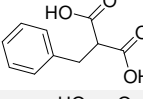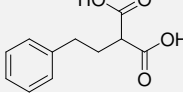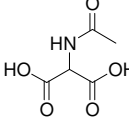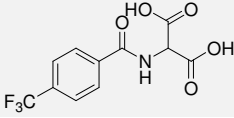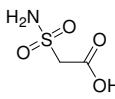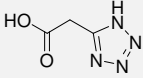
Compound	Structure	hSR %residual Activity	Ki(µM)
16		84	> 600
17		35	~ 90
18[a]			122±75
19[b]		100	>1500
20[b]		100	>1500
21[b]		100	>1500
22[b]		100	>1500
23[b]		100	>1500
24[b]		100	>1500

TABLE 3. Biological activity of compounds 1-15 on hSR evaluating β-eliminase reaction rate.
  a) Compound 18 is a possible substrate of LDH, therefore the activity assay was conducted by a titration of the hSR with the ligand, recording a different fluorimetric spectra for each concentration. Fitting the intensity of fluorimetric emission with ligand concentration is possible to deduce the Ki.
  b) This compound was tested at 660 µM concentration.

With regard to the malonate analogues, although the weak activity of the molecules tested, a few SAR clues can be described. compound **18** was found to show the best activity, being more active than the malonate itself. This might be consistent with a stronger interaction at the target binding site with polar aminoacid, warranted by the nature of H-bond donor/acceptor of the hydroxyl group. Indeed, the amino group, showing a similar pattern of interaction, was reported to have weak activity. When a more lipophilic group such as the methyl, unable to establuish H-bond, is put in place of the OH, the activity decreases, and it is completely lost when the group substituting the OH, beside lipophilic, is also particularly bulky (benzyl, phenylethyl). Since it seems that in that position a H-bond donor acceptor is necessary, an amide functionality was inserted. However, the compound resulted to be inactive, as well as for the bulkier derivative (compound **22**). Finally, it looked important to investigate whether the hydrogen of the OH played a role in the interaction with the enzyme-binding pocket; since compound **18** is quite tolerated, we may conclude that, although the presence of the O atom is crucial for the activity, the double nature of H-bond donor/acceptor of the OH warrant a better activity. Finally, it appears clear that the carboxylic moieties must have an extremely specific interaction with the target binding site, as the substitution of the carboxylic acid with its isosteres lead to loss of activity. In conclusion, the take-home message is that the range of modifications that this molecule can tolerate is extremely limited.

8.3 Fluoro-vinyl Glycine analogues.

The described compounds were tested on hSR with a time-dependent assay.
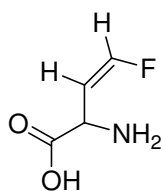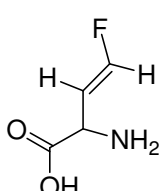
The compounds were incubated with the enzyme at 37°C in a basic pH (pH=8) for two hours. The mixture was then diluted and the assay was performed as previously reported measuring the rate of L-Serine β-elimination reaction, by the coupling with lactate dehydrogenase (LDH).

25

26

Time (min)	V0 (μM/min) hSR only	V0 (μM/min) + Comp.25	V0 (μM/min) + Comp.26
10	16.7	17.3	14.0
75	14.7	14.2	7.7
150	16.9	12.2	5.4
225	15.0	11.4	3.6

TABLE 4. Biological results on Compounds 25, 26. The table shows the time depend decrease of enzyme rate

From the data it is clear that compound **26** exhibits a time dependent inhibition, and after 75 min the enzyme activity is reduced by 50%.
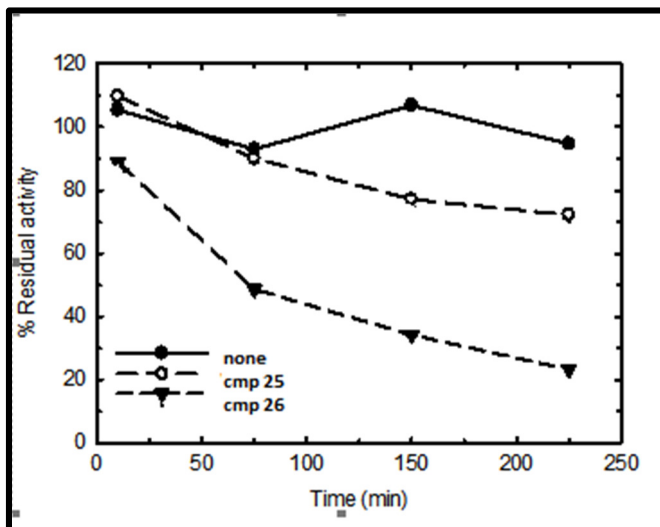
Scheme 9.Residual activity of SR

Although these data are only a preliminary evaluation of compound activity, it is quite clear the these covalent binder hold promise for further development as hSR inhibitors and, as such, represent an interesting starting point. Of course, further studies on the mechanism of inhibition and binding to PLP are needed.

8.4 Docking Studies.

Unfortunately, the only SAR information retrieved from this study is that the structural requisites for such a molecule to interact with active site of SR are so stringent that also the less relevant modification results to be detrimental for the activity, at the experimental conditions tested. In order to rationalize the experimental data, a docking study both on non-covalent inhibitor and on covalent ones was performed.

Set up of the docking study.

To perform docking studies on hSR were considered three different receptor conformations, given the high degree of structural flexibility of the protein. The previous reported study of Bruno A. *et al.* investigated, using TMD simulation, the steps characterizing the closure process. Therefore, for the docking study were selected three different protein conformations derived from this work:

1. the closed conformation of the crystal structure of hSR (PDB ID:3L6B);

2. the open form of hSR; since no human crystal structure is available in this form, we used the human model built using as template the open form of rSR (PDB ID: 3HMK) and used as starting point for the MD simulation

3. An intermediate protein conformation, extracted from the molecular dynamic simulation.

To performed the docking study, all the protein conformations have been prepared using Protein Preparation Wizard[130] from Maestro. For the crystal structure of 3L6B, the Protein Preparation tool was used to add hydrogen atoms at pH 7.0 ±1, to optimize the hydrogen bonding network and refine the protein structure with a maximum RMSD of tolerance of 0.3 Å. For the other two conformations, the starting point and an intermediate structure of the MD experiment, Protein Preparation Wizard was used only to minimize the hydrogen position. Two water molecules, coordinated to the PLP phosphate group and located in proximity of the binding site were conserved during docking studies, since from the analysis of all the available crystal structures from different species, they are always conserved, suggesting their important role in coordinating and shielding the phosphate group in the binding cavity. Docking were performed with Glide SP[131] available in Maestro, collecting ten poses for each molecule. Several serine and threonine residues are present in the binding site or are located closed to the binding pocket.

Therefore, during docking experiments hydroxylic groups were allowed to freely rotate, to optimize the hydrogen bonds formed with the ligands and to better resemble the physiological conditions. The binding poses of the compounds were visually analyzed in comparison with malonic acid, the inhibitor co-crystallized with hSR.
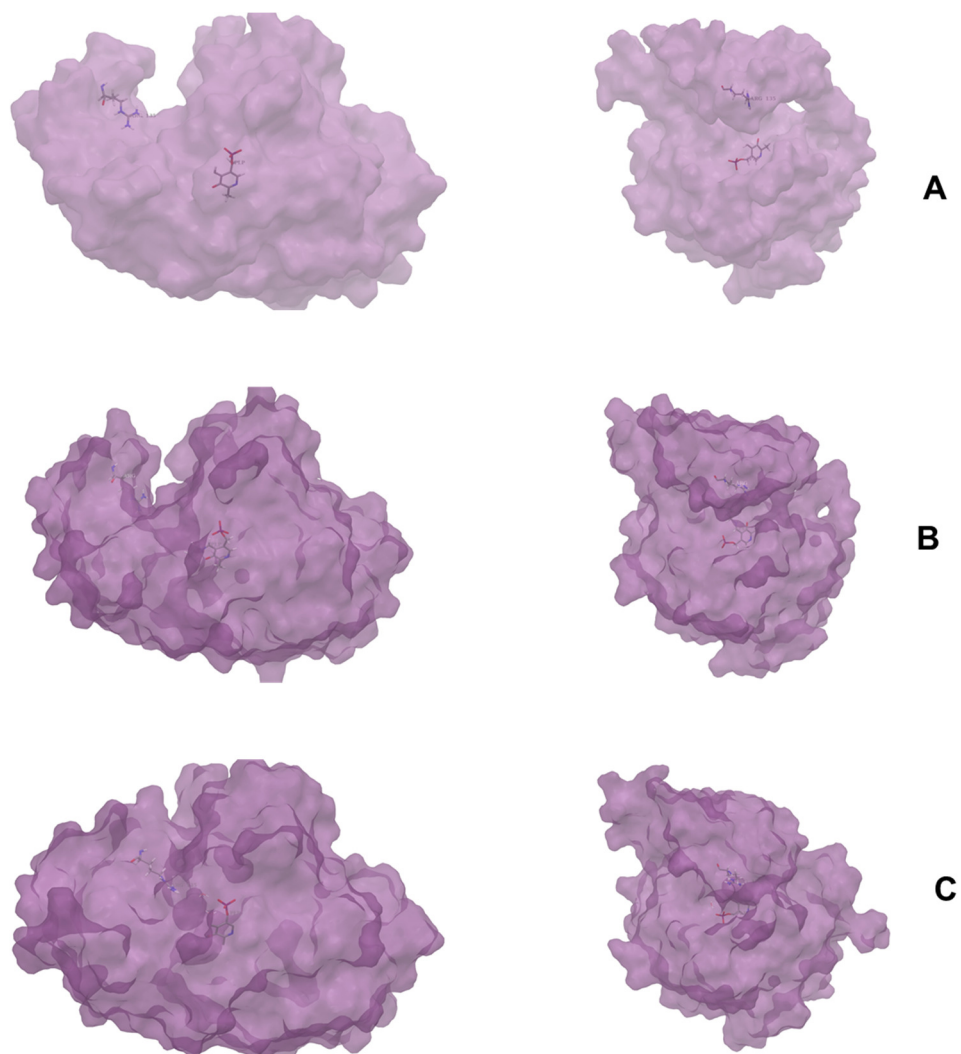
Figure17. Structure of hSR in the open form (A), intermediate conformation (B) and in the close conformation (C) in presence of the inhibitor malonate. Analyzing the different structure is evident the conformational change which undergoes the enzyme upon the ligand binding.

Docking analyses on cyclopropane scaffolds

Docking of compound **1**, that exhibits a K$_i$ of 240 µM, elucidates its binding mode on the active site of the enzyme in the close conformation. By comparing the pose of compound 1 with the malonate binding pose, it seems that the molecule maintains those interactions that are considered important for the enzyme affinity.
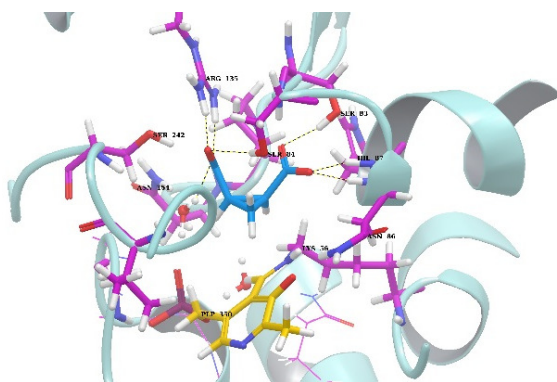
Figure 18. Docking of *cis*-(1,3)-cyclopropane dicarboxylic acid (in blue) in the close conformations.

The molecules establish three hydrogen bonds with the hydroxyl groups of Ser83, Ser84 and a water molecule and interacts with the nitrogen backbone of Arg135 and His87. The linkage with Arg135 shows a bidentate interaction similar to that made by the malonate, but the link angle with His87 reveals that the molecule is slightly shifted in respect to the malonate, and losses the interaction with Ser242.

Compound **2** differs from **1** only in the conformational geometry *trans* of the two dicarboxylic moieties. This difference leads to the loss of a considerable number of interactions. Indeed, it maintains the bond with Ser83, but not with Ser84 and, more importantly, the bidentate connection with Arg135 is replaced by a single hydrogen

bond, stressing the pivotal role of this amino acid in the active site of SR.
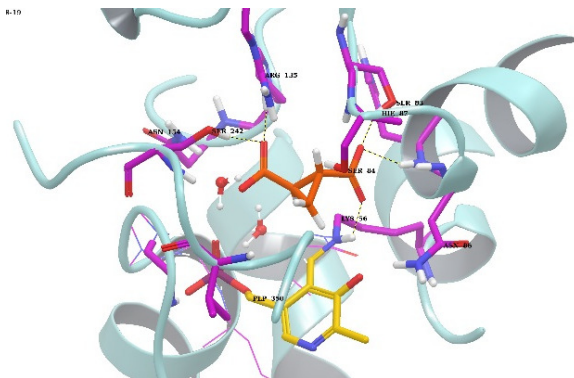
Figure 19. Docking of ***trans*-(1,2)-cyclopropane dicarboxylic acid (in red) in the close conformations.**

As regarding (1',2')-1,2-substituted cyclopropanes dicarboxylic acids, docking analysis on the close conformation of the enzyme reveals that only the monomethyl substituted cyclopropane (compound **10**) can access to the binding pocket. However, the methyl group interacts with the phosphate moiety of PLP cofactor, making unstable the interactions of the dicarboxylic groups of the molecules.

Docking analyses on vinyl glycine derivatives.

From the biological assays results only the *Trans* conformation of the fluoro-vinyl moiety inhibits the enzyme.
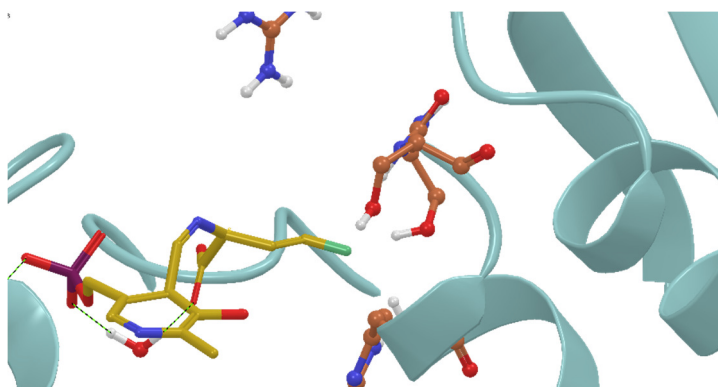
Figure 20. Docking on R isomers of (E)-fluoro vinyl glycine derivatives (orange).

Analyzing the binding mode of the two enantiomers of compound **26**, it seems that the S- enantiomer makes an H-bond with a water molecules while the R is connected to A135, underling once again the importance of this residue in stabilizing the catalytic site of the enzyme.
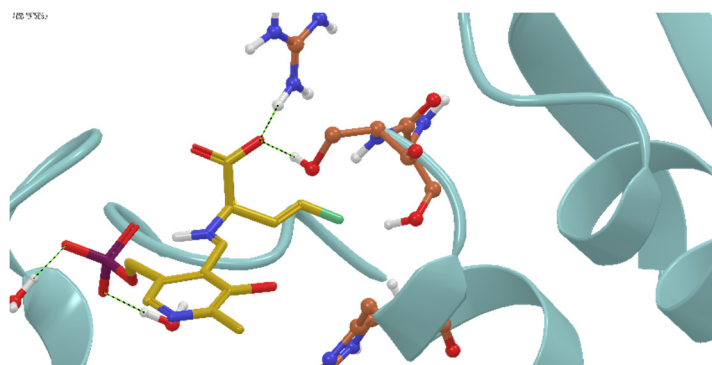
Figure 21. Docking on S isomers of (E)- fluoro vinyl glycine derivatives (orange).

Moreover both the enantiomers could be involved in a fluorine-H-bond with Ser83, and this interaction might be responsible for the activity shown only by the *trans* isomer.

9. CONCLUSIONS AND FUTURE PROSPECTIVES.

The study around small molecules as potential inhibitors of Human Serine Racemase reveals that the structure of malonate is hardly manageable: only modifications with small functionalities are tolerated, whereas bulky groups lead to a firm decrease of the affinity.

The analysis of the enzyme flexibility and binding pocket suggests that SR susceptibility is due to the small space in the cavity as well as a strictly interactions with crucial residues that cannot be modified (i.e. the Arg135 bidentate H bond).

In spite of this, some speculation for a further development of molecules that interact in a non-covalent mode could be done.

First of all, the TMD simulations on the open-close conformation reveal that the rearrangement of some residues is essential for a correct conformation of the active site. Under this prospective, the enzyme may be inhibited using more bulky molecules to prevent the enzyme closure and the active residues rearrangement. A first step in pursuing this strategy should be testing in a time–dependent manner those compounds that cannot access the binding site in the close conformation, such as the (1',2')-1,2-dicarboxylic acid disubstitute cyclopropanes, to verify if they impede enzyme closure.

A second consideration might be done regarding the biochemical assays. The activity of

could be studied measuring both the β-eliminase reaction and the racemization rate, since they occur at the same site. However, mutagenesis studies disclosed that different residues are involved in the two mechanism and suggest the stereospecificity of the racemase reaction. Considering that the compound do not interact directly with the PLP cofactor, it should be important to follow the progress of both reactions to elucidate if the binding of a molecule with different amino acids moieties can affect only one reaction or both.

The synthesis of vinyl glycine analogs lead to the best results, nevertheless the design of a inhibitor which interacts selectively with the PLP moiety of SR is a hard goal. Also in this case it is important to establish if the tested compounds interacts with the enzyme through the formation of a Michael adduct, and , if so, the residues involved in the interaction should be characterized. these information would be of great help in the future synthesis of novel and more potent inhibitors of SR.

10. EXPERIMENTAL SECTION (I)

10.1 Materials and methods.

All compound were obtained via classical synthetic procedures for reaction, purification and characterization, using organic chemistry lab wares at University of Parma.

Reactants were purchased both from Sigma-Aldrich® and TCI (Tokyo Chemical Industries)®, at reagent purity and, unless otherwise noted, used without further purification.

Solvent used in non-aqueous reaction were obtained by distillation of thecnical grade materials over appropriate dehydrating agents.

Reaction were monitored by thin layer chromatography on Kiesegel®60 F254 (DC-Alufolien, Merk®), at both 254 nm and 365 nm wavelengths.

Where indicated intermediates and final product were purified by silica gel flash chromatography (silica gel 0.040-0.063mm) using the described solvent mixtures.

Intermediates and final product were characterized by HPLC/MS analysis (HPLC:Agilent® 1100 series, equipped with Waters® Symmetry C18, 3.5 µm, 4.6x75 mm column; MS:Applied Biosystem/MDS SCIEX®, with API 150EX® ion source) and ^{1}H-NMR analysis(BRUKER AVANCE® 300MHz and   BRUKER AVANCE® 400MHz). Where indicated ^{13}C-NMR spectra were also recorded. Chemical shifts (δ scale) are reported in parts per million relative to

TMS. ¹H-NMR spectra are reported in this order: multiplicity, and number of protons. Singles were characterized as: *s* (singlet), *d*(doublet), *dd* (doublets of doublets), *t* (triplet), *q* (quartet), *m* (multiplet), *bs* (broad signal).

10.2 Synthetic procedures and products characterization.

General procedures for the synthesis of cis-(±) cyclopropane dicarboxylic acid and monoesters (1-4).

3-oxabicyclo[3.1.0]hexane-2,4-dione, 0.5 mMol, was suspended in water (or ethanol, isopropanol, isobutanol), reaction mixture was refluxed for two ours monitoring the disappearance of the SM with TLC(eluting with 8:2 petroleum ether/ethyl acetate). After this time, reaction mixture was evaporated under vacuum affording the desired compound in a quantitative yield.

Cis (±)-cyclopropane-1,2-dicarboxylic acid (1)

1H-NMR (MeOD 300 MHz):δ 1.27-1,29 (m, 1H), δ 1.49-1.55 (m, 1H), δ 2.07-2.12 (t,2H).

Cis (±)-2-(ethoxycarbonyl)cyclopropanecarboxylic acid(2).

1H-NMR (CDCl3 300 MHz):δ 1.16-1,29 (m, 3H), δ 1.65-1.67 (d, 1H), δ 2.07-2.12 (d,2H), δ 4.10-4.17 (d,2H).

Cis (±)-2-[(propan-2-yloxy)carbonyl] cyclopropanecarboxylic acid(3).

1H-NMR (CDCl3 300 MHz):δ 1.18-1,22 (t, 6H), δ 1.26-1.32 (m, 1H), δ 1.61-1.67 (q,1H), δ 2.07-2.14 (q,2H) δ 4.95-5.03 (m,1H), δ 8.53 (bs,1H).

Cis (±)-2-[(2-methylpropoxy)carbonyl] cyclopropanecarboxylic acid (4).

1H-NMR (CDCl3 300 MHz):δ 0.88-0.92 (d, 6H), δ 1.26-1.34 (m, 1H), δ 1.63-1.69 (t,1H), δ 1.88-1.05 (m,1H), δ 2.05-2.14 (m,2H), δ 3.81-3.91(m, 1H), δ 8.55 (bs,1H).

Synthesis of cis-(±)-2-{[4-(trifluoromethyl)phenoxy]carbonyl} cyclopropanecarboxylic acid (5).

Cis (±)-cyclopropane-1,2-dicarboxylic acid(1) (1eq.), 4-(trifluoromethyl)phenol (1eq.) and DMAP (0.1eq) were dissolved in dichloromethane, the mixture was cooled at 0°C and a solution of DCC in dichloromethane was added dropwise. The ice bath was removed and the mixture was stirred at room temperature overnight. TLC performed after 12 hours of reaction (eluting with 7:3 petroleum ether/ethyl acetate) show the complete consumption of (1) and the formation of two main spot. HPLC/MS analysis reveals the formation of the bi and mono substituted cyclopropanes.

Reaction was then filtered and the filtrated evaporated under vacuum.

The crude product was purified by flash column chromatography eluting with petroleum ether/ethyl acetate from 8:2 to 0:10 affording the desired product in a low yield(15%).

^{1}H-NMR (CDCl$_3$ 300 MHz):*δ* 1.42-1.49 *(m,* 1H), *δ* 1.82-1.88 (*q,* 1H), *δ* 12.18-2.22 (*q*,1H), *δ* 2.36-2.41 (*t*,1H), *δ* 6.95-6.97 (*d,*2H), *δ* 7.13-7.16(*d,* 2H).

Synthesis of Trans -(±)-(cyclopropane-1,2-dicarboxylic acid (6).

Diethyl -*trans*-cyclopropane-1,2-dicarboxylate was dissolved in aqueous KOH 6N. the mixture was refluxed for 2 hours. Starting material conversion was monitored by TLC eluting with petroleum ether and ethyl acetate 7:3.

The mixture was then washed with diethyl ether, and acidified to pH=3. The aqueous phase was extracted with diethyl ether for three times. The collected organic phases were dried over sodium sulfate and evaporated under vacuum to afford (6) as a colorless oil in a yield of 80%.

^{1}H-NMR (DMSO-d6 400 MHz):*δ* 1.25-1.99 *(t,* 2H), *δ* 1.87-1.91 (*t,* 2H), *δ* 12.59 (*bs,*1H).

Synthesis of Trans -(±)-2-(ethoxycarbonyl)cyclopropanecarboxylic acid(7).

Diethyl -*trans*-cyclopropane-1,2-dicarboxylate was dissolved in anidrous ethanol and refluxed for two hours. Starting material

conversion was monitored by TLC eluting with petroleum ether and Ethyl Acetate 7:3. The solution was evaporated under vacuum to afford the target product with a yield of 89%.

^{1}H-NMR (CDCl$_3$ 400 MHz):δ 1.27-1.31 *(t,* 3H), δ 1.49-1.51 *(m,* 2H), δ 2.15-2.26 (*dm,* 2H), δ 9.32 (*bs,*1H).

General procedure for the synthesis of (1',2')-substituted-cyclopropane-1,2 diethyl esters (8a, 9a,10a,11a,12a and 13a).

A stirred suspension of sodium hydride (60% suspension in mineral oil, 1.1eq.) in dry toluene was treated under nitrogen with the suitable ethyl 2-alocarboxylate (1 eq.) and ethyl 2-acrylate (1 eq.). The reaction temperature was maintained between 20 and 40 °C. After the addition, the reaction was monitored with TLC. At the end, (usually after 36-72h) residual sodium hydride was destroyed by addition of a small amount of methanol. Sufficient water was added to dissolve the sodium halide, and the mixture was extracted with Et$_2$O (×3 times), washed with water and brine, dried over MgSO$_4$, and concentrated. Crude residue was purified by silica gel flash chromatography with eluting mixture composed by petroleum ether/ethyl acetate in variable proportion comprised between 9:1 and 6:4.

Cis-(±)diethyl-1-methylcyclopropane-1,2-dicarboxylate (8a)

^{1}H-NMR (CDCl$_3$ 400 MHz):δ 0.65-0.69 *(d,* 1H), δ 1.04-1.06 *(t,* 1H), δ 1.25-1.27 (*t,* 6H), δ 1.45 (*s,*3H), δ 1.97-2.03 (*d,* 1H), δ 4.09-4.15 (*q,* 4H).

Cis-(±)diethyl -1,2-dimethylcyclopropane-1,2-dicarboxylate (9a)

^{1}H-NMR (CDCl$_3$ 400 MHz):δ 0.57-0.59 *(d,* 1H), δ 1.09-1.15 *(t,* 6H), δ 1.26 (*s,* 6H), δ 1.83-1.85 (*d,* 1H), δ 3.93-4.02(*q,* 4H).

Cis-(±)diethyl -1-ethylcyclopropane-1,2-dicarboxylate(10a)

^{1}H-NMR (CDCl$_3$ 400 MHz):δ 0.88-0.90 *(m,* 1H), δ 1.00-1.07 *(t,* 3H), δ 1.15-1.19 (d*,* 1H), δ 1.18-1.2 (*t,* 6H), δ 1.376-1.43 (*m,* 1H), δ 1.92-1.99 (*m,* 2H), δ 3.9-4.1 (*m,* 4H).

Cis-(±)diethyl -1-phenylcyclopropane-1,2-dicarboxylate(11a)

^{1}H-NMR (CDCl$_3$ 400 MHz):δ 0.88-0.90 *(d,* 1H), δ 1.18-1.22 *(t,* 6H), δ 1.51-1.53 (*d,* 1H), δ 2.1-2.23 (*d,* 1H), δ 4.09-4.14(*q,* 4H), δ 7.23-7.30 (*m,* 6H).

Cis-(±)diethyl -1-methyl-2-phenylcyclopropane-1,2-dicarboxylate (12a)

^{1}H-NMR (CDCl$_3$ 400 MHz):δ 0.86-0.88 *(d,* 1H), δ 1.04 *(s,* 3H), δ 1.12-1.28 *(m,* 6H), δ 2.28-2.29 (*d,* 1H), δ 4.03-4.24(*m,* 4H), δ 7.29-7.34 (*m,* 3H), δ 7.43-7.05 (*m,* 2H).

Cis-(±)diethyl-1-benzyl-2-methylcyclopropane-1,2-dicarboxylate (13a)

^{1}H-NMR (CDCl$_3$ 400 MHz):δ 0.97-0.99 *(d,* 1H), δ 1.51 *(s,* 3H), δ 1.09-1.23 *(m,* 6H) δ 2.09-2.11 (*d,* 1H), δ 2.75-2.79 (*d,* 1H), δ 3.30-3.34 (*d,* 1H), δ 4.05-4.27(*m,* 4H), δ 7.25-7.30 (*m,* 5H).

General Procedures for (1',2')-substituted-cyclopropane-1,2 diethyl esters hydrolysis (8, 9,10,11,12 and 13).

Diethyl dicarboxylate was dissolved in a mixture of THF/water (1:2) and reaction was cooled to 0°C. A solution of aqueous potassium hydroxide 1N was added dropwise. Reaction was the stirred at 50°C for four days monitored by TLC. The mixture was then washed with diethyl ether, and acidified to pH=3 with hydrochloric aqueous solution 1N. The aqueous phase was extracted with diethyl ether for three times. The collected organic phases were dried over sodium sulfate and evaporated under vacuum to afford target product as a white solid in a good yield.

Cis-(±)1-methylcyclopropane-1,2-dicarboxylic acid (8)

1H-NMR (CDCl3 400 MHz):δ 1.18-1.26 (q, 1H), δ 1.46 (s, 3H), δ 1.87-1.95 (m, 2H), δ 8.94 (bs,1.5H).

Cis-(±)-1,2-dimethylcyclopropane-1,2-dicarboxylic acid (9)

1H-NMR (CDCl3 400 MHz):δ 0.82-0.84 (d, 1H), δ 1.43 (s, 6H), δ 2.02-2.04 (d, 1H), δ 8.94 (bs,2H).

Cis-(±)-1-ethylcyclopropane-1,2-dicarboxylic acid (10)

1H-NMR (CDCl3 400 MHz):δ 0.88-0.90 (m, 1H), δ 1.00-1.07 (t, 3H), δ 1.15-1.19 (q, 1H), δ 1.37-1.45 (m, 1H), δ 1.81-1.92 (m, 1H), δ 1.97-2.06 (m, 1H), δ 8.17 (bs,2H).

Cis-(±)-1-phenylcyclopropane-1,2-dicarboxylic acid (11).

1H-NMR (DMSO-d6 400 MHz):δ 1.56-1.64 (t, 1H), δ 1.74-1.76 (t, 1H), δ 2.19-2.22 (t, 1H), δ 7.24-7.29 (m, 5H).

Cis-(±)-1-methyl-2-phenylcyclopropane-1,2-dicarboxylic acid (12).

1H-NMR (CDCl3 400 MHz):δ 1.035 (s, 3H), δ 1.42-1.44 (d, 1H), δ 2.29-2.33 (d, 1H), δ 7.33-7.41(m, 5H).

Cis-(±)-1-benzyl-2-methylcyclopropane-1,2-dicarboxylic acid (13).

1H-NMR (CDCl3 400 MHz):δ 1.04-1.05 (d, 1H), δ 1.51 (s, 3H), δ 2.12-2.13 (d, 1H), δ 2.81-2.85 (d, 1H), δ 3.32-3.36 (d, 1H), δ 7.25-7.30 (m, 5H).

Synthesis of disodium oxopropanedioate(18).

Diethyl oxopropanedioate was dissolved in THF/water (1:2) and a stoichiometric amount of aqueous solution of NaOH (1N) was added.

Reaction was then stirred art for 12 h monitoring starting material conversion by TLC.

When reaction was complete, the mixture was evaporated under vacuum and the residues was crystallized from ethanol/chloroform to obtain a white solid .Y=62%,

^{13}C-NMR (DMSO-d6 100 MHz): *δ 169*, *δ* 191. MS (APCI) m/z : 117 [M+H]+, calculated 116.03.

Diethyl benzylpropanedioate (19a) and diethyl (2-phenylethyl)propanedioate (20a) synthesis.

Diethyl malonate was dissolved in dry THF the solution was cooled to 0°C by an ice bath, and sodium hydride was added portionwise under nitrogen atmosphere. After stirring the suspension for 15 minutes, a solution of benzene derivative in dry THF was added. The ice bath was removed and the mixture was stirred at room temperature for 12h following the product formation by TLC. At the end residual sodium hydride was destroyed with a small amount of methanol and reaction was diluted with water.

The aqueous phase was extracted with Et$_2$O (×3 times), the organic layers washed with water and brine, dried over MgSO$_4$, and concentrated. Crude residues was purified by silica gel flash chromatography with eluting mixture composed by petroleum ether/ethyl acetate from 9:1 to 7:3.

Diethyl benzylpropanedioate (19a)

1H-NMR (CDCl3 400 MHz): δ 1.22-1.25 (t, 6H), δ 3.23-3.25 (d, 2H), δ 3.63-3.66 (t, 1H), δ 4.15-4.23 (m, 1H), δ 7.22-7.25 (q, 1H), δ 7.55-7.58 (m, 4H),δ 8.49-8.50 (m, 2H).

(2-phenylethyl)propanedioate (20a).

1H-NMR (CDCl3 400 MHz): δ 1.11-1.28 (t, 6H), δ 1.92-1.96 (q, 2H), δ 2.47-2.57 (t, 2H), δ 3.05-3.09 (t, 1H), δ 3.98-5.06 (q, 4H), δ 7.15-7.29 (m, 5H).

Benzylpropanedioic acid (19) and (2-phenylethyl)propanedioic acid (20) synthesis

Compound 19a or 20a was dissolved in an aqueous solution of sodium hydroxide 1N, and stirred at room temperature for 48h. After the complete hydrolyses of the diethyl moieties, the mixture was washed with diethyl ether, and acidified to pH=3 with hydrochloric acid solution 1N. The aqueous phase was extracted with diethyl ether for three times. The collected organic phases were dried over sodium sulfate and evaporated under vacuum to afford target product as a white solid in a good yield.

Benzylpropanedioic acid (19)

1H-NMR (DMSO-d6 400 MHz):δ 3.02-3.04 (d, 2H), δ 3.55-3.58 (t, 1H), δ 7.17-7.29 (m, 5H).

(2-phenylethyl)propanedioic acid (20).

1H-NMR (DMSO-d6 400 MHz):δ 1.99-2.04 (q, 2H), δ 2.51-2.58 (t, 2H), δ 3.16-3.32 (t, 2H), δ 7.17-7.32 (m, 5H), δ 12.75 (bs, 2H).

Diethyl (acetylamino)propanedioate (21a) and diethyl (benzoylamino)propanedioate (22a) synthesis.

Diethyl-2-amino malonate hydrochloride (1eq.) was suspended in acetonitrile , triethylamine (2.2eq.) was added and the mixture was stirred for 15 minutes. Then the corresponding acyl chloride was added and the reaction was stirred overnight at room temperature.

When TLC revealed starting material consumption, the reaction mixture was concentrated, and then water was added to the residual gum.

Aqueous phase was extracted with diethyl ether for three times and the collected organic phases were dried over sodium sulfate and evaporated under vacuum, The crude material was then purified by silica gel flash chromatography eluting with petroleum ether/ Ethyl acetate 7/3.

Diethyl (acetylamino)propanedioate (21a)

1H-NMR (DMSO-d6 400 MHz):δ 1.18-1.24 (t, 6H), δ 1.91 (s, 3H), δ 4.13-4.19 (m, 4H), δ 4.88-4.90 (d, 1H), δ 8.65-8.66 (d, NH).

Diethyl (benzoylamino)propanedioate (22a)

1H-NMR (CDCl3 400 MHz):δ 1.33-1.37 (t, 6H), δ 4.29-4.38 (m, 4H), δ 5.36-5.34 (d, 1H), δ 7.2 (bs, 0.5H), δ 7.74-7.76 (d, 2H), δ 7.97-7.99 (d, 2H).

(Acetylamino)propanedioic acid (21) and (benzoylamino)propanedioic acid (22) synthesis.

Compound 21a or 22a was dissolved in a mixture of THF/water (1:2) and reaction was cooled to 0°C. A solution of aqueous lithium hydroxide 1N was added dropwise. Reaction was then stirred at room temperature for 48-72 hours monitored by TLC. The mixture was then washed with diethyl ether, and acidified to pH=3 with hydrochloric aqueous solution 1N. The aqueous phase was

extracted with diethyl ether for three times. The collected organic phases were dried over sodium sulfate and evaporated under vacuum to afford target product as a white solid.

(Acetylamino)propanedioic acid (21)

1H-NMR (DMSO-d6 400 MHz): δ 1.91 (s, 3H), δ 4.96-4.98 (d, 1H), δ 8.64-8.67 (d, NH), δ 13.46 (bs, 1.5H).

(benzoylamino)propanedioic acid (22)

1H-NMR (DMSO-d6 400 MHz): δ 5.16-5.18 (d, 1H), δ 7.86-7.88 (d, 2H), δ 8.1-8.12 (d, 2H), δ 9.31-9.33 (d, 1H), δ 13.36 (bs, 1.5H).

13C-NMR (DMSO-d6 100 MHz):δ 56.62, δ 58.02, δ 124, δ 125, δ 126, δ 128.23, δ 128.3, δ 129.87, δ 131, δ 132, δ 137, δ 165, δ 168.

Synthesis of Fluoro-vinyl glycine analogues.

2-[(tert-butoxycarbonyl)amino]-3-hydroxypropanoic acid synthesis (27)

Serine was dissolved in an aqueous solution of sodium hydroxide 1N and cooled to 0°C by an ice bath. A solution of di-*tert*-butyl dicarbonate (1.2 eq.) in dioxane was added dropwise over a period of 15 minutes.

Reaction was then stirred for 30 minutes, the ice bath was then removed and the mixture was stirred at room temperature for two hours. Reaction evolution was monitored by TLC.

Reaction mixture was concentrated to half of its volume by rotary evaporation, cooled on ice and acidified to pH=3 by slow addition of a solution of $KHSO_4$ 1M.

The resulting mixture was extracted with ethyl acetate (four times) and the combined organic phases were dried over sodium sulfate and evaporated to dryness affording a sticky foam. Yield: 87% the product was use as crude in the next step of reaction.

Methyl 2-[(tert-butoxycarbonyl)amino]-3-hydroxypropanoate synthesis (28)

2-[(tert-butoxycarbonyl)amino]-3-hydroxypropanoic acid and potassium carbonate (1.1 eq.) were dissolved in DMF. The resulting

suspension was cooled to 0°C by an ice bath. Methyl iodide(2 eq.) was added dropwise over one hour. After this time the mixture was warmed to room temperature and stirred for three hours. TLC shown the complete starting material consumption.

Reaction was diluted with water and extracted with ethyl acetate (five times). The combined organic phases were washed with brine, dried over sodium sulfate and evaporated to dryness.

The crude was purified by silica gel flash chromatography eluting with petroleum ether/ethyl acetate from 7:3 to 6:4. Collected fractions were evaporated affording the titled compound in a yield of 88%.

^{1}H-NMR (CDCl$_3$ 400 MHz):δ 1.46-1.48 *(t,* 9H), δ 3.78-3.80 (*d,* 3H), δ 3.89-4.01 (*m,* 2H), δ 4.4 (*bs,* 0.5H), δ 5.47-5.49 (b*d,* 1H).

3-tert-butyl 4-methyl 2,2-dimethyl-1,3-oxazolidine-3,4-dicarboxylate synthesis (29)

A solution of Methyl 2-[(tert-butoxycarbonyl)amino]-3-hydroxypropanoate, dimethoxy propane (2 eq.) and *para*-toluensulfonic acid monohydrate (0.15 eq.) in toluene, was heated under reflux for two hours meanwhile methanol was slowly distilled off.

TLC of the reaction in petroleum ether/ ethyl acetate 1:1 show the clear formation of the product.

The cooled solution was partitioned between a saturated solution of sodium bicarbonate and diethyl ether. The separated organic layer was washed with a saturated solution of sodium bicarbonate and brine, then dried over sodium sulfate and concentrated to give a crude oil.

The crude product was purified by silica gel flash chromatography eluting with petroleum ether/ethyl acetate from 95:5 to 85:15 to give the desired product in a 74% yield.

^{1}H-NMR (CDCl$_3$ 400 MHz): δ 1.38-1.64 *(m,* 15H), δ 3.72 (*s,* 3H), δ 3.89-4.03(*td,* 1H), δ 4.1-4.14 (*m,* 1H), δ 4.34-4.36 (*dd,* 0.5H), δ 4.44-4.46 (*dd,* 0.5H).

Tert-butyl 4-formyl-2,2-dimethyl-1,3-oxazolidine-3-carboxylate synthesis (30)

To a -78°C solution of 3-tert-butyl 4-methyl 2,2-dimethyl-1,3-oxazolidine-3,4-dicarboxylate in dry diethyl esther a solution of 1M DIBAL in cyclohexane (1.7 eq.) was added dropwise over a period of 30 minutes, under nitrogen atmosphere and keeping the internal temperature below -65°C. the reaction mixture was stirred for an additional hour to -78°C and TLC (petroleum ether/ethyl acetate 9:1) shown the clear formation of product with only a trace of starting material.

Reaction was quenched by slowly addition of methanol, always maintaining the internal temperature below -65°C. The resulting emulsion was poured into ice-cold solution of hydrochloric acid 1N, and the aqueous mixture was the extracted with ethyl acetate (3 times). The organic phase was dried over sodium sulfate and evaporated to dryness affording a crude oil, which was purified by silica gel flash chromatography eluting with petroleum ether/ ethyl acetate from 100:0 to 85:15. Overall yield: 90%

^{1}H-NMR (CDCl$_3$ 400 MHz): δ 1.25-1.65 *(m,* 15H), δ 4.06-4.12 (*m,* 2H), δ 4.19-4.20 (*d,* 0.5H), δ 4.32-4.33 (*d,* 0.5H), δ 9.54-9.60 (*dd,* 1H).

(E)-(Z)-tert-butyl-4-[(2-fluoro-2-(phenylsulfonyl)ethenyl]-2,2-dimethyl-1,3-oxazolidine-3-carboxylate synthesis (31).

To a cooled solution (-78°C) of fluoromethylphenyl sulfone (1.5 eq.) in dry THF, under nitrogen atmosphere, diethyl chlorophosphate (1.5 eq.) was added dropwise. The mixture was stirred at -78°C for ten minutes and then a solution of lithium bis(trimethylsilyl) amide (1M solution in THF, 3 eq.) was added followed by a solution of Tert-butyl 4-formyl-2,2-dimethyl-1,3-oxazolidine-3-carboxylate in THF, with the temperature maintained to -78°C. The reaction mixture was gently warmed at room temperature and stirred overnight.

TLC petroleum ether/ ethyl acetate 8:2 clearly shown the formation of the isomer E and Z.

A saturated solution of ammonium chloride was added and reaction mixture was extracted with diethyl ether (four times). The combined extracts were dried over sodium sulfate and concentrated to give an orange oil.

Crude product was purified by silica gel flash chromatography eluting with hexane/ethyl acetate 8:2, affording a mixture of the Z/E isomers. The reported ^{1}H-NMR analysis is on the mixture of the two isomers.

^{1}H-NMR (CDCl₃ 400 MHz): _δ_ 1.22 _(s,_ 18H), _δ_ 1.52 _(s,_ 6H), _δ_ 1.67 _(s,_ 6H), _δ_ 3.81-3.83 _(d,_ 2H), _δ_ 4.10-4.14 _(q,_ 2H), _δ_ 4.67-4.71 _(bt,_ 1.5H), _δ_ 4.79 _(bs,_ 0.5H), _δ_ 6.19-6.22 _(d,_ 1H), _δ_ 6.27-6.19 _(d,_ 1H), _δ_ 7.60-7.66 _(m,_ 4H), _δ_ 7.71-7.73 _(d,_ 2H), _δ_ 7.79-8.00 _(d,_ 4H).

(E)-(Z)-4-[2-fluoro-2-(tributylstannyl)ethenyl]-2,2-dimethyl-3-oxazolidinecarboxylic   acid-1,1-dimethylethylester synthesis (32, 33).

A mixture of the two isomers, (E)-(Z)-tert-butyl-4-[(2-fluoro-2-(phenylsulfonyl)ethenyl]-2,2-dimethyl-1,3-oxazolidine-3-carboxylate, tributyltin hydride (2 eq.) and a catalytic amount of 2,2-azobis(2-methylpropionitrile) (0.1 eq.) in dry toluene was reflux under nitrogen atmosphere and the reaction was monitored by TLC (hexane/ethyl acetate 9:1). After 3 hours, additional tributyltin hydride (2 eq.) was added, and reflux continued for an additional 8 hours, at which time TLC indicated the reaction to be complete.

The reaction mixture was concentrated under reduced pressure to give a viscous colorless oil, which was chromatographed on silica gel eluting with 1% of diethyl ether in hexane to afford E isomer (y:11%) and Z isomer(70%).

(E)-4-[2-fluoro-2-(tributylstannyl)ethenyl]-2,2-dimethyl-3-oxazolidinecarboxylic acid-1,1-dimethylethylester (32).

1H-NMR (DMSO-d6 300 MHz): δ 0.84-0.88 (t, 9H), δ 1.04-1.14 (m, 27H), δ 1.46-1.55 (m, 6H), δ 3.61-3.64 (d, 1H j=9.6 Hz), δ 4.00-4.02 (t, 1H j= 7.44Hz and 6.93Hz), δ 4.12 (bs, 1H), δ 5.74-5.89 (dd, 1H j=10.41Hz and 37.53Hz).

(Z)-4-[2-fluoro-2-(tributylstannyl)ethenyl]-2,2-dimethyl-3-oxazolidinecarboxylic acid-1,1-dimethylethylester (33).

1H-NMR (DMSO-d6 400 MHz): δ 0.84-0.88 (t, 9H), δ 0.97-1.41 (m, 27H), δ 1.5-1.54 (m, 6H), δ 3.59-3.61 (d, 1H j=8.76 Hz), δ 4.02-4.05 (dd, 1H j= 6Hz and 8.68Hz), δ 4.75-4.78 (t, 1H, j=6..24Hz and 6.28Hz), δ 4.86-5.02 (dd, 1H j=8.5Hz and 53Hz).

(E)-(Z)-tert-butyl 4-[2-fluoroethenyl]-2,2-dimethyl-1,3-oxazolidine-3-carboxylate synthesis (34, 36).

To a solution of sodium methoxyde in dry methanol (32) or (33) were added. The mixture was heated to 50°C under nitrogen atmosphere for 5 hours and concentrated under reduced pressure. The residues was chromatographed on silica gel with 1% of ethyl acetate in hexane to give a quantitative yield of 34 or 90% yield of 36.

Tert-butyl 4-[(Z)-2-fluoroethenyl]-2,2-dimethyl-1,3-oxazolidine-3-carboxylate (34).

1H-NMR (CDCl3 300 MHz): δ 1.46 (s, 9H), δ 1.52 (s, 3H), δ 1.61 (s, 3H), δ 3.37-3.76 (d, 1H), δ 4.06-4.11 (dd, 1H), δ 4.83 (bs, 1.5H), δ 4.95-5.00 (dd, 0.5H), δ 6.35 (s, 0.5H), δ 6.62-6.64 (dd, 0.5H).

Tert-butyl 4-[(E)-2-fluoroethenyl]-2,2-dimethyl-1,3-oxazolidine-3-carboxylate (36).

1H-NMR (CDCl3 300 MHz): δ 1.45 (s, 9H), δ 1.48 (s, 3H), δ 1.58 (s, 3H), δ 3.69-3.72 (d, 1H), δ 3.99-4.04 (m, 1H), δ 4.21 (bs, 1H), δ

4.32-4.34 (dd, 1H), δ 5.33-5.46 (m, 1H), δ 6.48-6.62 (dd, 0.5H), δ 6.76-6.91 (dd, 0.5H).

(Z)-(E)-tert-butyl [4-fluoro-1-hydroxybut-3-en-2-yl]carbamate synthesis (35),(37)

A mixture of (34) or (36), p-toluensulfonic acid monohydrate (0.1 eq.) and methanol was refluxed under nitrogen atmosphere for 48h. Reaction progress was monitored by TLC (hexane/ ethyl acetate 9:1). The mixture was then concentrated and the crude residues was purified by silica gel chromatography eluting with dichloromethane/ methanol 95:5 affording the titled compounds in a yield of 75%.

Tert-butyl [(3Z)-4-fluoro-1-hydroxybut-3-en-2-yl]carbamate(35).

1H-NMR (CDCl3 400 MHz): δ 1.46 (s, 9H), δ 3.63-3.75 (m, 2H), δ 4.59 (bs, 1H), δ 4.83-4.86 (m, 0.5H), δ 4.94-4.97 (m, 0.5H), δ 5.01-5.02 (bd, 0.8H NH), δ 6.41-6.43 (d, 0.5H), δ 6.62-6.64 (d, 0.5H).

Tert-butyl [(3E)-4-fluoro-1-hydroxybut-3-en-2-yl]carbamate (37).

1H-NMR (CDCl3 300 MHz): δ 1.46 (s, 9H), δ 3.63-3.75 (m, 2H), δ 4.59 (bs, 1H), δ 4.83-4.86 (m, 0.5H), δ 4.94-4.97 (m, 0.5H), δ 5.01-5.02 (bd, 0.8H NH), δ 6.41-6.43 (d, 0.5H), δ 6.62-6.64 (d, 0.5H).

(Z)-(E)-2-amino-4-fluorobut-3-enoic acid synthesis (25) (26)

A mixture of (35) or (37) and pyridinium dichromate (10 eq.) in acetic acid was stirred at room temperature for 4 h. The reaction mixture was then diluted with water and extracted with ethyl acetate (3 times). The combined organic layers were washed with water and extracted with aqueous saturated solution of sodium bicarbonate (3 times). The basic aqueous layers were acidified to pH=2 with hydrochloric acid 2N and extracted with ethyl acetate (5 times). The combined organic extract were dried over sodium sulfate and evaporated giving a clear crud oil, which was homogeneous by TLC. MS m/z: 220 (MH$^+$).

The crude was then dissolved in a solution of hydrochloric acid /ethyl acetate and stirred at room temperature for one hours. The solvent was removed under reduced pressure and the clear oil was precipitated with diethyl ether affording a white solid. (Compound **25** yield 50%, compound **26** yield 59%.)

(3Z)-2-amino-4-fluorobut-3-enoic acid hydrochloride (25)

1H-NMR (DMSO-d6 400 MHz): δ 4.16-4.19 (d, 1H, j=10.04Hz), δ 4.16-5.34 (ddd, 1H j=4.52Hz, 9.76Hz, 14.72Hz, 41.24Hz), δ 6.73-6.95 (dd, 1H j=4.56 Hz and 83.68Hz).

(3E)-2-amino-4-fluorobut-3-enoic acid hydrochloride (26)

1H-NMR (DMSO-d6 400 MHz): δ 4.73-4.75 (d, 1H, j=9.8Hz), δ 5.02-5.06 (ddd, 1H j=4.6Hz, 9.84Hz,14.48Hz, 39.6Hz), δ 6.88-7.10 (dd, 1H j=4.04 Hz and 82.16Hz).

11. SYNTHESIS OF 2' SUBSTITUTED (2*S*,1'*R*,2'*S*)-2-(CARBOXYCYCLOPROPYL)GLYCINE ((*S*)-CCG-IV) ANALOGUES.

During the third year of my doctorate, I worked at Department of Drug Design and Pharmacology at Copenhagen University, under the supervision of Prof. Rasmus Prætorius Clausen.

One of the main research topic from this department is the development of subunit -selective ligand for glutamate receptors both as pharmacological tools and as therapeutically useful agents.

To date few subtypes-selective ligands are known, especially among the NMDAR class, due to the high conserved region in the binding site of the subunits.

During the period spent to this department, I was interested in the development of selective ligands on NR2 subunit, and in particular in the development of constricted analogues based on (carboxycyclopropil) glycine (CCG) scaffold.

To better contextualize my work I will proceed in a brief introduction about current selective ligands on NMDAR and the past work conducted by this group.

11.1 NMDAR subunit -selective agonists.

NMDARs have always triggered an intense interest as potential therapeutic drug targets because they are involved in many brain disorders. Traditionally, NMDARs are best known for their role in excitotoxicity, a process during which excessive glutamate release causes over activation of NMDARs, accumulation of intracellular calcium and, eventually, neuronal death. This excitotoxic mechanism is well kown to occur during cerebral ischemia (following stroke or brain trauma) and in neurodegenerative disorders such as PD and HD. Most NMDAR antagonists developed in the 1980s and 1990s to treat these disorders failed in clinical trials because of unacceptable side effects (e.g. hallucinations, and memory and motor deficits).

The better understanding of NMDAR subunit organization and pharmacology renovated the interest towards the development of new subunit-selective NMDAR ligands, that appear to have a much improved side effect profile compared with broad-spectrum antagonists.

NMDAR are assembled from two GluN1 subunits and two GluN2 subunits. GluN3 subunits can also co-assemble with GluN1 and GluN2, but the function and physiological roles of these triheteromeric GluN1/GluN2/GluN3 receptors are less well understood. Glycine, D-Serine and glutamate are the endogenous agonists at the GluN1 and GluN2 subunits of the NMDAR, respectively. Simultaneous binding of glutamate and the co-agonist

(glycine or D-Serine) activates the NMDAR by opening a central cation-conducting channel.

The different NMDAR subunits (GluN1, GluN2A–D, and GluN3A–B) offer opportunities for the development of selective agonists, partial agonists, antagonists, and modulators However, progress in the development of subunit-selective agonists and competitive antagonists has been impeded by the high sequence identity of the GluN2 agonist-binding domain. The overall sequence identity of the agonist-binding domain of GluN2A–D is 63 %, but the residues that directly interact with the agonist, as well as the neighboring residues, are 100 % conserved among the GluN2 subunits. In comparison, the sequence identity of the GluN2 transmembrane domains is 73 %, whereas it is as low as 19 and 2 % for the N- and C-terminal domains, respectively.

A large variety of agonists for the NMDARs with diverse structures has been evaluated. These agonists are characterized by containing a free amino acid moiety, a free carboxylic acid or a bioisostere, corresponding to the distal carboxylate group in glutamate (Fig.22). Different bioisosteres, such as 1-hydroxy-pyrazoles, 3-hydroxy-isoxazoles, 3-hydroxy-isothiazoles, and tetrazoles have been successfully applied in NMDAR ligand design as bioisosteres for the distal carboxylate.
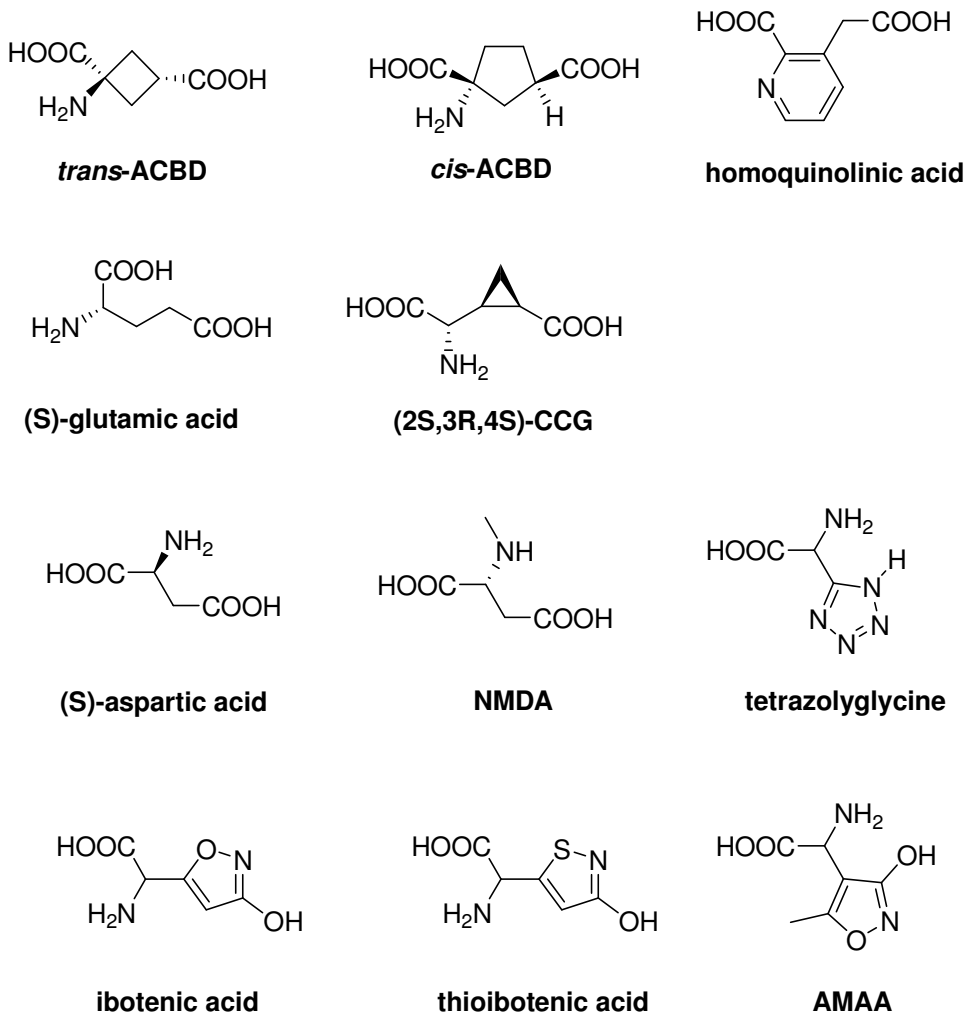
Figure 22. Structure of some subunit-selective ligand on NMDAR

Among them, an important family on selective ligand derive from the naturally occurring amino ibotenic acid, isolated from the mushroom *Amanita Muscaria* [132].

Modifications of ibotenic acid led to thioibotenic acid and the selective NMDAR agonist AMAA, which possess a E_{C50} of 12µM.

Another important class of agonist derive from carboxycyclopropyl-glycines (CCGs). CCGs are naturally occurring glutamate analogues isolated from seeds of *Aesculus parviflora* and *Blighia sapida*, belonging to the family Sapindaceae, and seeds of *Ephedra altissima* belonging to the family Ephedraceae. These have been important lead structures for the development of a range of selective GluR agonists and antagonists. CCGs incorporate the glutamate structure in a rigid ring, mimicking the partially folded conformation of (S)-glutamate. Three of the stereoisomers are very potent NMDAR agonists and may serve as lead structures for obtaining subtype selective NMDAR ligands. Indeed (2*S*,1′*R*,2′*S*)-2-(carboxycyclopropyl)glycine ((*S*)-CCG-IV) constitutes one of the most potent selective NMDAR ligand with an potency in the micro molar range and a specificity directed towards NR2B subunit.

The work I followed at Copenhagen University was finalize to the synthesis of (*S*)-CCG-IV analogs with substituent in the 2'-position since there are no analogues described.

11.2 2'- Alkyl substituted analogs of (S)-CCG-IV.

The synthesis and pharmacological characterization of 2'-Alkyl substituted analogs of (S)-CCG-IV (Fig.23) has been previously reported by the same group[133].

A R= H, (S)-CCG-IV
B R= Me
C R= Et
D R= nPr
E R= nBu
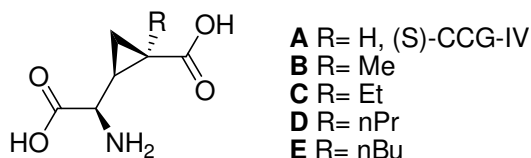
Figure 23. 2'-Alkyl substituted analogs of (S)-CCG-IV

The rational that supported this investigation, was a docking studies o subunit NR2A. The study underlines a substituent in the 2' position of (S)-CCG-IV protrudes into a region of the binding poked where non conserved residues are present, indeed could confers to the derivative a higher selectivity towards the different subunit.

A first panel of compound reported in figure 23 were synthetized and tested on recombinant GluN1/N2A-D receptors and the results are summarized in table 5

Pharmacological characterization of the new analogues revealed that although some potency is lost when introducing larger alkyl groups in the 2′-position, the analogues are indeed more potent than previously published glutamate analogues.[134]

Propyl-substituted **D** activates GluN2A and GluN2B with 67% and 105%, respectively, thus significant differences are achievable. Furthermore, differences in potency is also observed, for example,

for compound **C** that is 15-folds more potent at GluN2D compared to GluN2A and thus **C** is one of the most potent and selective agonists toward the GluN2D.

Comp.	R	subtype	EC$_{50}$ (μM)	rel I$_{max}$
A	H	GluN1/GluN2A	0.262	0.99
		GluN1/GluN2B	0.083	1.23
		GluN1/GluN2C	0.110	0.90
		GluN1/GluN2D	0.036	1.11
B	Me	GluN1/GluN2A	0.277[0.261;0.292]	0.94 ± 0.01
		GluN1/GluN2B	0.045[0.043;0.047]	1.14 ± 0.02
		GluN1/GluN2C	0.124[0.120;0.129]	0.81 ± 0.04
		GluN1/GluN2D	0.026[0.025;0.026]	0.83 ± 0.02
C	Et	GluN1/GluN2A	1.18[0.673;1.40]	0.83 ± 0.03
		GluN1/GluN2B	0.272[0.257;0.286]	1.02 ± 0.04
		GluN1/GluN2C	0.540[0.519;0.559]	0. 81 ± 0.02
		GluN1/GluN2D	0.080[0.077;0.083]	0. 91 ± 0.01
D	n-Pr	GluN1/GluN2A	46.3[45.2;47.4]	0.67 ± 0.01
		GluN1/GluN2B	15.8[15.2;16.3]	1.05 ± 0.02
		GluN1/GluN2C	29.9[29.3;30.5]	0. 70 ± 0.02
		GluN1/GluN2D	6.56 [6.15;6.90]	0. 89 ± 0.01
E	n-Bu	GluN1/GluN2A	28.8[28.4;29.2]	0.65 ± 0.02
		GluN1/GluN2B	10.2[9.82;10.5]	1.07 ± 0.01
		GluN1/GluN2C	16.0[15.6;16.5]	0.85 ± 0.02
		GluN1/GluN2D	3.30 [3.21;3.39]	0.94 ± 0.01

Table 5. Potency and Efficacy Relative to Glutammate of Compounds A–E at Recombinant GluN1/GluN2A–D Receptors   Expressed in Xenopus Ocytes.

The study demonstrated it is possible to introduce substituents in the 2′ position of (*S*)-CCG-IV.

A subsequent step in class exploration was to introduce more polar groups in position 2'. However, the synthetic pathways to obtain these derivatives needed to be explored in order to facilitate the synthesis of such compounds.

Synthetic strategy for 2'-subtituted (S)-CCG-IV analogs.
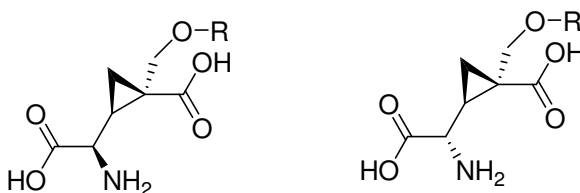
R = H, Bn, Et, *i*Pr

Figure 24. Proposed substitution in 2' position.

The project focus was to synthetize a small class of 2' alchoxy (S)-CCG-IV derivatives, in order to verify if a polar substitution could be tolerated and could enhance the selectivity and potency of the previous reported class. To pursue this goal an efficient synthetic pathway is fundamental.

In order to functionalize (s)-CCG-IV in position 2 was followed the synthetic strategy depicted in scheme 10.
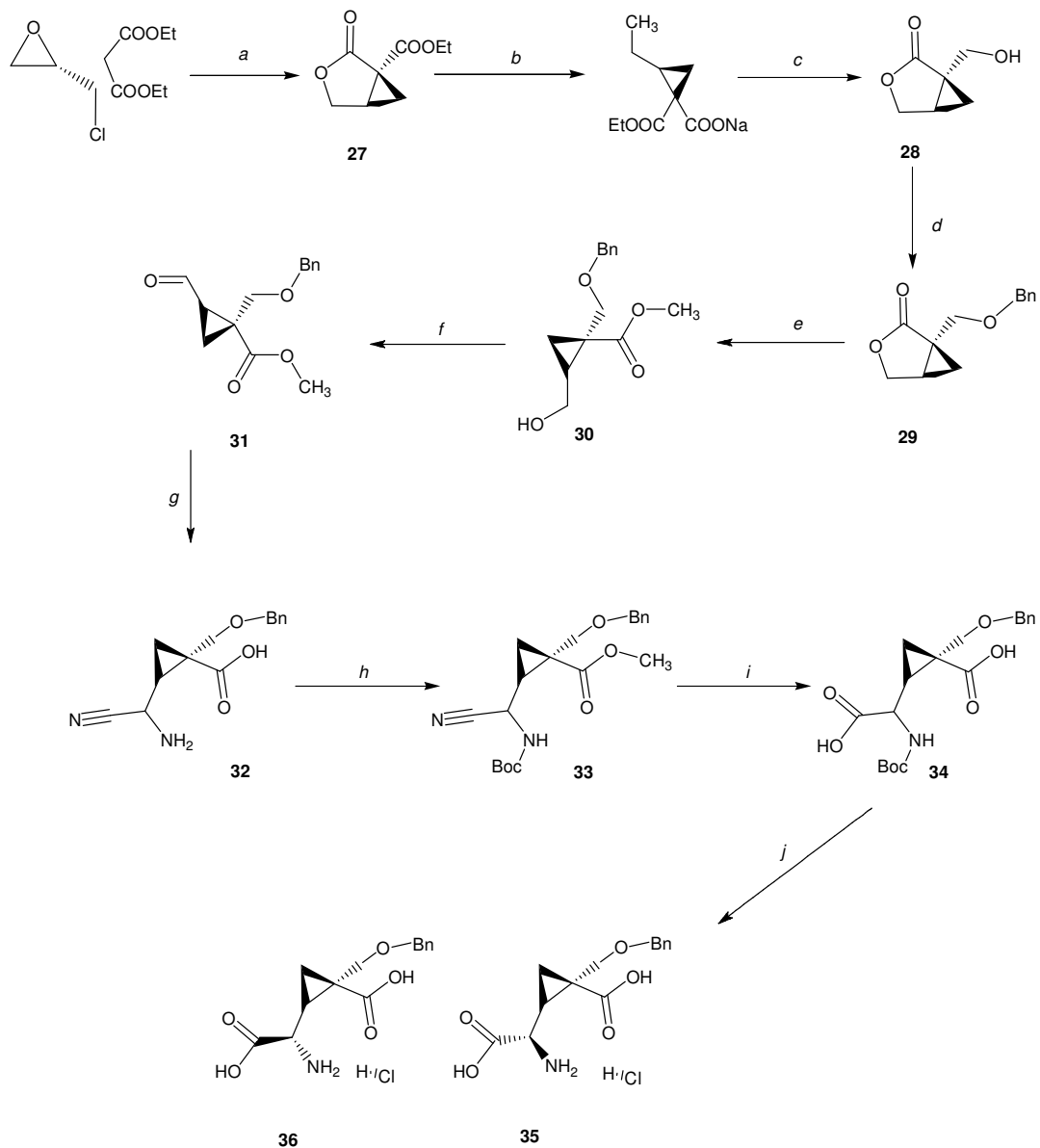
Scheme 10. Reagents and conditions. *a)* Na°, EtOH, from 0°C to RT, 20h. *b)* NaOH**,** EtOH, RT 12h. *c)* NaBH₄, EtOH, reflux 3h, HCl 2N rt 48h. *d)* Ag₂O, TBAI, Benzyl bromide, DMF,36h. *e)* NaOH, EtOH, RT 1h. DMS, DMSO toluene RT 2h. *f)* Dess-Martin, DCM, RT 1h. *g)* KCN, NH₄Cl, ammonia 28%, RT 2h. *h)* (Boc₂)O, DIPEA, DCM, RT 4h. *i)* NaOH 2N, EtOH, 70°C 1 week. *j)* HCl in EtOAc, RT 2h.

This strategy exploits the stereoselective formation of a cyclopropane fused ɣ-lactone functionalized with a 2 alchoxy moiety.

Compound **27** was synthetized according the procedures reported by Young Park and co. workers[135].

Reaction of R-epichlorohydrine with diethyl malonate and sodium metal gave cyclopropane fused ɣ-lactone 27 via tandem alkylation followed by lactonisation.

Treatment of **27** with sodium hydroxide in ethanol afforded the mono carboxylate sodium salt; then, the ester was selectively reduced by sodium borohydride under reflux, and then cyclized back under acidic conditions to give the ɣ-lactone **28**.
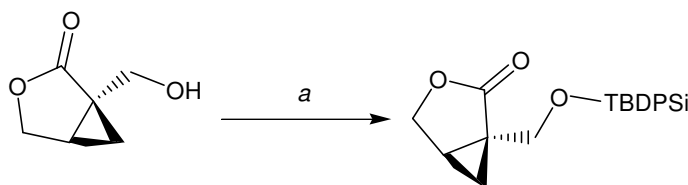
Scheme 32. Protection of the alkoxy moiety by tert-butyldi-phenyl chloride.Reagents and conditions. *a)* TBDPSi-Cl, imidazole, DCM, RT overnight.

The protection of hydroxyl group of **28**, was performed with both tert-buthyldi-phenylsilyl chloride to produce silyl ether, and with benzyl bromide to produce the benzyl ether.

Protection with the silyl chloride proceed under mild condition, in a good yields, without any particular problem, meanwhile the protection with the benzyl bromide require some attempts (Table 6) to obtain a satisfactory yields.

Condition	Time	Yield
1-NAH, THF, BENZYL BROMIDE	-	40%
2-DIPEA, BENZYL BROMIDE, DMF	48h; RT	No product
3-CS_2CO_3, BENZYL BROMIDE, DMF	48h; RT	<30%
4-CS_2CO_3, BENZYL BROMIDE, NAI, DMF	12h; 78°C	47%
5-AG_2O, BENZYL BROMIDE DCM	52h; RT	75%
6-AG_2O, BENZYL BROMIDE, TBAI, DMF	36h, RT	69%

Table 6. Overview of the attempted synthetic procedures for the protection of the alkoxy moiety.

Best results were obtained by using Ag_2O as a weak base, the reaction didn't proceed in quantitative yields, however it was possible to recover Starting material by purification trough silica gel chromatography.

The choice of Benzyl as a protecting group was impose by the subsequent reactions steps in which the silyl protecting group revealed an unexpected instability under the ring opening conditions.

In table 7 are summarized all the attempts done to open the lactone ring.

Condition	Time, temperature	yield
1-NaOH, EtHO	Rt, 12 h	silicium
2-NaOMe, THF	Rt, 12h	-
3-LiOMe, THF	Rt 12 h	-
4-KOtBu, THF	-reflux 12 h	silicium
5-NH$_3$, MeOH	RT,	-
6-PTSA, MeOH	50°C 5 h	degradation
7-HCl, MeOH	RT 8 h	degradation
8-LiOH, THF/H$_2$O, Et$_2$O	2h rt	Open salt

Table 7. Overview of the attempted synthetic procedures to open the γ-lactone 29

Usually strong basic conditions, or acidic conditions in alcohols are reported as classical procedure to open ɣ- lactones, in that case, the ring opening was especially unfavored, because of the cyclopropane constriction.

More over using silyl-protecting group a steric hindrance issue was added, and all the trials revealed an unexpected instability of the silyl group, not only in basic condition, but also in acidic ones.

Indeed, strong basic conditions favored the silyl group deprotection, and using less basic condition such as ammonia in methanol no reaction was detected, as far as using acidic condition (entry 6 and 7 of table 7).

Finally , ring lactone was open by treating it with 1.2 eq. of base, for a short time (1h), and without isolating it, was treated with dimethoxy

sulfate, affording the open methyl ester in a good yield (from 70 to 90%)

Reaction represented in entry 9 was performed successfully also on the benzyl ether protected lactone, with the same results.

However, TLC analysis of NMR samples of the open benzylated product revealed the product in solution reclosing to give the γ-lactons, this problem was bypassed by using direct the crude of reaction in the next step of alcohol oxidation.

Alkoxy moiety **30** was then oxidized to aldehyde **31** by using Dess-Martin periodinane, and on the aldehyde was attempted a Strecker reaction to obtain the amino nitrile portion.

Strecker reaction was performed both using TMSCN and in classical condition by using KCN/NH4Cl.

The first attempt, by using TMSCN lead to a very low yield (less than 20%) and a difficult product purification, probably because of the formation of the carboxylic acid in position 2.

Classical Strecker reaction conditions by using KCN and NH_4Cl lead to the formation of two diastereoisomers **32**, in a good yield (75%). The amino-nitrile was then protected with Boc (**33**) and hydrolyzed in basic condition, in order to obtain the dicarboxylic derivative (**34**).

Basic hydrolysis required one week, and afforded a mixture of the amide and dicarboxylic acid in a 2:1 ratio, which was separated by chromatography.

Finally, the Boc protected dicarboxylic acid was teated with HCl to afford the hydrochloric salt of the first two desired product **35** and **36**, which could be separated by preparative HPLC.

Conclusion.

In this work, I was able to project and develop an efficient synthetic pathway that led to a reproducible chemistry to obtain 2'-CCG-VI analogues. Notably the introduction of chemical diversity can be accomplished in the last step of the synthesis by the deprotection and functionalization of the hydroxyl moiety. This feature can be exploited for a class exploration, in order to create a tool of new subunit selective NMDAR molecules, useful both as pharmacological scaffold as potential drugs.

12. EXPERIMENTAL PROCEDURES (II)

12.1 Materials and method

All compound were obtained via classical synthetic procedures for reaction, purification and characterization, using organic chemistry lab wares at Copenhagen University

Reactants were purchased from Sigma-Aldrich® at reagent purity and, unless otherwise noted, used without further purification.

Solvent used in non-aqueous reaction were obtained by distillation of technical grade materials over appropriate dehydrating agents.

Reaction were monitored by thin layer chromatography on Kiesegel®60 F254 (DC-Alufolien, Merk®), at both 254 nm and 365 nm wavelengths.

Where indicated intermediates and final product were purified by silica gel flash chromatography (silica gel 0.040-0.063mm) using the described solvent mixtures.

Intermediates and final product were characterized by NMR analysis(BRUKER ® 400MHz) recording ^{13}C-NMR and ^{1}H-NMR. Data from characterization are not reported in this section.

12.2 Synthetic procedures.

(1S,5R)-Ethyl 2-oxo-3-oxabicyclo[3.1.0]hexane-1-carboxylate (27).

Sodium (2.42 g, 105 mmol) was carefully dissolved in EtOH (195 mL) at 0°C, and diethyl malonate (16.7 mL, 110 mmol) was added at 0 °C over 5 min to the solution. (R)-(-)-Epichlorohydrin (7.8 ml, 100 mmol) in EtOH, was added dropwise at room temperature over 1h, and the reaction mixuture was refluxed for 48 h. The mixture was filtered, and the filtrate was evaporated under reduced pressure. The residue was dissolved in methylene chloride and washed with H_2O. The organic layer was dried over anhydrous $MgSO_4$ and evaporated under reduced pressure.

The residue was purified by silica gel column chromatography using hexanes and ethyl acetate (3:1) as the eluent to give cyclopropane-fused lactone (11.40 g, 67%) as a colorless oil.

(1S,5R)-1-(Hydroxymethyl)-3-oxa-bicyclo[3.1.0] hexan-2-one (28).

A solution of (_)-(1S,5R)-Ethyl 2-oxo-3-oxabicyclo[3.1.0]hexane-1-carboxylate (2 g, 11.9 mmol) in EtOH (38 mL) was treated with sodium hydroxide (571mg. 14.28 mmol) in EtOH (38 mL). After stirring for 16 h at room temperature, the reaction mixture was treated with sodium borohydride (2.25 g,59.5 mmol) and refluxed for 3 h. After cooling to room temperature, 2 N HCl (40 mL) was added

slowly at 0 °C. EtOH in the reaction mixture was evaporated off under reduced pressure and to the resulting solution was added 2 N HCl (40 mL). After being stirred for 48 h at room temperature, the aqueous layer was extracted with methylene chloride several times. The organic layer was dried over anhydrous $MgSO_4$, filtered, and concentrated in vacuo. The residue was purified by silica gel column chromatography using methylene chloride and MeOH (20:1) as the eluent to give lactone (1.1 g. 8.59mmol, 72.2%y) as a colorless oil.

(1S,5R)-1-[(benzyloxy)methyl]-3-oxabicyclo[3.1.0]hexan-2-one (29).

(_)-(1S,5R)-1-(Hydroxymethyl)-3-oxa-bicyclo[3.1.0] hexan-2-one (600 mg, 4.68mmol) was dissolved in dry DMF,Ag_2O(1.62 g, 7.03 mmol) and TBAI (1,72 g, 4.68 mmol) were added, followed by BnBr (0.836 mL, 7,03 mmol). After 36 h, the reaction mixture was diluted with Et_2O filtered through Celite and washed with Et_2O.

The filtrate was washed with aqueous $NaHCO_3$ and with brine, and the organic layer was separated, dried, and concentrated to give the crude product, which was purified by using column chromatog4.49raphy on silica gel to give (1S,5R)-1-[(benzyloxy)methyl]-3-oxabicyclo[3.1.0]hexan-2-one as a colorless oil (662 mg, 70%).

Methyl (1R,2S)-1-[(benzyloxy)methyl]-2-(hydroxymethyl)cyclopropanecarboxylate (30)

To a solution of (1S,5R)-1-[(benzyloxy)methyl]-3-oxabicyclo[3.1.0]hexan-2-one (850 mg, 3.89 mmol) in H_2O (5 mL) and ethanol (20 mL) was added NaOH (187 mg, 4.67 mmol) and the reaction mixture was stirred at ambient temperature for 1 h and concentrated in vacuo. Without further purification, the resulting residue was dissolved in DMSO (5 mL) and toluene (1.2 mL). To this mixture was added dimethyl sulfate (0.4438 mL, 4.67 mmol) slowly and stirred at ambient temperature for another 1 h.

The mixture was evaporated and the residue was poured into ethyl acetate (20 mL) and water (10 mL). The organic layer was separated, washed with brine (10 mL) and dried (MgSO₄), filtered, and evaporated. The residue was purified by silica gel column chromatography (heptanes:ethyl acetate) from 95:5 to 6:4 to give Methyl (1R,2S)-1-[(benzyloxy)methyl]-2-(hydroxymethyl)cyclopropanecarboxylate (605 mg., 69%) as a colorless oil.

Methyl (1R,2S)-1-[(benzyloxy)methyl]-2-formylcyclopropanecarboxylate (31).

Methyl (1R,2S)-1-[(benzyloxy)methyl]-2-(hydroxymethyl)cyclopropanecarboxylate (137mg, 0.54 mmol) was dissolved in DCM (3 ml), and Dess-Martin periodinane (464 mg. 1.96 mmol) was added to the solution. Reaction was stirred at room

temperature for 1.5h, then diluted with NaOH 1N (10ml). The organic phase was separated and washed several times with NaOH 1 N, until it was clear, the it was dried over Na_2SO_4 and evaporated to driness affording Methyl (1R,2S)-1-[(benzyloxy)methyl]-2-formylcyclopropanecarboxylate (110 mg. 0.44 mmmol, 88.7%y) as a colourless oil

Methyl (1R,2S)-2-[amino(cyano)methyl]-1[(benzyloxy)methyl]cyclopropanecarboxylate (32).

A solution of Methyl (1R,2S)-1-[(benzyloxy)methyl]-2-formylcyclopropanecarboxylate (360mg, 1.45 mmol) in EtOH (1.5 ml), was added to a solution of KCN (113 mg. 1.74 mmol) and NH_4CL (155 mg. 2.90 mmol) in ammonia 28% (5ml), and the mixture was stirred at room temperature for 2h.

Reaction was then diluted with EtOAc (10 ml). the aqueous phases were washed several times with EtOAc. All the collected organic phases were dried over Na_2SO_4 and evaporated to dryness affording a crude oil which was purified by silica gel chromatography eluting with Hept:EtOAC from 1.9 to 100% EtOAc (1%NH3).

Collected fractions gave Methyl (1R,2S)-2-[amino(cyano)methyl]1[(benzyloxy)methyl]cyclopropanecarboxylate (300mg, 1.09 mmol 75%

Methyl (1R,2S)-2-[Boc-amino(cyano)methyl]-1[(benzyloxy)methyl]cyclopropanecarboxylate (33).

Methyl (1R,2S)-2-[amino(cyano)methyl]-1[(benzyloxy)methyl]cyclopropanecarboxylate, (320 mg, 1.09 mmol) was dissolved in DCM (10ml) and DIPEA (04 ml) and (Boc)$_2$O (334 mg, 1.53 mmol) were added reaction was stirred at room temperature for 2h. The reaction was diluted with water and the organic phase was separated, dried over Na$_2$SO$_4$ and evaporated in vacuo affording a crude product (390mg) which was use directly in the next step of reaction.

(1R,2S)-2-[Boc-amino(carboxy)methyl]-1-[(benzyloxy)methyl]cyclopropanecarboxylic acid (34).

Methyl (1R,2S)-2-[Boc-amino(cyano)methyl]-1[(benzyloxy)methyl]cyclopropanecarboxylate (390 mg) was dissolved in EtOH (5ml) and NaOH 1N (1ml) was added and the mixture was stirred at 80°C for 6 days. After this time reaction was evaporated and the residues diluted with DCM (5Ml) and water.

Organic phase was separated and the aqueous one was acidified to pH 4 with KHSO$_4$, and extracted with DCM (5ml x3t.). these organic phases were dried over Na$_2$SO$_4$, evaporated and purified by silica gel chromatography eluting with DCM:ETOAc from 100:0 to 90:10 (1% formic acid). Collected fractions gave 98mg of target compound.

(1R,2S)-2-[amino(carboxy)methyl]-1-[(benzyloxy)methyl]cyclopropanecarboxylic acid hydrochloride (35) and (36).

(1R,2S)-2-[Boc-amino(carboxy)methyl]-1-[(benzyloxy)methyl]cyclopropanecarboxylic acid (98 mg.) was dissolved in a solution of HCl in Ethyl Acetate (3ml) and stirred at room temperature for three hours. The reaction mixture was evaporated under vacuum to obtain a crude slurry that was precipitated with diethyl ether/ ethyl acetate (8:2), affording the desired products as a withe solid (51 mg.).

13. LIST OF PAPERS.

Further Insights in 5-phenyl-2-[2-(1-piperidinylcarbonyl) Phenyl]-2,3-dihydro-1H-pyrrolo[1,2-c]imidazol-1-ones, a Recently Disclosed Class of Neuropeptide S Antagonists.

Gabriele Costantino*,[a], Marco Mor[a,] Chiara Pecchini[a], Gian Paolo Vallerini[a], Elisa Della Turca[a],Fabrizio Micheli[*,b], Angela Worby[*,c], Romano Di Fabio[b], Angelo Giacometti[b], Adelheid Roth[b], Emilio Merlo-Pich[c], Matteo Biagetti[d] [b], Giorgio Bonanomi[b], Dino Montanari[b], Luca Tarsi[b], Federica Tonelli[b], Raffaele Longhi[e] and Anna Maria Capelli[b,d].

Abstract.

In this paper, a recently reported series of NPS antagonists is further expanded and biologically evaluated. The ligand efficiency and ADMET score concepts were then applied to the newly disclosed 5-phenyl-2-[2-(1-piperidinylcarbonyl) phenyl]-2,3-dihydro-1H-pyrrolo[1,2-c]imidazol-1-ones, to limit the SAR exploration. Important pharmacophoric features were identified suggesting potential way forward for the identification of further developable templates.

14. REFERENCES

[1] James N. C. Kew, John A. Kemp **2005**, *Psychopharmacology* 179, 1, 4-29.

[2] Conn PJ, Pin JP, **1997**, *Annu Rev Pharmacol Toxicol.*, 37:205-37.

[3] Ferraguti and Shigemoto , **2006** , *Cell Tissue Res*, 326:483–504,

[4] Shigemoto and Mizuno, **1997**, *The Journal of Neuroscience,* 17(19): 7503-7522.

[5] Holmann, Heineman **1994**, *Annu.Rev.Neurosci.* 17, 31-108.

[6] Sommer, B., Keinanen, K., Verdoorn, T. A., Wisden, W., Burnashev, N., Herb, A., Kohler, M., Takagi, T., Sakmann, B. and Seeburg, P. H. **1990,** *Science* 249, 1580– 1585.

[7] Lambolez, B., Ropert, N., Perrais, D., Rossier, J. and Hestrin, S. **1996**, *Proc. Natl. Acad. Sci. U.S.A.* 93, 1797– 1802.

[8] Seeburg PH, Hartner J, **2003**, *Curr. Opin. Neurobiol.* 13:279–283.

[9] Liu SQ, Cull-Candy SG. **2000***, Nature*, 25;405(6785):454-8.

[10] Dong H, O'Brien RJ, Fung ET, Lanahan AA, Worley PF, Huganir RL. **1997**, *Nature.* 20;386(6622):279-84.

[11] Gallyas F, Ball SM, Molnar E ,**2003**, J Neurochem 86:1414–1427

[12] J. Lerma, **2003**, *Nat. Rev. Neurosci.* 4, 481–495

[13] R.J. Rodrigues, J. Lerma, **2012**, *Membrane Transport and Signaling*, 1, 399–410.

[14] Stuart Cull-Candy, Stephen Brickley and Mark Farrant, **2001**, *Current Opinion in Neurobiology*, 11:327–335.

[15] .Schorge S, Colquhoun D., **2003,** *J Neurosci.*, 23, 1151-8.

[16] Schüler T, Mesic I, Madry C, Bartholomäus I, Laube B., **2008**, *J Biol Chem.*, 283, 37-46.

[17] Dingledine R, Borges K, Bowie D, Traynelis SF., **1999**, *Pharmacol Rev.*;51(1):7-61.

[18] Sendtner M, *et al.*, **2000**, *Cell Tissue Res.*;301:71–84.

[19] Martins RA, *et al.,* **2005***, J Neurochem*; 95:244–253.

[20] Mattson MP. *et al.,* **1996***, Perspect Dev Neurobiol.*;3:79–91.

[21][21] Marini AM, *et al.*, **1998**, *J Biol Chem.*;273:29394–29399.

[22] Kitayama *et al.*, **2004**, *Journal of Neuroscience Research,* 76, 5, 599–612.

[23] Petralia RS, *et al.* **2010**, *Neuroscience*; 167:68–87

[24] Hardingham GE, Bading H., **2010**, *Nat Rev Neurosci.* (10):682-96.

[25] Milnerwood A, *et al.,* **2010***, Neuron.*; 65:178–190.

[26] Gouix E, Léveillé F, Nicole O, Melon C, Had-Aissouni L, Buisson A., **2009**, *Mol Cell Neurosci.*;40,4:463-73.

[27] Shankar GM, Bloodgood BL, Townsend M, Walsh DM, Selkoe DJ, Sabatini BL, **2007**, *J Neurosci.*;27:2866-75.

[28] Snyder EM, Nong Y, Almeida CG, Paul S, Moran T, Choi EY, *et-al.*, **2005**, *Nat Neurosci.*;8:1051-8.

[29] Dingledine R, Borges K, Bowie D, Traynelis SF. **1999,** *Pharmacol Rev.*; 51(1):7-61.

[30] Fadda E, Danysz W, Wroblewski JT, Costa E., **1988**, *Neuropharmacology*;27(11):1183-5.

[31] Nong Y, *et al.* **2003,** *Nature.* 20;422(6929):302-7.

[32] Shan Q, Nevin ST, Haddrill JL, Lynch JW. **2003,** *J Neurochem.*; 86(2):498-507.

[33] Cubelos B, Giménez C, Zafra F., **2005,** *Cereb Cortex.*; 15(4):448-59.

[34] **Hashimoto** A, Nishikawa T, Oka T, Takahashi K., **1993**, *J Neurochem.*;60(2):783-6

[35] Mothet JP, **2000** , *Proc Natl Acad Sci U S A.*;97(9):4926-31

[36] Furukawa H, Gouaux E. , **2003**, *EMBO J*. Jun 16;22(12):2873-85.

[37] Wolosker *et al.,* **1999***, Proc.Natl. Acad.Sci. USA,* 96, 721-725.

[38] Wolosker *et al.,* **1999***, Proc.Natl. Acad.Sci. USA*, 96, 13409-13414.

[39] Schell MJ, Snyder SH, **1997**, *J.Neurosci*, 17,1604-1615.

[40] Stevens ER, **2003**, *Proc. Natl. Acad. sci. USA*, 100(11),6789-6794.

[41] Schell MJ, Molliver ME, Snyder SH., **1995**, *Proc Natl Acad Sci USA*.;92:3948–52

[42] Mothet JP, Pollegioni L, **2005**, Proc *Natl Acad Sci USA*, 102, 5606-5611.

[43] Wolosker H, **2006**, *J.Biol. Chem.*, 281, 14151-14162.

[44] Mori, H. & R. Inoue., **2010**, *Chemistry and Biodiversity*, 7, 1573-1578.

[45] Fuchs SA*,* Dorland L*,* de Sain-van der Velden MG*,* Hendriks M*,* Klomp LW*,* Berger R *&* de Koning TJ *,***2006***, Ann Neurol* 60*,* 476–480*.*

[46] H.A. Krebs, **1935,** *Biochem. J.* 29, 1620-1644.

[47] A. Hashimoto, T. Nishikawa, R. Konno, A. Niwa, Y. Yasumura, T. Oka, K. Takahashi, **1993,** *Neurosci. Lett*. 152, 33-36.

[48] A. Morikawa, K. Hamase, T. Inoue, R. Konno, A. Niwa, K. Zaitsu, **2001,** *J. Chromatogr. B Biomed. Sci Appl.* 757 ,119-125.

[49] A. D'Aniello, A. Vetere, L. Petrucelli, **1993**, *Biochem. Physiol B* 105, 731-734.

[50] Y. Nagata, R. Konno, Y. Yasumura, T. Akino, **1989**, *Biochem. J.* 257, 291-292.

[51] L.Z. Wang, X.Z. Zhu, **2003**, *Acta Pharmacol. Sin.* 24 965-974.

[52] K. Strisovsky, **2003,** *FEBS Lett.,* 535, 44–48.

[54] Rosenberg, D., & H. Wolosker: **2010**, *Faseb J*, 24, 2951–2961.

[54] S.M. Williams, R.K. Sullivan, **2006**, *Glia,* 53, 401–411.

[55] P.M. Kim *et al.,* **2005**, *Proc. Natl. Acad. Sci. U. S. A.*, 102 , 2105–2110.

[56] C.S. Ribeiro *et al.,* **2002**, *Brain Res.*, 929, 202–209.

[57] E. Kartvelishvily *et al.,* **2006**, *J. Biol. Chem.*, 281, 14151–14162.

[58] Wu S. et al., **2007** , *Current Alzheimer Research*, 4, pp. 243-251(9)

[59] Rutter *et al.,* **2007**, *European Journal of Neuroscience* 25, 6, 1757–1766.

[60] D.C. Javitt *et al.,* **2002**, *Brain Res.*, 941, 146–149.

[61] M.J. Schell *et al.* **1997**, *J. Neurosci.*, 17, pp. 1604–1615

[62] Mothet et al., **2000**, *Proc Natl Acad Sci U S A.*;97(9):4926-31.

[63] R.A. Nicoll Philos., **2003**,*Trans. R. Soc. Lond. B Biol. Sci.*, 358, 721–726.

[64] Y. Yang *et al.,* **2003**, *Proc. Natl. Acad. Sci. U. S. A.*, 100, 15194–15199.

[65] Oliet SH, Mothet JP., **2006**, *Glia*. 15;54(7):726-37.

[66] Turpin *et al.* **2006**, *J Neurochem.*;98(4):1159-66.

[67] Panatier A. *et al.* **2006** , *Cell*.19;125(4):775-84.

[68] S. Yang *et al.* **2005**, *Neurosci. Lett.,* 379, 7–12

[69] K. Wake *et al.* **2001**, *Neurosci. Lett.,* 297, 25–28

[70] X. Xie *et al.,* **2005***, Brain Res.*, 1052, 212–221

[71] E.R. Stevens *et al.,* **2003***, Proc. Natl. Acad. Sci. U. S. A.*, 100, 6789–6794

[72] D. Dememes *et al.,* **2006***, Neuroscience*, 137, 991–997

[73] S.Z. Wu *et al.* **2004***, J. Neuroinflammation*, 1, 2

[74] M.E. Hatten, **1999**, *Annu. Rev. Neurosci.*, 22, 511–539

[75] E. Yacubova, H. Komuro, **2003**, Cell *Biochem. Biophys.* 37, 213–234.

[76] D. Boehning, S.H. Snyder, **2003**, *Annu. Rev. Neurosci.* 26, 105–131.

[77] F. Hepner *et al.,* **2005***,* J. *Neural Transm.,* 112, 805–811.

[78] Z. Chen *et al.,* **2004**, *J. Soc. Gynecol. Investig.*, 11, 294–303.

[79] L.M. Ritter *et al.,* **2001***,* Dev. *Brain Res.*, 127, 123–133.

[80] P. Reiprich *et al.*, **2005**, Cereb. Cortex, 15, 349–358.

[81] S. Taharaguchi *et al.* **2003***, Virology*, 307, 243–254.

[82] G.E. Hardingham, H. Bading, **(2003)**, J. *Neural Transm,* 81–89.

[83] Katsuki H, **2004**, *J. Pharmacol. Exp. Ther.* 311, 836-844.

[84] Katsuki H, Watanabe Y, **2007**, *Life Sci.*, 81, 740-749.

[85] S. Wu, S.W. Barger, **2004**, *Ann. N. Y. Acad. Sci.*, 1035,133–146.

[86] S.A. Lipton, **2004**, *NeuroRx*, 1, 101–110.

[87] S. Wu, S.W. Barger, **2004**, Ann. *N. Y. Acad. Sci.*, 1035, 133–146.

[88] G. Fisher *et al.*, **1998**, *Amino Acids*, 15, 263–269.

[89] Sasabe J, et al, **2007**, *EMBO J.* 26, 4149–4159.

[90] M. Shleper *et al.,* **2005***,* J. *Neurosci.*, 25, 9413–9417.

[91] Bendikov I, , Wolosker H & Agam G ,**2007**, *Schizophr Res* 90, 41–51.

[92] Hashimoto K, et al. ,**2003**,. *Arch Gen Psychiatry* 60, 572–576.

[93] Chumakov I, et al. ,**2002**,. *Proc Natl Acad Sci U S A* 99, 13675–13680.

[94] Baumgart,F et Rodriguez-Crespo, **2008**, *FEBS J.* 275,3538-3545.

[95] Smith, M. A., B. Felicetti, M. Wood, A. Cesura & J. Barker:, **2010 ,** *J Biol Chem*, 285, 12873-81.

[96] Goto, M.,*et al.,* **2009***, J Biol Chem*, 284, 25944-52.

[97] Yamauchi, T., M. Goto, **2009**, *J Biochem*, 145, 421-4.

[98] I. Rodriguez-Crespo., **2002**, *J Biol Chem*, 277, 27782-92.

[99] Strisovsky, K., J. Jiraskova, & J. Konvalinka. **2005**, *Biochemistry*, 44, 13091-100.

[100] Goto M., Ito T. et al., **2013**, *Amino Acids* 44; 1073-1084.

[101] Hoffman, H *et al.,* **2010***, Collect. Czech. Chem. Commun.*, 75, 59-79.

[102] Jiraskova-Vanickova, J, H. E. Hoffman *et al.*, **2011**, *Current Drug Targets*, 12, 1037-1055.

[103] Yoshimura T. and Goto M.,**2008**, *FEBS J.* 275, 3527-3537.

[104] Neidle, A. & D. S. Dunlop., **2002**, *Neurochem Res*, 27, 1719-24.

[105] De Miranda, J., R. Panizzutti, V. N. Foltyn & H. Wolosker., **2002**, *Proc Natl Acad Sci U S A*, 99, 14542-7.

[106] Wolosker, H *et al* . , **1999**, *Proc Natl Acad Sci U S A*, 96, 721-725.

[107] Cook, S. P., I. Galve-Roperh, A. Martinez del Pozo & I. Rodriguez-Crespo, **2002**, J *Biol Chem*, 277, 27782-92.

[108] Baumgart, F., J. Mancheno & J. R. Crespo, **2007**, *Febs Journal*, 274, 293-293.

[109] Shoji K, Mariotto S, Ciampa AR, Suzuki H., **2006**, *Neurosci Lett.*,392(1-2):75-8.

[110] Shoji K, Mariotto S, Ciampa AR, Suzuki H., **2006**, *Neurosci Lett.* Feb 20; 394(3):163-7.

[111] Mustafa, A. K., A. Kumar, B. Selvakumar, G. P. H. Ho, J. T. Ehmsen, R. K. Barrow, L. M. Amzel & S. H. Snyder:, **2007**, *Proc Natl Acad Sci U S A*, 104, 2950–2955.

[112] Mustafa, A. K., **2009**, *Proc Natl Acad Sci U S A*, 106, 2921-2926.

[113] Balan, L., & H. Wolosker, **2009**, *Proc Natl Acad Sci U S A* , 106, 7589-7594.

[114] Kim, P. M., *et al* , **2005** , *Proc Natl Acad Sci U S A*, 102, 2105-2110.

[115] Fujii, K., *et al* , **2006**,*Mol Psychiatry*, 11, 150-7.

[116] Hikida, T., **2008,** *Biol Psychiatry*, 63, 997-1000.

[117] Dumin, E., I. Bendikov, V. N. Foltyn, Y. Misumi, Y. Ikehara, E. Kartvelishvily & H. Wolosker: **2006,** *J Biol Chem*, 281, 20291-302.

[118] Ma, T. M., S. Abazyan, B. Abazyan, J. Nomura, C. Yang, S. Seshadri, A. Sawa, S. H. Snyder & M. V. Pletnikov: **2012,** *Mol Psychiatry* 2105-2110.

[119] Panizzutti *et al.*, **2001,** *Proc Natl Acad Sci U S A*; 98; 5294-5299.

[120] Cook SP. *et al.*, **2002,** *J.Biol.Chem.*;277; 27782-9.

[121] Hoffman, H. E., J. Jiraskova, **2009,** *J Med Chem*, 52, 6032-41.

[122] Dixon, S. M., P. Li, R. Liu, H. Wolosker, K. S. Lam, M. J. Kurth & M. D. Toney, **2006**, *J Med Chem*, 49, 2388-97.

[123] Bruno, A., L. Amori & G. Costantino. **2011,** *Molecular Informatics*, 30, 317-328.

[124] L.L. McCoy , **1958,** *J. Am. Chem. Soc.*, 80, 6568.

[125] Qiong Zhao, Henry N.C. Wong, **2007**, Tetrahedron 63, 27, 6296–6305.

[126] Liang, F.; Kirsch, J. F. *Biochemistry* **2000**, *39*, 2436–2444.

[127] Jung, M. J.; Palfreyman, M. G. *Vigabatrin. In Antiepileptic Drugs*, 4th ed.; Levy, R. H., Mattson, R. H., Eds.; Raven: New York, **1995.**

[128] Silverman, R. B.; Bichler, K. A.; Leon, A., **1996**, J. *J. Am. Chem. Soc., 118*, 1253–1261.

[129] McCarthy, J. R.; Huber, E. W.; Le, T.-B.; Laskovics, F. M.; Matthews, D. P., **1996,** *Tetrahedron*, *52*, 45–58.

[130] *Protein Preparation Wizard; Epik version 2.0; Impact version 5.5; Prime version 2.1.*, Schrödinger, LLC, New York, NY, **2009**.

[131] Halgren, T. A.; Murphy, R. B.; Friesner, R. A.; Beard, H. S.; Frye, L. L.; Pollard, W. T.; Banks, J. L., Glide. *J. Med. Chem.* **2004,** *47*, 7, 1750-1759.

[132] C. H. Eugster, G. F. Muller, R. Good*, 1965, Tetrahedron Lett. 6, 1813.*

[133] Risgaard, R , Nielsen, SD , Hansen, KB , Jensen, CM , Nielsen, B , Traynelis, SF & Clausen, RP **2013**, *Journal of Medicinal Chemistry* , 56, 10, 4071-4081.

[134] Erreger, K.; Geballe, M. T.; Kristensen, A.; Chen, P. E.; Hansen, K. B.; Lee, C. J.; Yuan, H.; Le, P.; Lyuboslavsky, P. N.; Micale, N.; Jorgensen, L.; Clausen, R. P.; Wyllie, D. J.; Snyder, J. P.; Traynelis, S. F., **2007**, *Mol. Pharmacol.*, 72, 907– 920.

[135] Park, Ah-Young *et al.* **2011**, *Bioorganic & Medicinal Chemistry*, 19(13), 3945-3955.